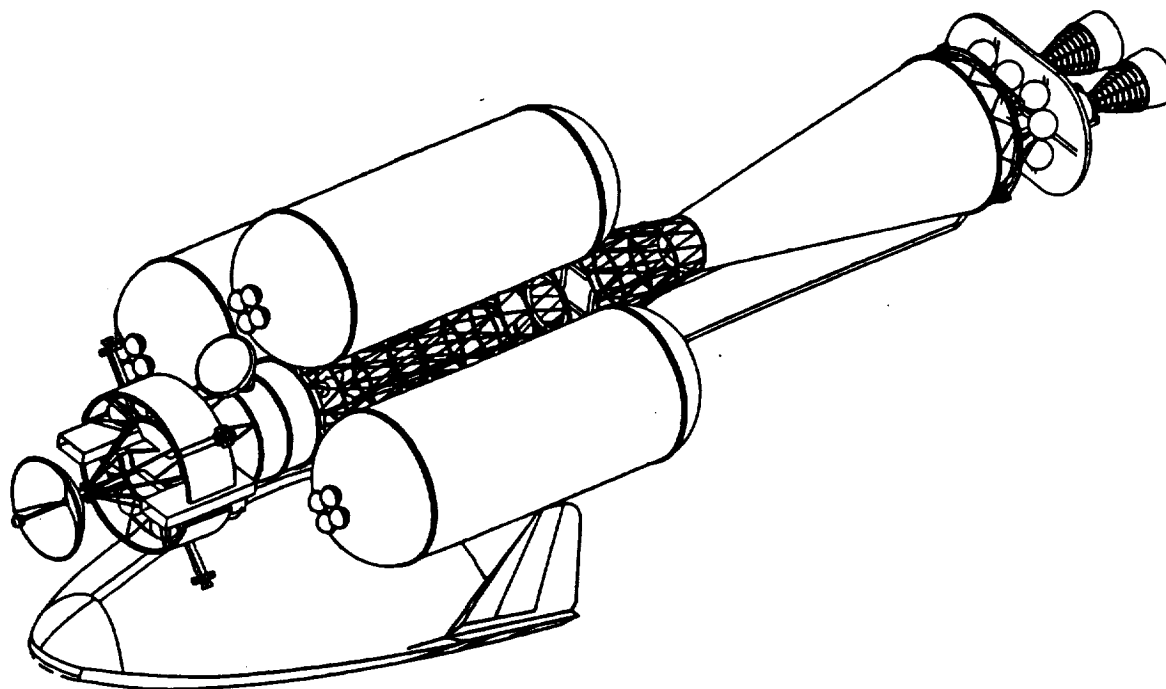


John Edwards
PT41

Space Transfer Concepts and Analyses for Exploration Missions

Final Report
Technical Directive 10
February 1992



Boeing Defense and Space Group
Advanced Civil Space Systems
Huntsville, Alabama

Contract NAS8-37857

D615-10051

(NASA-CR-184309) SPACE TRANSFER CONCEPTS
AND ANALYSES FOR EXPLORATION MISSIONS:
TECHNICAL DIRECTIVE 10 Final Report, Oct.
1991 - Jan. 1992 (Boeing Aerospace Co.)
111 p

N92-24048

Unclas
CSCL 22A G3/12 0086911



Space Transfer Concepts and Analyses for Exploration Missions


Contract NAS-37857

Technical Directive 10

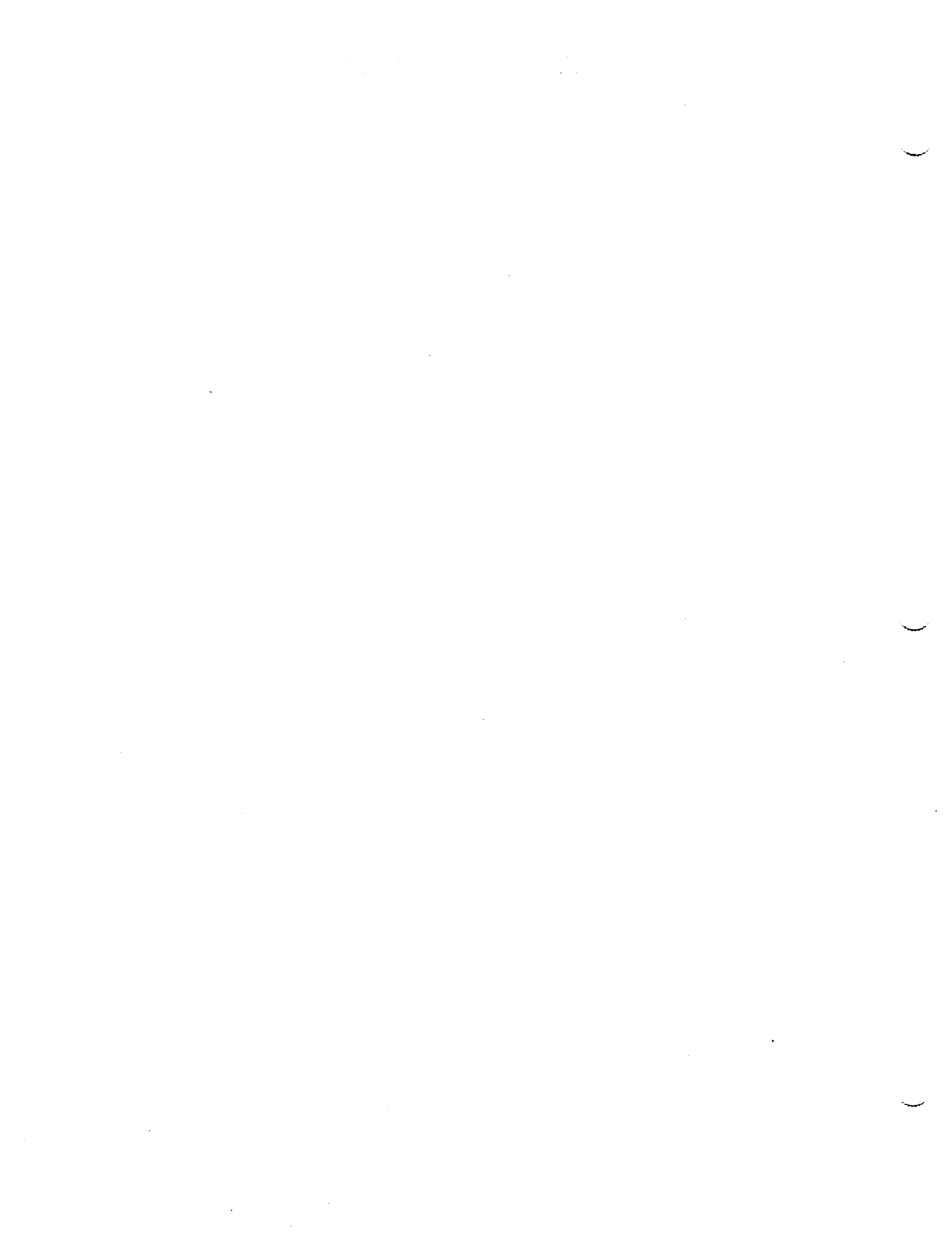
Final Report

February 1992

**Boeing Defense & Space Group
Advanced Civil Space Systems
Huntsville, Alabama**


**Gordon R. Woodcock
Study Manager**

D615-10051



BOEING

CAGE CODE 81205

THIS DOCUMENT IS:

CONTROLLED BY Advanced Civil Space Systems

ALL REVISIONS TO THIS DOCUMENT SHALL BE APPROVED BY THE ABOVE ORGANIZATION PRIOR TO RELEASE.

PREPARED UNDER CONTRACT NO. NAS8-37857

IR&D

OTHER

PREPARED ON DOCUMENT NO. D615-10051

FILED UNDER MODEL

TITLE Space Transfer Concepts and Analyses for Exploration Missions, Technical Directive 10, Final Report

THE INFORMATION CONTAINED HEREIN IS NOT PROPRIETARY.

THE INFORMATION CONTAINED HEREIN IS PROPRIETARY TO THE BOEING COMPANY AND SHALL NOT BE REPRODUCED OR DISCLOSED IN WHOLE OR IN PART OR USED FOR ANY DESIGN OR MANUFACTURE EXCEPT WHEN SUCH USER POSSESSES DIRECT, WRITTEN AUTHORIZATION FROM THE BOEING COMPANY.

ORIGINAL RELEASE DATE *S.G. 92-02-28*

ISSUE NO. TO DATE

ADDITIONAL LIMITATIONS IMPOSED ON THIS DOCUMENT WILL BE FOUND ON A SEPARATE LIMITATIONS PAGE.

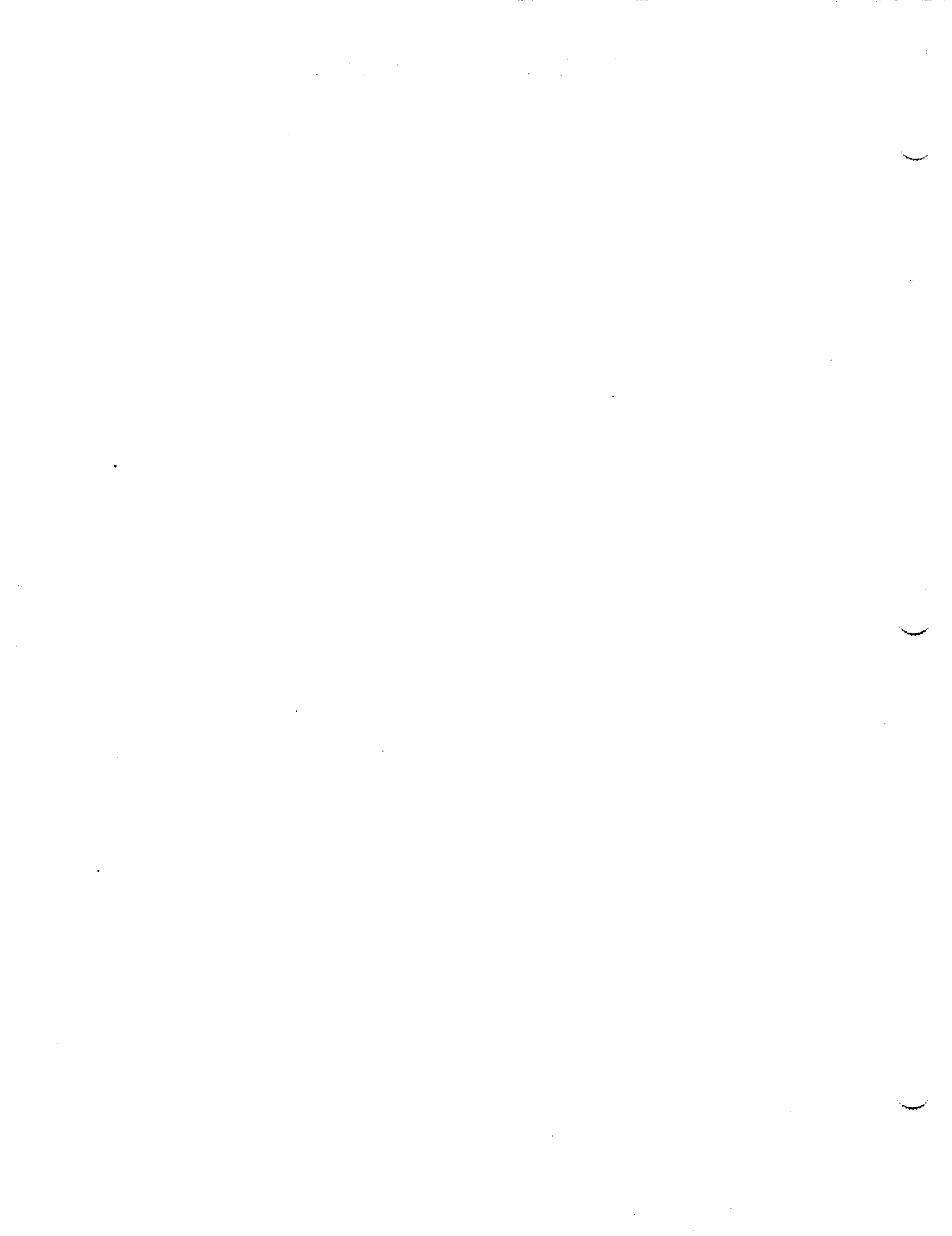
PREPARED BY STCAEM Team 2-H895 92-2-28

CHECKED BY Irwin E. Vas *Irwin E. Vas* 2-H895 92-2-28

SUPERVISED BY *Gordon K. Woodcock* Gordon K. Woodcock 2-H895 92-2-28

APPROVED BY J. E. Kingsbury (see below)

J. E. Kingsbury
SIGNATURE 2-H890 92-2-28
J. E. Kingsbury ORGN DATE



FOREWORD

The study entitled "Space Transfer Concepts and Analyses for Exploration Missions" (STCAEM) was performed by Boeing Missiles and Space, Huntsville, for the George C. Marshall Space Flight Center (MSFC). The current activities were carried out under Technical Directive 10 during the period October 1991 through January 1992. The Boeing program manager was Gordon Woodcock, and the MSFC Contracting Officer's Technical Representative was Alan Adams. The task activities were led by M. Appleby, P. Buddington, B. Donahue, and I. Vas, with technical support from J. Burrell, S. Capps, M. Cupples, R. Fowler, K. Imtiaz, S. LeDoux, J. McGhee, J. Nordwall, T. Ruff, R. Schorr, B. Sherwood, R. Tanner, and B. Wallace.

CONTENTS

	Page
1. INTRODUCTION	1
2. LAUNCH VEHICLE SIZE TRADE	3
2.1 Assembly Options and Concepts	3
2.1.1 Shroud Packaging	9
2.1.2 Length Sizing by Pad-Wind Loading	11
2.2 Platform Concepts	16
2.2.1 I-Beam Platform	18
2.2.2 Saddle Platform	21
2.3 Meteoroid/Orbital Debris Program (MOD)	24
2.4 Delta-V and Descent Analysis	26
2.4.1 Introduction	26
2.4.2 Delta-V Sets	26
2.4.3 Mars Parking Orbit Descriptions	30
2.4.4 2016 TEI Reduction	32
2.4.5 Low-L/D MEV Landing Site Access	35
2.4.6 High-L/D MEV Landing Site Access	36
2.4.7 Nuclear Reactor Disposal	38
2.4.8 Summary	41
3. MEV OPTIONS	42
3.1 Symmetric Biconic Concepts	42
3.1.1 Parametric Study	42
3.1.2 Additional Studies	47
3.1.3 Biconic MEV Configuration Layout	53
3.1.4 Biconic MEV Summary	54
3.2 Structural Analysis of Low L/D Aerobrake	54
3.2.1 Material properties	54
3.2.2 Loading	56
3.2.3 Baseline Analysis Results	56
3.2.4 Aerobrake Configuration Update	56
3.2.5 Revised Rim	57
3.2.6 Thermal Loading	59
3.3 High L/D Biconic MEV	60
3.3.1 Loading	60
3.3.2 Analysis	62
4. LUNAR DRESS REHEARSAL ANALYSIS	63
4.1 Introduction	63
4.1.1 Specific Areas of Investigation	64
4-2 Mission Profile	64
4.2.1 Earth-Moon-Earth Transfer	64
4.2.2 Reuse	65
4.2.3 Abort Modes	65
4.3 Validation of Mars Mission Unique Hardware	65
4.4 Space Transfer Vehicle Description	66
4.4.1 Transfer Vehicle Systems	66
4.4.2 Transfer Vehicle Performance and Mass	67

CONTENTS (Concluded)

	Page
4.4.3 Transfer Vehicle Propulsion System	67
4.4.4 Transfer Vehicle Crew Systems	69
4.4.5 Radiation Sources	69
4.4.6 Transfer Vehicle Attitude Control Propulsion System ..	71
4.4.7 Transfer Vehicle Truss Strongback/Interconnect System (Structures)	71
4.4.8 Earth-to-Orbit Vehicle Flight Manifests	72
4.5 Validation of Mars Mission Unique Operations	72
4.5.1 On-Orbit Assembly/Assembly Platform	72
4.5.2 Outbound Flight/Lunar Arrival/Lunar Orbit	73
4.5.3 Surface Operations	73
4.5.4 Inbound Flight	74
4.5.5 Earth Return	74
4.6 Surface Manifest	74
4.7 Surface Habitat System Delivery	75
4.7.1 Lunar Lander Design and Application	76
4.7.2 Lander Cargo Downloading	77
4.7.3 Lander Mass and Performance	77
4.8 Mars Ascent Stage Checkout Test at the Moon	77
4.8.1 Flight Plan for Propulsion and Flight Control Systems ..	78
4.8.2 Cryogenic Propellant Thermal Insulation Validation ...	79
4.8.3 Mars Descent Aerobrake Qualification Flight	80
4.9 Lunar Dress Rehearsal Mission Schedules	80
4.10 Follow On Lunar Missions	81
5. RADIATION ANALYSIS - LUNAR CREW RETURN VEHICLE (LCRV)	91
5.1 Introduction	91
5.2 Modules and Methods	91
5.2.1 Background and Description of the Analysis	91
5.2.2 Natural Radiation Environment Models	92
5.2.3 The Boeing Radiation Exposure Model	92
5.2.4 Solid Modeling	93
5.3 Analysis Results	94
REFERENCES	97

FIGURES

	<u>Page</u>
2-1. Assembly Options/Concepts	3
2-2. Trade Study NTP Vehicle Data Sheets - Summary	3
2-3a. Data Sheet 1	4
2-3b. Data Sheet 2	5
2-3c. Data Sheet 3	6
2-3d. Data Sheet 4	7
2-3e. Data Sheet 5	8
2-4. Baseline NTP Manifest 12 m Diameter Shroud	9
2-5. Baseline NTP Vehicle Configured for 14 m Diameter Launch Shroud	10
2-6a. Launch Optimized NTP Vehicle and Biconic MEV (Configuration)	12
2-6b. Launch Optimized NTP Vehicle and Biconic MEV (Manifest)	13
2-7. Launch Vehicle Comparison	14
2-8. Windload Data	15
2-9. Shroud Size Study	16
2-10. MTV Assembly Platform Full-Service Concept	17
2-11. NTP Platform Full-Up Configuration	17
2-12. Saddle Platform CAD Model	18
2-13a. Assembly Platform Parts List (I-Beam)	18
2-13b. Assembly Platform Parts List (I-Beam)	19
2-13c. Assembly Platform Parts List (I-Beam)	20
2-14. Saddle Assembly On Vehicle Core	21
2-15a. Saddle Assembly Platform	22
2-15b. Saddle Platform: Top View	22
2-15c. Saddle Platform: Side View	23

FIGURES (Continued)

	<u>Page</u>
2-15d. Saddle Platform: End View	23
2-16. Robotic Arm Detail	23
2-17. Saddle Assembly Platform Parts List	24
2-18a. LEO Debris Shielding Model-1	25
2-18b. LEO Debris Shielding Model-2	25
2-18c. LEO Debris Shielding Model-3	26
2-19. 2012 - 2020 Mission Delta-V Data	27
2-20. Reference Delta - Set, Synthesis Report	30
2-21. 2014 Reserves, Losses, Midcourse	30
2-22. Mars Parking Orbits	31
2-23. Parking Orbit Delta-V	32
2-24. 2016 Opposition, Split Delta-V	33
2-25. Definition of Angle Psi	34
2-26. 2016 Split Delta-V	34
2-27. 2014 Landing Site Access	36
2-28. 2018 Landing Site Access	37
2-29. Polar Access with HMEV Lander	38
2-30. Polar Access with Biconic Lander	39
2-31. Reactor Disposal Delta-V	40
3-1. Types of Aerobrake Shapes Examined	43
3-2. Biconic Geometry Parameters	43
3-3. Biconic Lift and Drag Values	45
3-4. Nose Cone Angle Effects	46
3-5. Center of Pressure Locations	46
3-6. Concept 408.7033 Aerodynamic Parameters	47

FIGURES (Continued)

	<u>Page</u>
3-7. Comparison of Biconic Shapes	49
3-8. Biconic Lift and Drag Values	50
3-9. Scaled Peak Heating Rates for BMEV Descent	50
3-10. Aerodynamic Coefficients for BMEV and HMEV	51
3-11. Lift-to-Drag Ratios for BMEV and HMEV	52
3-12. Moment Coefficient for Concept 414.7516	52
3-13. BMEV Conceptual Configurations	53
3-14. Loads and Boundary Conditions	55
3-15. Aerobrake Honeycomb Sandwich Structure	55
3-16. Sandwich Structure Physical Characteristics	55
3-17. Revised Rim Configuration	56
3-18. Exaggerated Deformed Shape, Blue - Undeformed, Black - Deformed	57
3-19. Magnitude of Total Displacements (meters)	58
3-20. Major Principal Stresses on the Outer Surface (Pa)	59
3-21. Summary of Structural Results	59
3-22. Concept 408.7033, Loading, Shear, and Moment Diagrams	61
4-1. Lunar Dress Rehearsal Vehicle Sketch and Launch Manifest	67
4-2. Vehicle Mass Variation with Surface Payload	68
4-3. Validation of Mars Mission Unique Operations at the Moon	73
4-4. Mars Surface Exploration Manifest - 2014 90-day stay	75
4-5. Lander Mass Variation with Surface Payload	76
4-6. Mars Ascent Stage Lunar Checkout Flight	79
4-7. Lunar Dress Rehearsal - Top Level Development Schedule	82
4-8a. Lunar Dress Rehearsal - Man-Rating Approach	83

FIGURES (Concluded)

	<u>Page</u>
4-8b. Lunar Dress Rehearsal - Man-Rating Approach	84
4-8c. Lunar Dress Rehearsal - Man-Rating Approach	85
4-9. Lunar Dress Rehearsal - NTP Engine Development	86
4-10. Lunar Dress Rehearsal - 3-Way Airlock	87
4-11. Lunar Dress Rehearsal - Vehicle Habitat	88
4-12. Lunar Dress Rehearsal - Self-Check Capability Development . . .	89
4-13. Lunar Dress Rehearsal - Structures	90
5-1. LCRV Dose Equivalent in Rem/Event	94

ABBREVIATIONS AND ACRONYMS

A/B	Aerobrake
Al	Aluminum
ALARA	As Low as Reasonably Achievable
ALSPE	Anomalous Large Solar Proton Event
AOA	Angle of Attack
ASE	Airborne Support Equipment
AU	Astronomical Unit (=149.6 million km)
BFO	Blood-Forming Organs
BLAP	Boundary Layer Analysis Program
BMEV	Biconic Mars Excursion Vehicle
BREM	Boeing Radiation Exposure Model
CAD/CAM	Computer-Aided Design/Computer-Aided Manufacturing
CAM	Computer Anatomical Man
C _D , Cd	Drag Coefficient
c.g.	Center of Gravity
CM	Center of Mass, Moment Coefficient
C _p , CP	Center of Pressure, specific heat at constant pressure
CRV	Crew Recovery Vehicle, Crew Return Vehicle
CTV	Cargo Transfer Vehicle
delta-V, ΔV	Velocity Change (m/s or km/s)
ECLS	Environmental Control and Life Support
EOC	Earth Orbit Capture
ETO	Earth-To-Orbit
FEM	Finite Element Model
F.S.D.	Full Scale Development
g	Acceleration in Earth Gravities (acceleration 9.80665 m/s ²)
HLLV	Heavy Lift Launch Vehicle
HLV	Heavy Launch Vehicle
H ₂	Hydrogen
i	Inclination, degrees
I	Moment of inertia
IMLEO	Initial Mass in Low Earth Orbit
Isp	Specific Impulse (= thrust/mass flow rate)
JSC	Johnson Space Center
K	Temperature in Kelvin Units
kg	kilograms
km	kilometers
km/sec	kilometers/second
kts	Wind Speed, Knots

ABBREVIATIONS AND ACRONYMS (Continued)

L	Lift, shroud length, vehicle length
lbf	Pounds force
L/D	Lift-To-Drag Ratio
LCRV	Lunar Crew Return Vehicle
LCV	Lunar Crew Vehicle
LDR	Lunar Dress Rehearsal
LEO	Low Earth Orbit
LEM	Lunar Excursion Module
LEV	Lunar Excursion Vehicle
Level II	Space Exploration Initiative Project Office, Johnson Space Center
LH ₂	Liquid Hydrogen
LOC	Lunar Orbit Capture
LO ₂	Liquid Oxygen
LTV	Lunar Transfer Vehicle
m	meters
MCRV	Mars Crew Return Vehicle
MEV	Mars Excursion Vehicle
MIEA	Modified Integrated Equipment Assembly
MOC	Mars Orbit Capture
MOD	Meteoroid/Orbital Debris Program
MSFC	Marshall Space Flight Center
mt	Metric Ton (1000kg)
NTR	Nuclear Thermal Rocket
Pa	Pascals
P _B	Base Pressure
PDOSE	Proton Dose Code
P/L	Payload
PNP	Probability of No Penetration
psi	Angle relative to velocities
q	Heat Flux, dynamic pressure
Q	Heat Flux (Joules per Square Centimeter), Radiation Quality Factor
R	Radians
RCS	Reaction Control System
RF	Radio Frequency
RMS	Remote Manipulator System
s	seconds
SEI	Space Exploration Initiative
SPE	Solar Proton Events
SSF	Space Station Freedom
STCAEM	Space Transfer Concepts and Analyses for Exploration Missions
t	metric tons (1000 kg), thickness
TEI	Trans-Earth Injection
Ti	Titanium
TLI	Trans-Lunar Injection

ABBREVIATIONS AND ACRONYMS (Concluded)

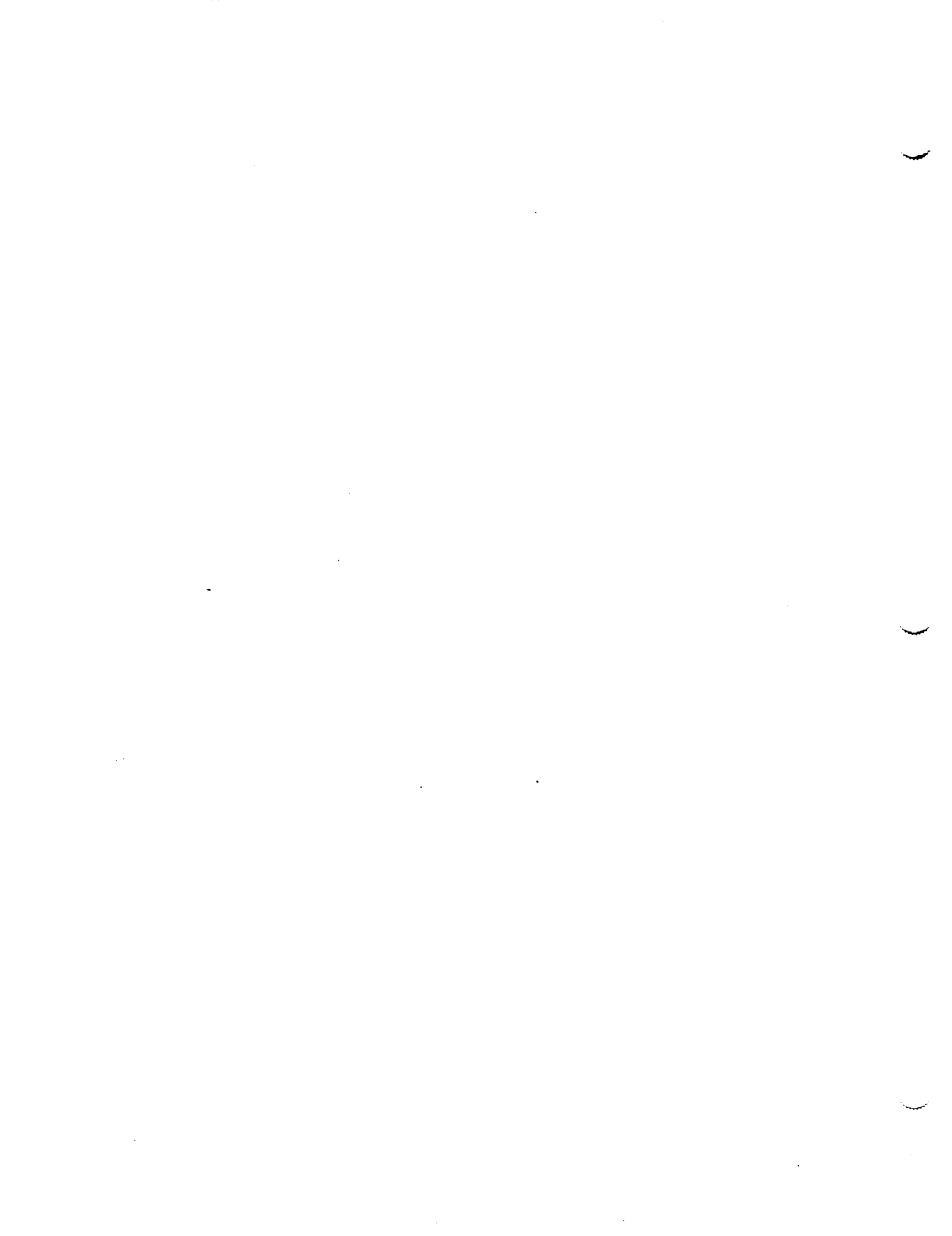
TMI	Trans-Mars Injection
TPS	Thermal Protection System
VECTRACE	Vector Trace
Vhp	Velocity, relative to a central body of a spacecraft a great distance from the central body
VSB	Venus Swing-by
Δ	Delta
θ	Angle of a Attack, Degrees
	Specific mass, power and propulsion dry mass divided by electric thruster input power, kg/kW_e
σ	Half Angle relative to body geometry
ρ	density
E	Modulus of Elasticity (Pa)
G	Modulus of Rigidity (Pa)
μ	Poisson's Ratio
σ_{ty}	Allowable Tensile Yield Stress (Pa)
σ_{ey}	Allowable Compressive Yield Stress (Pa)
σ_{sv}	Allowable Shear Yield Stress (Pa)

SUBSCRIPT

b	base
i	intermediate
n	nose
ref	reference value

ABSTRACT

The current technical effort is part of the third phase of a broad-scoped and systematic study of space transfer concepts for human lunar and Mars missions. The study addressed issues that were raised during the previous phases but specifically on launch vehicle size trades and MEV options.



1. INTRODUCTION

The "Space Transfer Concepts and Analyses for Exploration Missions" (STCAEM) study was initiated in August, 1989 to address in-space transportation systems for human exploration missions to the Moon and Mars. Detailed investigations carried out in the study have been documented in two technical reports (references 1 and 2). A broad range of topics were covered in these studies including orbit-to-orbit transfer vehicles, with emphasis on nuclear thermal propulsion, landing and ascent vehicles, lunar rover, concepts, technology requirements and costs. This report describes results of tasks dealing with particular aspects of lunar and Mars missions that were identified as important issues during Phases 1 and 2 of the present study. The reader is referred to the final reports of these phases, and to a nuclear thermal propulsion Mars transportation system concept baseline document now in preparation for a more general treatment of study results and findings. The current activity, commencing phase 3 of the overall study, addresses specific aspects of launch vehicle capabilities.

Study tasks reported herein include:

- a. Completion of a launch vehicle payload capability and shroud size trade in which launch manifesting of certain Mars transportation system options is described.
- b. Discussion of MEV options and results of analyses of high L/D biconic configurations and a structural analysis of a monocoque structural configuration of the L/D 0.5 Mars aerobrake from Phase 1 of the study. The monocoque configuration was investigated because configurations with rib/spar stiffeners proved difficult to package for launch.
- c. Lunar dress rehearsal analysis: One of the recommendations of the Stafford Synthesis Report was that a lunar mission be carried out as a dress rehearsal for the first piloted Mars mission; this section presents an analysis of such a mission with particular attention to what can be adequately demonstrated and how demonstration requirements drive the mission configuration and operations.
- d. Lunar crew return vehicle radiation analysis: This task was "left over" from Phase 2; funding limits caused the radiation analysis to be postponed until the present phase. The results indicate that the Apollo-like lunar CRV provides enough inherent protection to keep crew dose below the Space Station Freedom 30-day exposure guidelines for solar proton events of the magnitude of the August 1972 and October 1989 events. However, the "as low as reasonable achievable" (ALARA) principle

merits further optimization of the configuration for radiation protection and may lead to consideration of adding some dedicated shielding.

2.0 LAUNCH VEHICLE SIZE TRADE

2.1 ASSEMBLY OPTIONS AND CONCEPTS

A review was made of tank sizing and assembly criteria and analysis, as well as, design and manifesting assessments. Both the I-Beam and Saddle platform designs were considered. The features of these designs are given in figure 2-1 and further defined under the individual headings listed below.

Two Concepts	
I-Beam Concept	<ul style="list-style-type: none"> ● Designed to have the most of the service functions located on the platform ● Allows checkout of the vehicle systems with platform backup ● Vehicle systems are conserved for the Mars departure (management of MTBF on critical systems) ● Served as an "at hand" parts storage area ● It is its own resource node.
"Saddle" Concept	<ul style="list-style-type: none"> ● Designed to use the vehicle systems as much as possible ● Long-term vehicle systems checkout prior to Mars departure ● Small and more easily reconfigurable with SSF support ● Does not appear to require a separate launch.

Figure 2-1. Assembly Options/Concepts

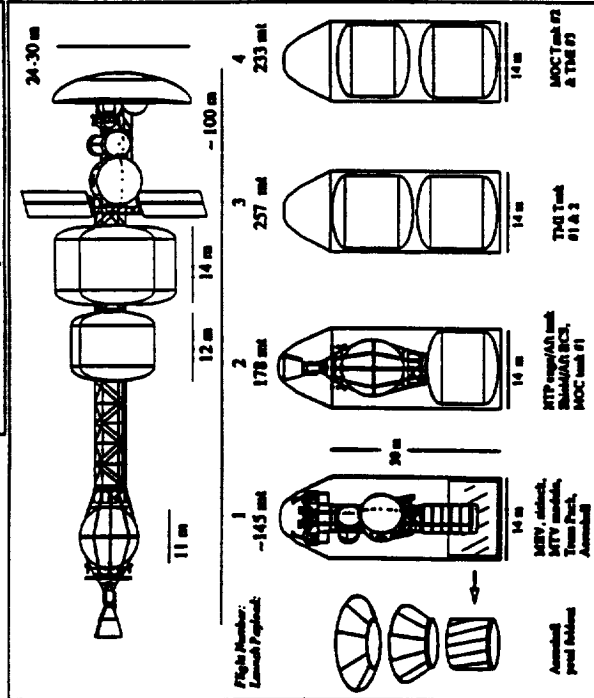
A launch vehicle size trade was supported with calculations of vehicle mass and tank size for manifesting considerations. A description of the conditions from which the data was generated is shown in figure 2-2, and the resultant vehicle parameters are shown in figures 2-3a through 2-3e. Additional orbital and flight mechanics work was done to answer specific questions on the capability of possible vehicle elements, landing site access and nuclear disposal questions. This information is given under its own separate heading in section 2.4.

Data Sheet	250 (mt) Payload Class ETO Vehicle: Shroud Sizes: 14 (m) dia by up to 30 (m) cyl length 257 (mt) payload actually delivered by Launch Veh
1	2014 Piloted NTR vehicle: ● IMLEO = 815 (mt) ● Four ETO flights are necessary for delivery to LEO ● Veh core up in two flights
2	2012 Cargo NTR vehicle: ● IMLEO = 216 (mt) ● Only one ETO flight is necessary for delivery to LEO
	150 (mt) Payload Class ETO Vehicle: Shroud Sizes: (1) 14 (m) dia by up to 30 (m) cyl length 115 (mt) p/l actually delivered by Launch Veh or (2) 10 (m) dia by up to 30 (m) cyl length 132 (mt) p/l actually delivered by Launch Veh
3	2014 Piloted NTR vehicle: ● IMLEO = 815 (mt) ● Seven ETO flights are necessary for delivery to LEO ● Veh core up in two flights
4	2012 Cargo NTR vehicle: ● IMLEO = 216 (mt) ● Two ETO flights are necessary for delivery to LEO
	Enhanced 150 (mt) Payload Class ETO Vehicle: Increase actual deliverable payload to 148 (mt) to LEO reduces required ETO flights by one, from seven to six.
5	2014 Piloted NTR vehicle: ● IMLEO = 815 (mt) ● Six ETO flights are necessary for delivery to LEO ● Veh core up in two flights

Figure 2-2. Trade Study NTP Vehicle Data Sheets - Summary

MARS SEI VEHICLE DATA SHEET

VEHICLE: NTP Flashed for 250 mt payload class ETO Vehicle
 LAST DATA UPDATE: 11/20/99 (launch veh actually delivers 257 mt P/L max)



Num Tank	Fluid(s)	Tank Size	Dry Mass (ca)	Prop Mass (ca)	Total Mass (ca)
1	TE1	11 m sphere	9918 kg	52067 kg	61985 kg
2	MOC	14 m by 12.0 m	13070 kg	80286 kg	93356 kg
2	TM1 1 & 2	14 m by 14.0 m	17990 kg	110510 kg	128500 kg
1	TM1 3	14 m by 15.0 m	19675 kg	120861 kg	140536 kg
6	TOTALS		91713 kg	554520 kg	646233 kg

SEI CASE NAME

COMMENTS

Veh sketch serves as representation; not definitive of latest configuration. Level II dV set with losses, 440 d transfer, 90 d stay, elliptical orbit, CRV returns to Earth, veh expended, crew of 6, shield weight equals engine weight. NTP engines operate at 2700K, nozzle area ratio of 400:1 - engine performance = 925 sec Imp.

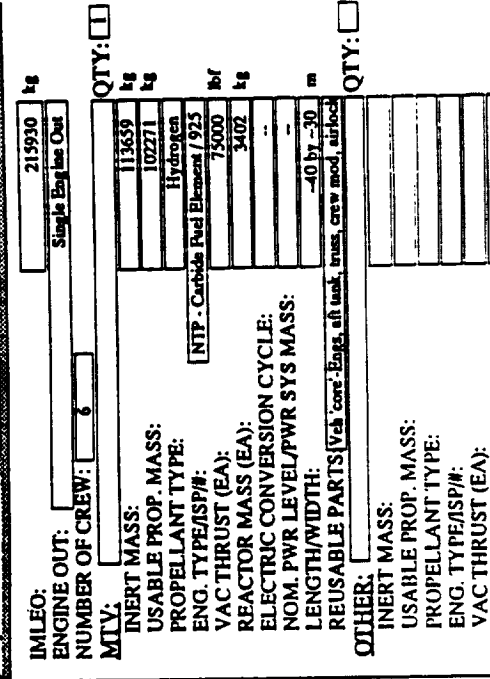
Surface Payload Mass: 5.7 mt payload to the surface
 Departure Orbit: 407 km, 407 km, 28.3 deg

IMLEO: 814890 kg
 ENGINE OUT: Single Engine Out
 NUMBER OF CREW: 6
 MTV: QTY: 1
 INERT MASS: 260360 kg
 USABLE PROP. MASS: 554520 kg
 PROPELLANT TYPE: Hydrogen
 ENG. TYPE/ISP/#: [NTP - Carbide Fuel Element / 925] m/s
 VAC THRUST (EA): 75000 mN
 REACTOR MASS (EA): 3403 kg
 ELECTRIC CONVERSION CYCLE: --
 NOM. PWR LEVEL/PWR SYS MASS: --
 LENGTH/WIDTH: -100 by -30 m
 REUSABLE PARTS: Veh tank-Bays, all tank, trans, crew mod, airlock QTY: 0
 OTHER:
 INERT MASS:
 USABLE PROP. MASS:
 PROPELLANT TYPE:
 ENG. TYPE/ISP/#:
 VAC THRUST (EA):
 LENGTH/WIDTH:
 A/B SIZE/MASS:
 REUSABLE PARTS:
 MEV: 1017/01.02 L/D, storable, 3.7 ton down cargo w Asc BR, 18 522 kg
 INERT MASS: 15,427 kg
 USABLE PROP. MASS: 48,670 kg
 PROPELLANT TYPE (Descent/Asc): [N2O4/MMH N2O4/MMH]
 ENGINES (Descent/Asc): 4/2
 THRUST (EA) (Descent/Asc): 30,000/30,000 mN
 ISP (Descent/Asc): 340 sec
 LENGTH/WIDTH: 24-30 by 24-30 m
 A/B SIZE/MASS: 8725 - (12.5 %) sec/m
 REUSABLE PARTS: none

REFERENCES:
 102591 Performance/statement: Boeing STCAEM B. Donahue 205/461-3712 (see sec 4.9)
 9/10/91 Trajectory/dV set: Level II; g-load/plane change dV Boeing STCAEM M. Cripples
 10/15/91 MEV Performance/statement: Boeing STCAEM B. Donahue (see sec 4.10)
 OTHER MASS includes masses Not included in MTV, OTHER, MEV, Prop Tanks, or Payload. Describe OTHER MASS Below:

Figure 2-3a. Data Sheet 1

MARS SEI VEHICLE DATA SHEET
 VEHICLE: NTP Cargo for 250 mt ETO Vehicle
 LAST DATA UPDATE: 1031/91
 250 ton launch vehicle



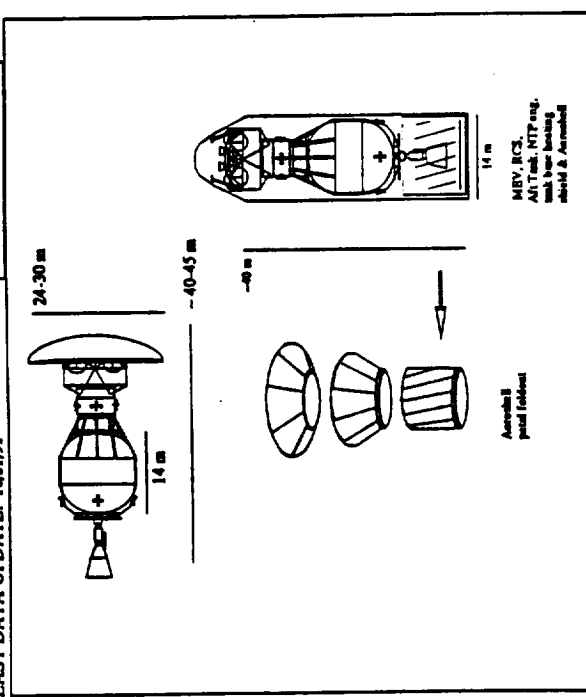
IMLEO: 219930 kg
 ENGINE OUT: Single Engine Out
 NUMBER OF CREW: 6
 QTY: 1
 INERT MASS: 113659 kg
 USABLE PROP. MASS: 102271 kg
 PROPELLANT TYPE: Hydrogen
 ENG. TYPE/ISP/#: NTP - Carbide Fuel Element / 925
 VAC THRUST (EA): 75000 lbf
 REACTOR MASS (EA): 3402 kg
 ELECTRIC CONVERSION CYCLE: ...
 NOM. PWR LEVEL/PWR SYS MASS: ...
 LENGTH/WIDTH: -40 by -30 m
 REUSABLE PARTS (Veh, core, Eng, aft tank, truss, crew mod, aeroshell) QTY: 0
 OTHER:

INERT MASS:
 USABLE PROP. MASS:
 PROPELLANT TYPE:
 ENG. TYPE/ISP/#:
 VAC THRUST (EA):
 LENGTH/WIDTH:
 A/B SIZE/MASS:
 REUSABLE PARTS:
 MEV: [1017/91] 0.2 LD, storable, 3.7 ton down cargo w Asc sig 78.522 kg
 INERT MASS: 7,124 kg
 USABLE PRO. MASS: 17,673 kg
 PROPELLANT TYPE (Descent/Asc): [N2O/MMH/N2O/MMH]
 ENGINES (Descent/Asc): 4 / 2
 THRUST (EA) (Descent/Asc): 30,000 / 30,000 lbf
 ISP (Descent/Asc): 340 sec
 LENGTH/WIDTH: 24-30 by 24-30 m
 A/B SIZE/MASS: [8735 - (12.5 %)] kg
 REUSABLE PARTS: none

REFERENCES:
 1025/91 Performance/wt statement: Boeing STCAEM B. Donahue 205/461-3732
 9/10/91 Trajectory/dV set: Level II; g-loss/plane change dV Boeing STCAEM M. Cupples
 10/15/91 MEV Performance/wt statement: Boeing STCAEM B. Donahue

OTHER MASS includes masses Not included in MTY, OTHER, MEV, Prop Tanks, or Payload. Describe OTHER MASS Below:

MARS SEI VEHICLE DATA SHEET
 VEHICLE: NTP Cargo for 250 mt ETO Vehicle
 LAST DATA UPDATE: 1031/91
 250 ton launch vehicle



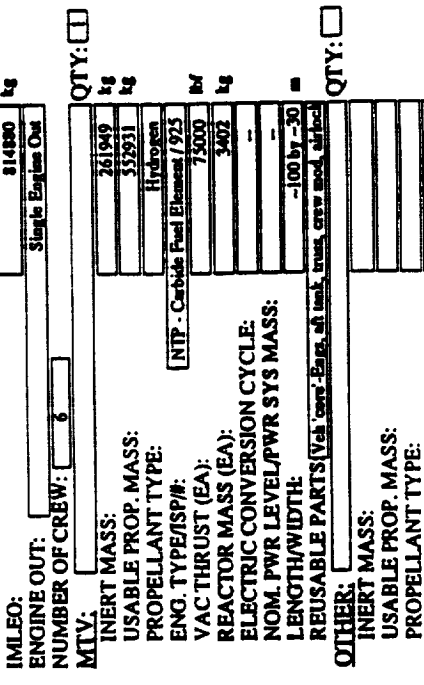
PROPELLANT TANKS			
Num Tanks	Fluid(s)	Tank Size	Dry Mass Prop Mass Total Mass (ca)
1	Air tank	10 m by 14 m	19496 kg 20576 kg 121767 kg
	MOC I2		
	TMI H2		
TOTALS			19496 kg 102271 kg 121767 kg

SEI CASE NAME

COMMENTS:
 Veh sketch serves as representation; not definitive of latest configuration. Level II dV set with losses, elliptical orbit, veh expended, shield weight equals engine weight. Single NTP engine operate at 2700K, nozzle area ratio of 400:1 - engine performance = 925 sec ISP.

Figure 2-3b. Data Sheet 2

MARS SEI VEHICLE DATA SHEET
 VEHICLE: NTP Pilead for 150 mt payload class ETO Vehicle
 LAST DATA UPDATE: 102491 launch veh actually delivers 132 mt payload max



Numl Tank	Fluid(s)	Tank Name	Tank Size	Dry Mass (ca)	Prop Mass (ca)	Total Mass (ca)
1	H2	TBE	10 m by 13.0 m	9918 kg	32067 kg	61985 kg
1	MOC #1	MOC #1	10 m by 30.0 m	18300 kg	113500 kg	132000 kg
1	MOC #2	MOC #2	10 m by 8.5 m	5138 kg	31562 kg	36700 kg
1	MOC #3	MOC #3	10 m by 5.0 m	3000 kg	15302 kg	18302 kg
3	TME	TME	10 m by 30.0 m	18500 kg	113500 kg	132000 kg
7		TOTALS		92056 kg	552991 kg	644947 kg

COMMENTS
 Veh sketch serves as representation; not definitive of latest configuration. Level II dV set with losses, 440 d transfer, 90 d stay, elliptical orbits, CRV returns to Earth, veh expended, crew of 6, shield weight equals engine weight. NTP engines operate at 2700K, nozzle area ratio of 400:1 - engine performance = 925 msec lbp.

Surface Payload Mass: 5.7 mt payload to the surface
Departure Orbit: 407 km, 407 km, 28.3 deg

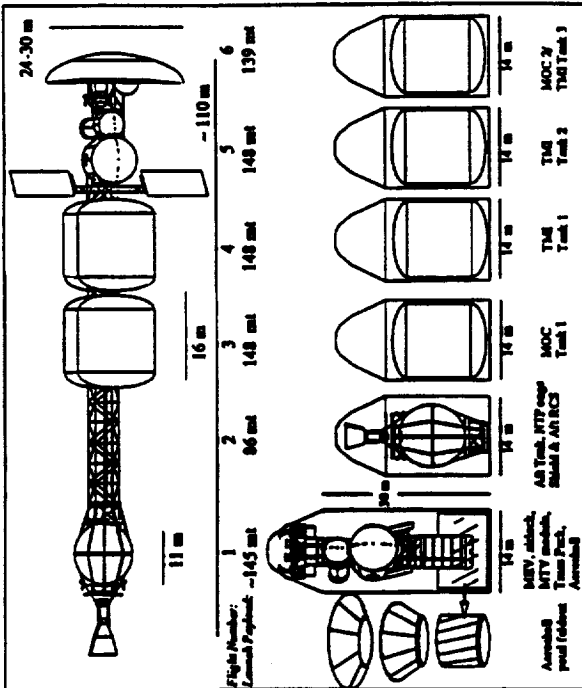
IMLEO: 814800 kg
ENGINE OUT: Single Engines Out
NUMBER OF CREW: 6
MTV: 261949 kg
USABLE PROP. MASS: 552931 kg
PROPELLANT TYPE: Hydrogen
ENG. TYPE/ISP#: NTP - Carbide Fuel Element / 925
VAC THRUST (EA): 75000 lbf
REACTOR MASS (EA): 3402 kg
ELECTRIC CONVERSION CYCLE: --
NOM. PWR LEVEL/PWR SYS MASS: --
LENGTH/WIDTH: --
REUSABLE PARTS (Veh, crew, parts, aft tank, trust, crew mod, airlock): -100 by -30
OTHER: QTY:
INERT MASS: --
USABLE PROP. MASS: --
PROPELLANT TYPE: --
ENG. TYPE/ISP#: --
VAC THRUST (EA): --
LENGTH/WIDTH: --
A/B SIZE/MASS: --
REUSABLE PARTS: --
MEV: 107191.03 L/D, storable, 5.7 ton down cargo w Asc strg, 78,522 kg
INERT MASS: 15,477 kg
USABLE PRO. MASS: 48,670 kg
PROPELLANT TYPE (Descent/Asc): N2O4/MMH N2O4/MMH
ENGINES (Descent/Asc): 4/2
THRUST (EA) (Descent/Asc): 30,000 / 30,000 lbf
ISP (Descent/Asc): 340 sec
LENGTH/WIDTH: 24.30 by 24.30 m (87.5 - (12.5 ft))
A/B SIZE/MASS: 24.30 by 24.30 m (87.5 - (12.5 ft))
REUSABLE PARTS: None

REFERENCES:
 1025/91 Performance/wt statement: Boeing STCAEM B. Doanbu 205/461-3732
 9/10/91 Trajectory/dV set: Level II; g-load plane change dV Boeing STCAEM M. Cuyler
 10/15/91 MEV Performance/wt statement: Boeing STCAEM B. Doanbu
OTHER MASS includes masses Not Included in MTV, OTHER, MEV, Prop Tanks, or Payload. Describe OTHER MASS Below:

Figure 2-3c. Data Sheet 3

MARS SEI VEHICLE DATA SHEET

VEHICLE: NTP Planned for 150 mt payload class ETO Vehicle
 LAST DATA UPDATE: 11/8/91 launch veh actually delivers 148 mt payload



Num Tank	Fluid(s)	Tank Size	Dry Mass (ca)	Prop Mass (ca)	Total Mass (ca)
1	H2	11 m sphere	9918 kg	52067 kg	61985 kg
1	MOC 1	14 m by 16 m	20720 kg	127280 kg	148000 kg
2	TML 1 & 2	14 m by 16 m	20720 kg	127280 kg	148000 kg
1	MOC 2/TMB 3	14 m by 15.5 m	19978 kg	119024 kg	139002 kg
5	TOTALS		92056 kg	529311 kg	641987 kg

SEI CASE NAME

COMMENTS
 Veh sketch serves as representation; not definitive of latest configuration. Level II dV set with losses, 440 d transfer, 90 d stay, elliptical orbits, CRV returns to Earth, veh expended, crew of 6, shield weight equals engine weight. NTP engines operate at 2700K, nozzle area ratio of 400:1 - engine performance = 925 sec/isp.

Surface Payload Mass: 5.7 mt payload to the surface
 Departure Orbit: 407 km 407 km 21.3 deg

IMLEO: 814880 kg
 ENGINE OUT: Single Engines Out
 NUMBER OF CREW: 6
 MTV: QTY:
 INERT MASS: 261949 kg
 USABLE PROP. MASS: 552931 kg
 PROPELLANT TYPE: Hydrogen
 ENG. TYPE/SP/R: NTP - Carbide Fuel Element / 925
 VAC THRUST (EA): 75000 lbf
 REACTOR MASS (EA): 3400 kg
 ELECTRIC CONVERSION CYCLE: --
 NOM. PWR LEVEL/PWR SYS MASS: --
 LENGTH/WIDTH: -100 by -30 m
 REUSABLE PARTS (Veh, tank, Eng, aft tank, truss, crew mod, airlock) QTY:

OTHER:
 INERT MASS:
 USABLE PROP. MASS:
 PROPELLANT TYPE:
 ENG. TYPE/SP/R:
 VAC THRUST (EA):
 LENGTH/WIDTH:
 A/B SIZE/MASS:
 REUSABLE PARTS:
 INERT MASS: 1071791.021 lb, storable, 3.7 mt down entry w/ Asc sig 713,522 kg
 USABLE PRO. MASS: 15,427 kg
 PROPELLANT TYPE (Descent/Asc): N2O4/MMH N2O4/MMH
 ENGINES (Descent/Ascent): 4/2
 THRUST (EA) (Descent/Ascent): 30,000/30,000 lbf
 ISP (Descent/Ascent): 340 sec
 LENGTH/WIDTH: 24.30 by 24.30 m 1775 (113%) kg
 A/B SIZE/MASS: none
 REUSABLE PARTS: none

1072591 Performance/vt statement: Boeing STCAEM B. Donahue 205/461-3732
 9/10/91 Trajectory/AV act: Level II; g-load/plane change dV Boeing STCAEM M. Cripples
 10/15/91 MEV Performance/vt statement: Boeing STCAEM B. Donahue
 OTHER MASS includes masses Not included in MTV, OTHER, MEV, Prop Tanks, or Payload. Describe OTHER MASS Below:

Figure 2-3e. Data Sheet 5

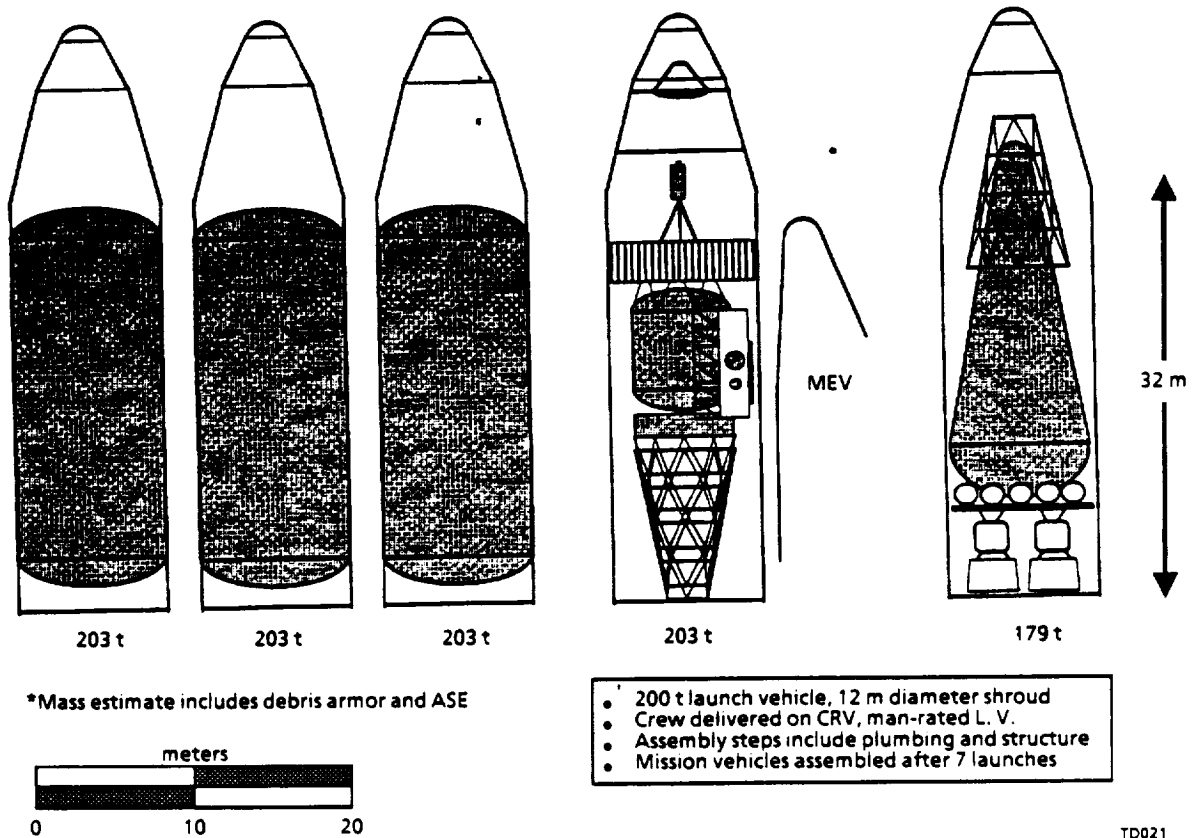


Figure 2-4. Baseline NTP Manifest 12 m Diameter Shroud

Additional work has been done in two areas: (a) the basic packaging of the new NTP vehicle in the 150 t and 250 t ETO, and (b) the shroud size optimization for the new NTP. The first area examined entails analysis of three options for manifest and launch. Two options involve the current NTP vehicle configuration with airborne support equipment (ASE) and debris shields (armor). The third option involves a launch optimized vehicle design that does not use the same criteria as was used in previous NTP configurations. The second part was to determine the optimum length for each of the vehicle shroud sizes based on wind loading on the launch pad. This analysis was begun with initial results presented.

2.1.1 Shroud Packaging

Three basic options for launch of the NTP Mars transfer vehicle have been investigated. These options are based on variations in payload shroud diameter and degree of vehicle assembly done on the ground. All configurations mass take into account debris shields (armor) and ASE packaging mass equal to 13% of the vehicle cargo sections (lofted mass).

The first option describes the baseline NTP vehicle. This vehicle was highly integrated and detailed, and the illustrations reflect the manifesting, figure 2-4. The next option illustrates the baseline NTP concept, including 7.6m diameter transfer habitat and subsystem array, configured for launch within a 14m diameter payload shroud, figure 2-5. The forward section of the vehicle is attached by truss structure to a plumbing manifold, and the vehicle structure consists of stacking truss sections. The shape of the section has been modified to adapt to a new TMI/MOC propellant tank length. The propellant tank length and diameter were changed to better utilize the larger payload shroud. The aft section of the NTP differs from the baseline by using a 14m diameter ellipsoidal TEI propellant tank, and the attached radiation shield and engine assembly are consistent with the baseline concept. On-orbit assembly is achieved by launching a single "core" and assembly platform, and then subsequently mating the TMI/MOC tanks in a four launch procedure, not including crew delivery. As a delta to this option, the payload shroud envelope was sized to include an MEV lander and descent aerobrake. The aerobrake shown folds down and away from the attached MEV, allowing the aerobrake to fit over the forward part of the core, reducing overall shroud length.

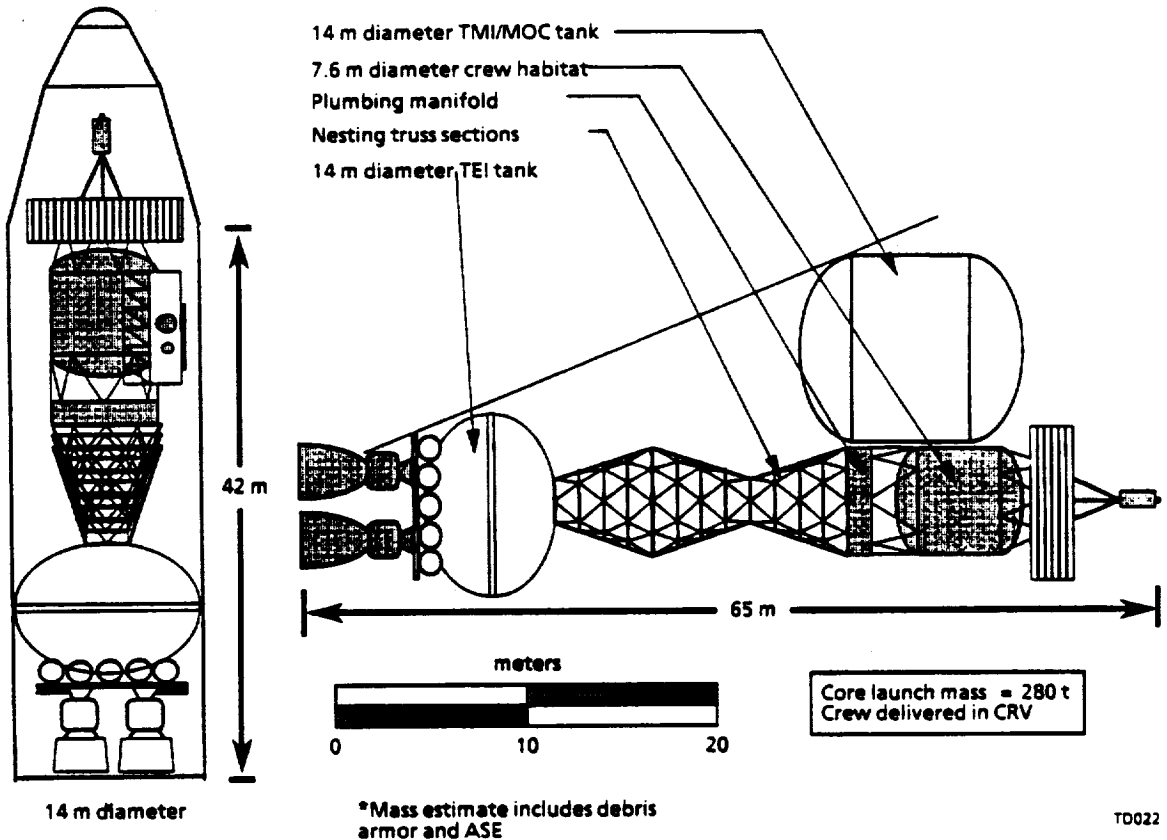


Figure 2-5. Baseline NTP Vehicle Configured for 14 m Diameter Launch Shroud

The last option makes use of current work on Biconic MEV landers, and integrates the "core" of the vehicle with the biconic on a single launch vehicle of 12-m diameter, and 250 tonne lift capacity, figure 2-6. This configuration requires minimal on orbit operations, limited to deployment of a telescoping truss section that extends the nuclear engines and shield approximately 20 meters beyond the forward core. This ensures minimal radioactive "scattering" at the crew habitat. This deployment also requires that plumbing from the manifold be extended and attached on orbit. This operation can probably be accomplished through robotics, and might even be done as part of the truss deployment. This launch option has the advantage of significantly reducing on-orbit assembly, reduces the number of launches to five, and could allow the crew to be launched with the transfer vehicle. However, it accepts radiation heating of the propellant in the drop tanks during the trans-Mars injection burn, a telescoping truss arrangement that still must be more defined to be workable and a Mars orbit ascent stage that is a portion of the piloted biconic nose section. A comparison of these three configurations and two all in one core stage launches, one with the lander/"flower petal" aerobrake and one without are shown in figure 2-7.

2.1.2 Length Sizing by Pad-Wind Loading

A parametric load/deflection analysis was carried out for an optimum payload shroud size selection. Shrouds of varying lengths and diameters were subjected to wind gusts of 50 to 100 kts.

Three shroud lengths were considered:	30m, 42m, 50m
Five shroud diameters were considered:	10m, 12m, 14m, 16m, 18m
Three wind velocities were considered:	50kts, 75kts, 100kts

Assumptions:

 Payload mass (including shroud) = 150 mt

 Launch load = 4g

 Sea Level air density

 Drag coefficient for a cylindrical shape, $C_d = 1.0$

 Shroud material = 7075 Aluminum

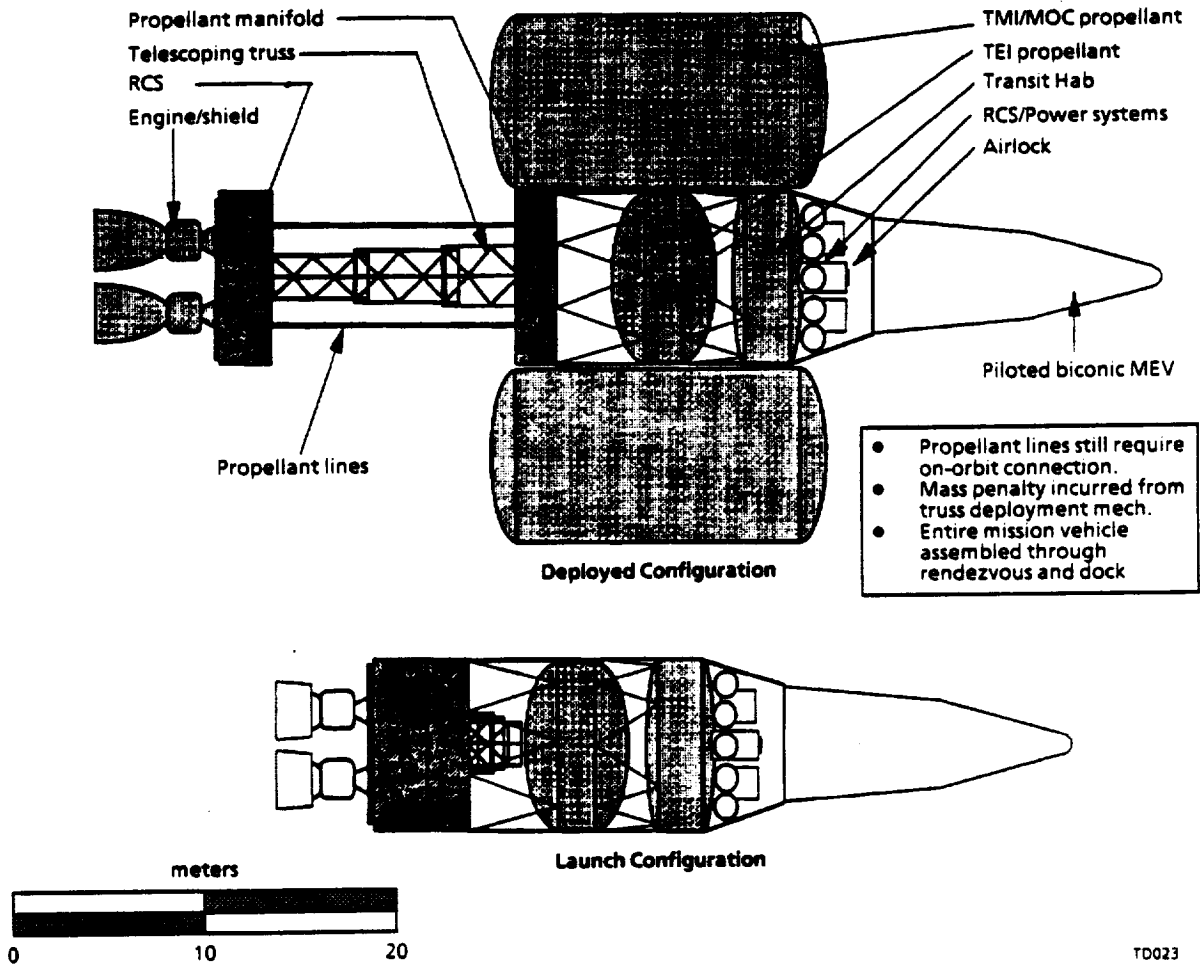
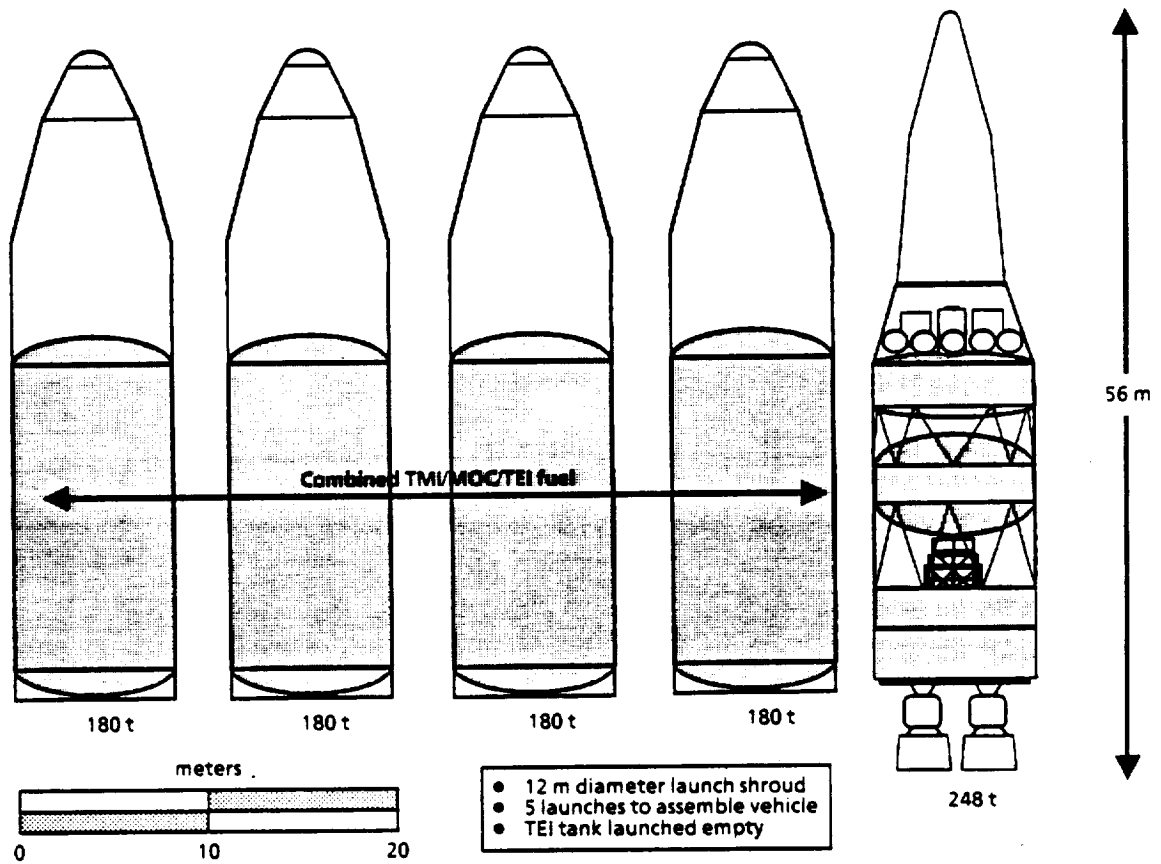


Figure 2-6a. Launch Optimized NTP Vehicle and Biconic MEV (Configuration)

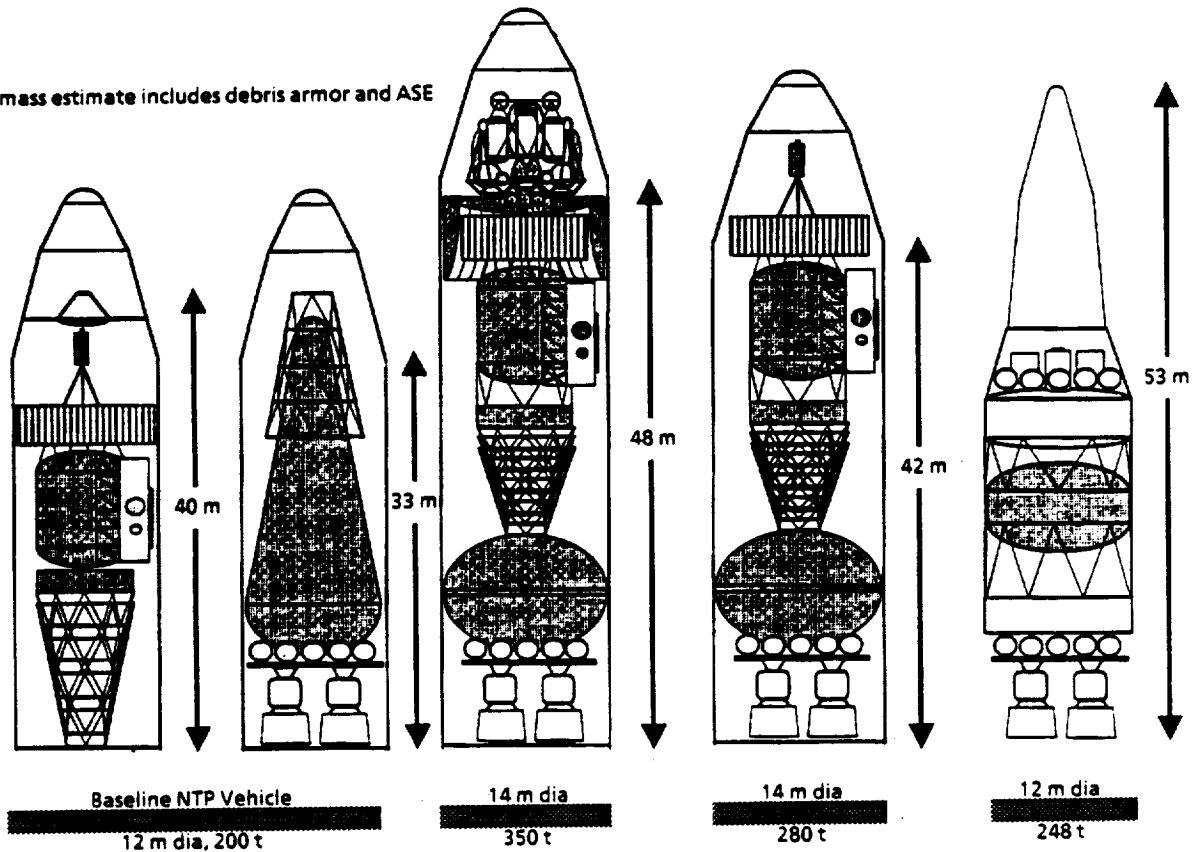


* mass estimate includes debris armor and ASE

T0024

Figure 2-6b. Launch Optimized NTP Vehicle and Biconic MEV (Manifest)

* mass estimate includes debris armor and ASE



TD025

Figure 2-7. Launch Vehicle Comparison

Procedure:

A preliminary sizing for the shroud was performed using 4g launch loading. Skin thickness and moment of inertias were calculated as functions of shroud diameter. Wind loading for each of the three cases (50 kts, 75 kts, and 100 kts) was computed as a function of shroud length and diameter. Maximum deflection was calculated for each variable. The results of these calculations are shown in figures 2-8 and 2-9.

Over the entire range of the parameters studied, the deflections ranged from 0.0023m to 0.1254m. The 30-m long shroud was shown to be the most promising length. It showed almost no change in deflection with varying diameter and very little change with varying wind gusts.

D615-10051

Total Mass = 15000 kg
 Total Load = 5883600 N @ 4g
 Shroud Area = 0.01422396 M²

Aluminum:
 E = 7.1008E + 10 Pa
 σyield = 4.14E + 08 Pa

Shroud Length L (m)	Shroud diameter D (m)	Wind velocity kts	Shroud thickness t (m)	Moment of inertia I m ⁴	Wind loading w (N/m)	Maximum deflection y (m)
30	10	50	0.00045	1.4224	4068	0.0041
	10	75	0.00045	1.4224	9152	0.0092
	10	100	0.00045	1.4224	16270	0.0163
	12	50	0.00038	2.0483	4881	0.0034
	12	75	0.00038	2.0483	10982	0.0076
	12	100	0.00038	2.0483	19524	0.0136
	14	50	0.00032	2.7879	5695	0.0029
	14	75	0.00032	2.7879	12813	0.0066
	14	100	0.00032	2.7879	22778	0.0116
	16	50	0.00028	3.6413	6508	0.0025
	16	75	0.00028	3.6413	14643	0.0057
	16	100	0.00028	3.6413	26032	0.0102
	18	50	0.00025	4.6086	7322	0.0023
	18	75	0.00025	4.6086	16473	0.0051
	18	100	0.00025	4.6086	29286	0.0091
42	10	50	0.00045	1.4224	4068	0.0157
	10	75	0.00045	1.4224	9152	0.0352
	10	100	0.00045	1.4224	16270	0.0627
	12	50	0.00038	2.0483	4881	0.0131
	12	75	0.00038	2.0483	10982	0.0294
	12	100	0.00038	2.0483	19524	0.0522
	14	50	0.00032	2.7879	5695	0.0112
	14	75	0.00032	2.7879	12813	0.0252
	14	100	0.00032	2.7879	22778	0.0448
	16	50	0.00028	3.6413	6508	0.0098
	16	75	0.00028	3.6413	14643	0.0220
	16	100	0.00028	3.6413	26032	0.0392
	18	50	0.00025	4.6086	7322	0.0087
	18	75	0.00025	4.6086	16473	0.0196
	18	100	0.00025	4.6086	29286	0.0348
50	10	50	0.00045	1.4224	4068	0.0315
	10	75	0.00045	1.4224	9152	0.0708
	10	100	0.00045	1.4224	16270	0.1258
	12	50	0.00038	2.0483	4881	0.0262
	12	75	0.00038	2.0483	10982	0.0590
	12	100	0.00038	2.0483	19524	0.1049
	14	50	0.00032	2.7879	5695	0.0225
	14	75	0.00032	2.7879	12813	0.0506
	14	100	0.00032	2.7879	22778	0.0899
	16	50	0.00028	3.6413	6508	0.0197
	16	75	0.00028	3.6413	14643	0.0442
	16	100	0.00028	3.6413	26032	0.0787
	18	50	0.00025	4.6086	7322	0.0175
	18	75	0.00025	4.6086	16473	0.0393
	18	100	0.00025	4.6086	29286	0.0699

Figure 2-8. Windload Data

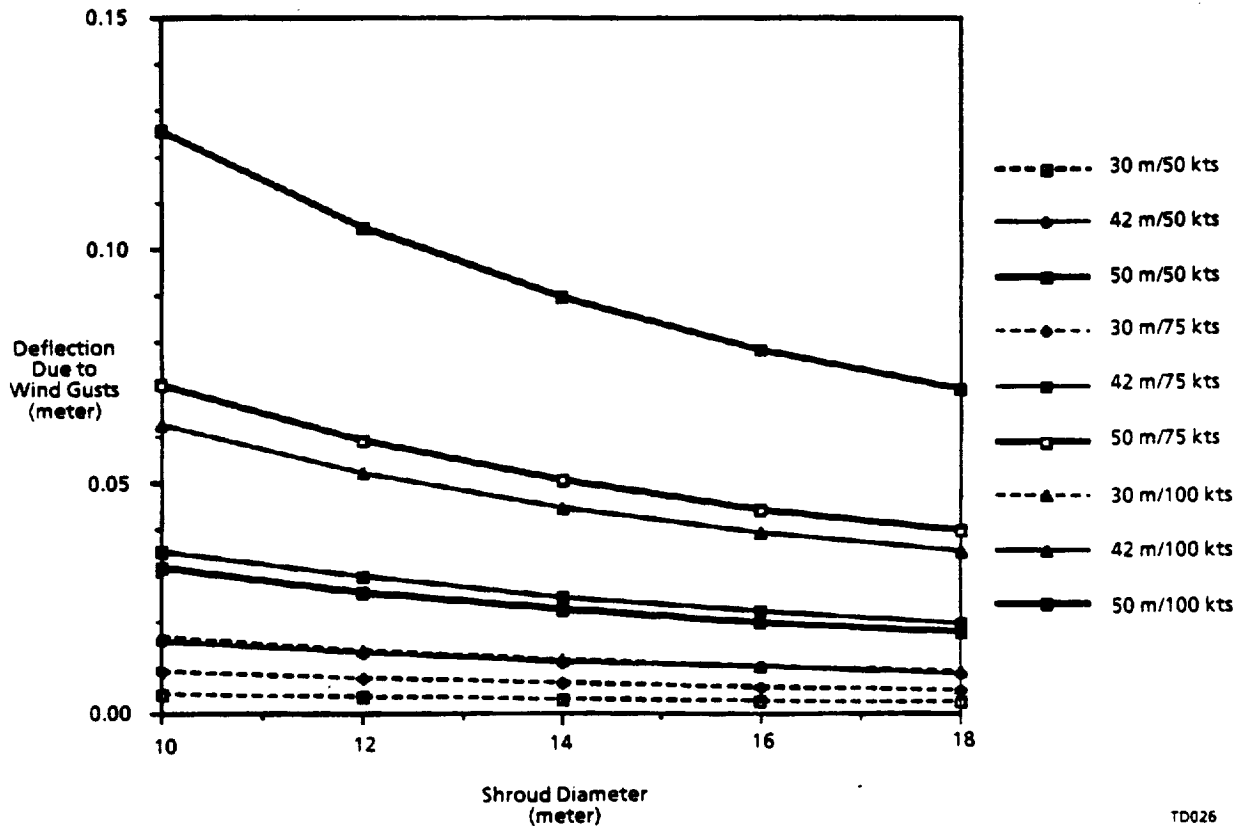


Figure 2-9. Shroud Size Study

2.2 PLATFORM CONCEPTS

Two concepts were investigated for LEO assembly utilities, with the I-beam (figs. 2-10 and 2-11) being a "large dry dock" for the growing NTP vehicle and the Saddle (fig. 2-12) being a "minimum" approach. The I-beam uses none of the NTP resources and, as a redundant resource, it can supply the vehicle with emergency power and communications if required. It is large enough to provide parts storage around the perimeter, decreasing if not eliminating the need for special CTV delivery/retrieval (debris shield) trips. The saddle is a smaller robotics and reaction control system (RCS) platform that uses the vehicle systems as much as possible. It provides maneuver capability to the vehicle before the propellant tanks are in place and the vehicle RCS is active. The robotic assembly walking arms used for assembly are controlled from this platform.

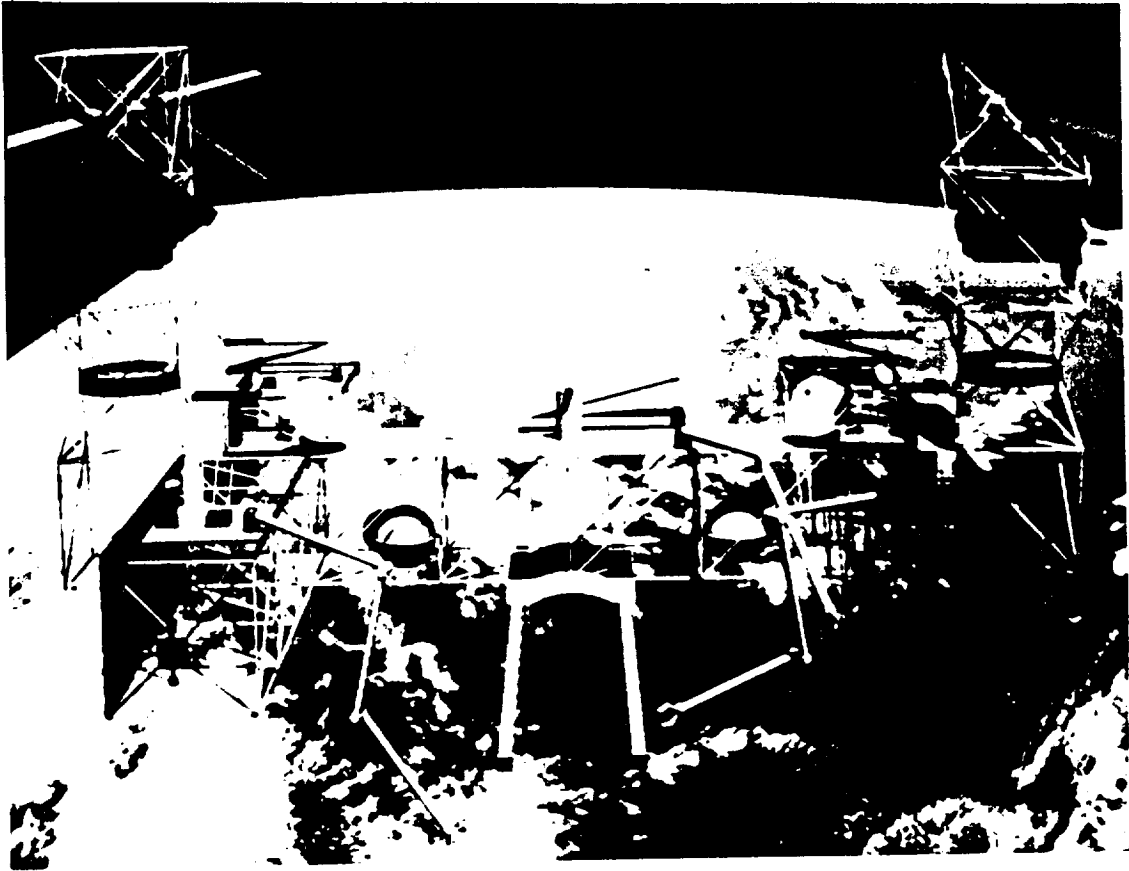


Figure 2-10. MTV Assembly Platform Full-Service Concept

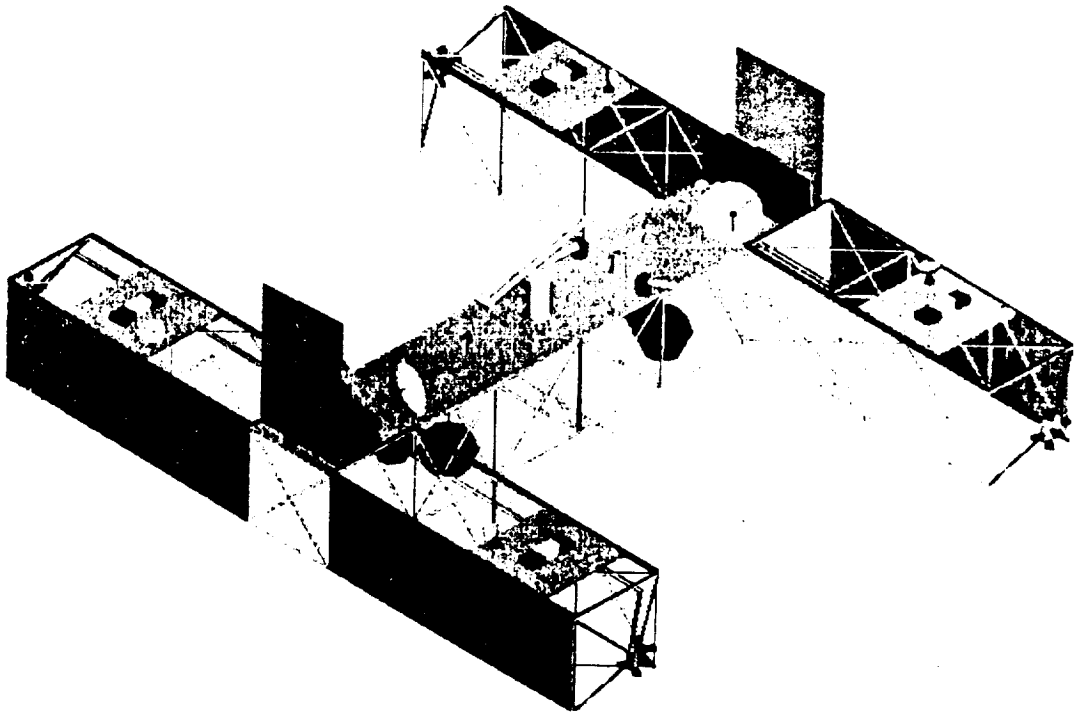


Figure 2-11. NTP Platform Full-Up Configuration

This page intentionally left blank

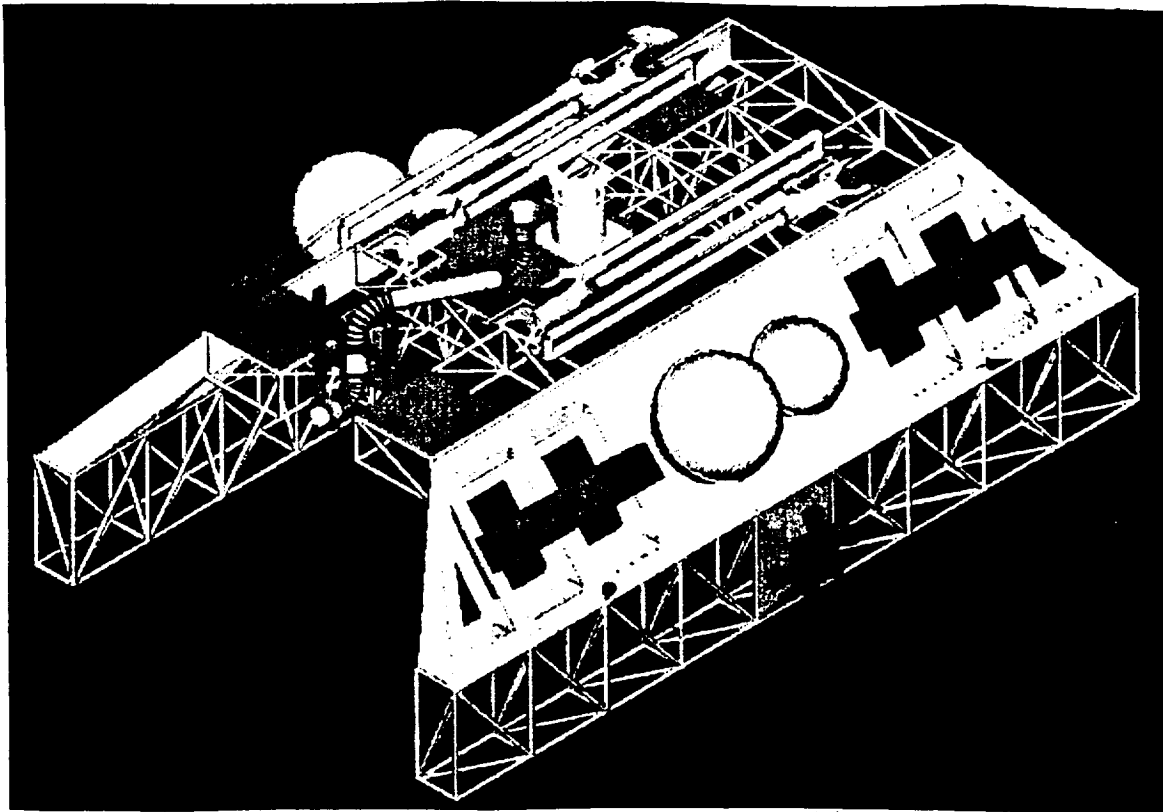


Figure 2-12. Saddle Platform CAD Model

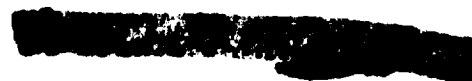
2.2.1 I-Beam Platform

A preliminary I-Beam Assembly Platform Parts List and Weights Statement has been completed. The results of the parts evaluation and the weight estimates are shown in figures 2-13a to 2-13b, Assembly Platform Parts List series.

Item	Item Description	Quantity	Mass	Source	Manufacturer
Solar array system	Photovoltaic arrays with radiators, modified integrated equipment assembly (MIEA), alpha joint, one beta joint, one set of PV arrays (SSF configuration from alpha joint to station 3), 5 m cubic truss	2	23 mt estimated (total)	Old Space Station design	Prime: Rockwell Alternate: TBD
Auxiliary batteries	Additional batteries not in the MIEA	2 sets	1 mt		
Truss structure	5m x 5m x 5m truss cube pattern of 10 cm dia. composite members with conductive wire embedded in the surface for charging control. Entire surface is seven bay end pieces on a 4-bay cross piece.	1 set	17 mt estimated (total)	Old Space Station design	Prime: McDonnell-Douglas Alternate: TBD
Thruster pod	5 thruster grouping of 25-pound thrust GO ₂ /H ₂ thrusters, initially built for the Space Station, manifolded together	4	16 kg each, 0.06t (total)	Old Space Station design	Prime: Rockwell International Alternate:
Propellant lines	Combination of fixed and flex lines of TBD length, that will deploy with the end pieces (flex) and be hardlined to the propellant tanks and thruster pod manifold 1 H ₂ line and 1 O ₂ line	4 sets	42 kg, 0.04t (total)	Current terrestrial design	Prime: Alternate:
Mobile Remote Manipulator System (MRMS)	15 meter "strongarm" used for maneuvering into place large assembly elements. It is on a mobile base that translates the length of the end piece but does not translate the central crosspiece. The base is on a rail system that will be part of the deployed truss.	4	TBD	From Space Station designs	

Figure 2-13a. Assembly Platform Parts List (I-Beam)

This page intentionally left blank



Item	Item Description	Quantity	Mass	Source	Manufacturer
GO ₂ tank and gas	Insulated tank, 2 meter dia., that can be removed and replaced	2	0.249t (197 kg each)	Space Station	Prime: Pressure Systems Inc.
GH ₂ tank and gas	Insulated tank, 2.7 meter dia., that can be removed and replaced	2	0.510t (255 kg each)	Space Station	Prime: Pressure Systems Inc.
Propellant Manifold	Manifold that allows one tank set to feed two thruster pods	2			
Control Moment Gyros (CMG)	Station keeping and position sensing	8	50 kg (total)	Current Available	Prime: Ithaco Alternate: TBD
Antennae:					
High Gain	Ground, SSF, and CTV com. 2.7 m dia.	2	0.2t (total)	Similar Pioneer upgraded electronics	
Omni-Directional	backup communications, 1 meter	4	0.04t (total)	TDRS/Comm. sats.	
Robot/Data	Visual, digital 1 meter dia.	2	0.12t (total)	Com. Sats.	
RF	Proximity operations, robot control 46cm by 23 cm cone	6	0.12t (total)	Com. sats., exploration vehicles	
Fixed Remote Manipulator System (FRMS)	12-meter arms fixed to the central crosspiece that will be used to guide in the HLLV cargo to the docking port, help remove the cargo and hand it off to the MRMS for assembly or storage	2	TBD	From Space Station/Space Shuttle designs	
Robot Walker	A TBD sized, self-contained system with dexterous manipulators that can "inchworm" itself along the platform, vehicle and HLLV to assist in actual assembly, component removal/storage and fine manipulation work	2 to 4	TBD	Various current walker designs (MacDonnel-Douglas, Carnegie-Mellon, etc)	
Power distribution net	Power distribution system that will handle the power demands from the temporary arrays for initial deployment, and any other functions not covered by the MIEAs in the permanent array package	2	2.0t (1.0 t ea. all electronics, cabling & shielding)	Standard requirement	
Data management system (DMS)	Handles communication linkage, robot control, data linkage, sensor system identifications,	2	1.5 t (.75 ea.)	Standard requirement	
Power switching unit (PSU)	Handles power switching during occultation that is not handled by the MIEAs in the permanent array package, and all switching with the temporary arrays	2	0.5 t (250 kg each)	Standard requirement	

Figure 2-13b. Assembly Platform Parts List (I-Beam)

Item	Item Description	Quantity	Mass	Source	Manufacturer
Berthing port	Standard berthing port on a 2-meter standoff for docking the HLLV to the platform	1	0.1 t (100 kg each)	Space Station	
Lighting/camera post	Swivel mounted camera and lighting assembly on a 1-meter post for wide angle observations	2	0.2 t (100 kg each)		
Temporary arrays	Small deployable/retractable arrays that will power the initial platform deployment. Each array has 2 panels 2 meters by 25 meters	2	0.4 t (200 kg each)		
Initial deployment mechanism (IDM)	Jackscrew/telescoping mechanism that pushes out the folded end pieces to deploy them on the initial flight	4	3.0 t (750 kg each)	Extendible exit cones, SSF deployment strategies	
Rail crawler	Supporting undercarriage that will extend a pulling mechanism that will work in both direction along the rails (forward and back)	1	5.0 t	SSF RMS translation strategies	
Rails	44.5 meter segmented rails that will be fitted along the truss of the vehicle (makes the platform independent of truss configuration), which will allow the platform to translate the vehicle for assembly. The rails are segmented to allow the removal of several sections to clear the tank installation area	2 (one set)	4.0 t (both rails)		
Outside panels	Lightweight paneling (Al/composite?) that will be set up with attachment points for part storage	14 maximum (5m x 5m) 12 nominal	14.2 t for 12		

Figure 2-13c. Assembly Platform Parts List (I-Beam)

2.2.2 Saddle Platform

The Saddle Platform design has been completed with a parts list/weights statement for this assembly platform configuration. A 1/200 scale drawing of the saddle platform on the first vehicle element as launched is shown in figure 2-14 and in more detail in figure 2-15. This platform will have four mobile (inchworm type) remotely controlled robotic arms (fig. 2-16) that grapple, carry and offload the payloads, disengage the packed major elements, manipulate them into position and perform the element attachments. It will additionally serve as the LEO reaction control system for the maneuvers that must be performed in order to station keep and co-orbit with the SSF. Its third main task is to provide a platform to perform top-off refueling of the full up vehicle prior to Mars departure. Communications for these operations is provided by six RF antennae with communications packages, one for each arm and each function (position communications and telemetry). One small one-meter antenna was added as a visual data and communications control link. Any additional storage needs not provided in the spaces of the platform truss (debris shielding) will be transferred to and from a CTV docked at the central berthing port. The platform will ride on a set of extending rails that run the length of the vehicle core (from the MCRV connection point to the beginning of the aft tank diameter expansion) that will allow access to the full extent of the core assembly points and clear the tank connection areas. Sketches of the Saddle platform have been made and the CAD model generated in figure 2-12. A mass statement for the saddle platform giving the expected mass for each of the vehicle parts with a 30% total mass growth is listed in figure 2-17.

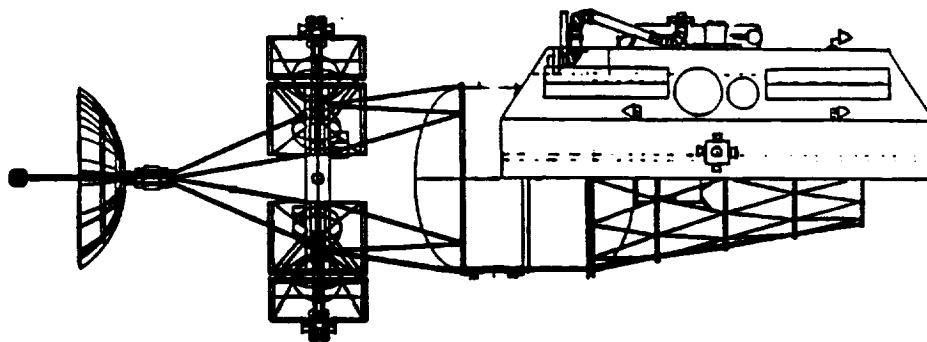


Figure 2-14. Saddle Assembly On Vehicle Core

TD030

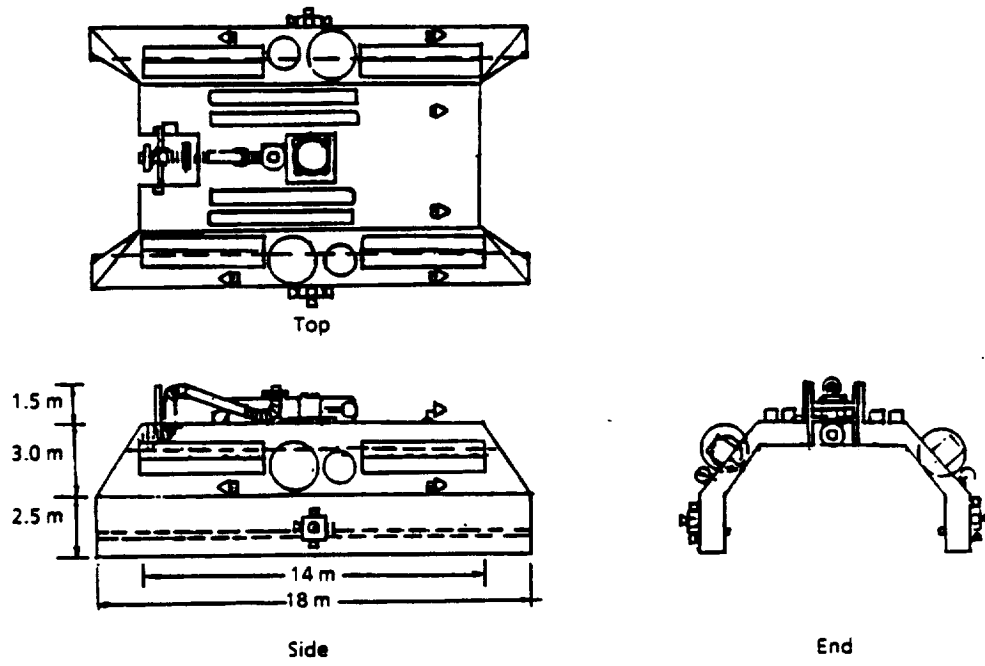


Figure 2-15a. Saddle Assembly Platform

TD031

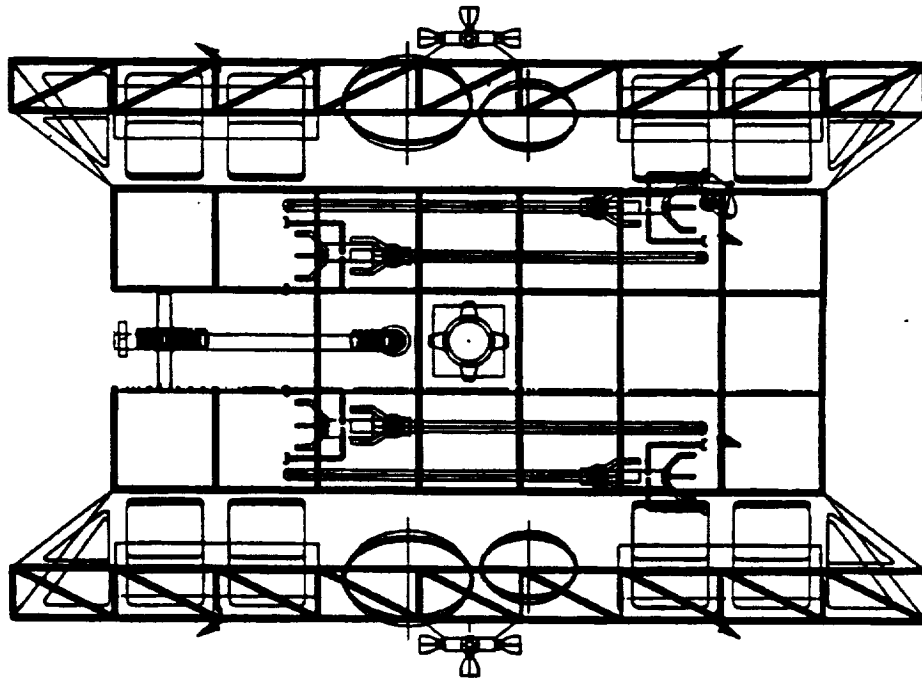


Figure 2-15b. Saddle Platform: Top View

TD032

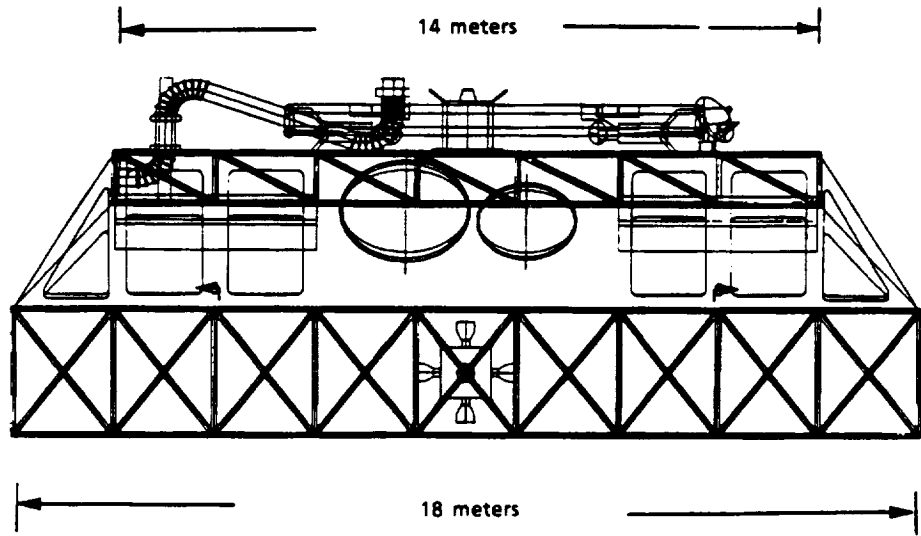


Figure 2-15c. Saddle Platform: Side View

TD033

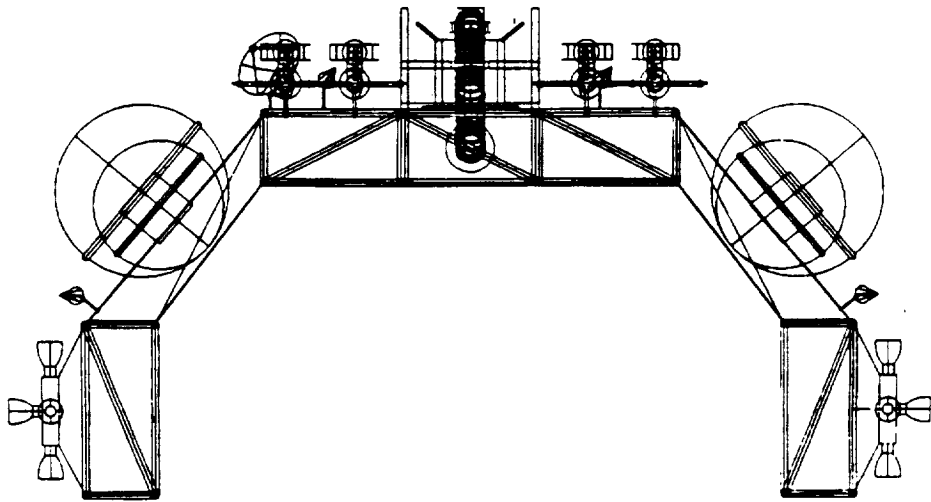


Figure 2-15d. Saddle Platform: End View

TD034

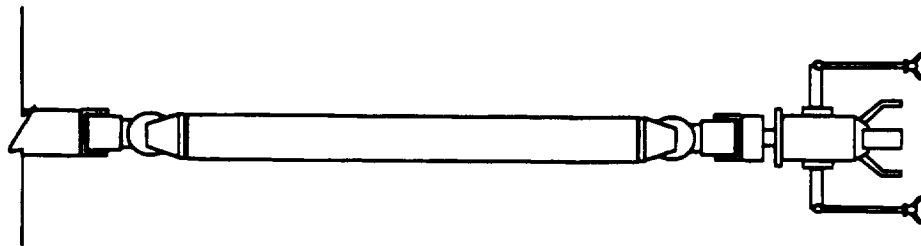


Figure 2-16. Robotic Arm Detail

TD035

Item	Item Description	Quantity	Mass
Antennae	Communications between ground, SSF, vehicle, platform and the walking robots	6	0.12 t total
Walking robotic arms	12-meter inchworm type arms with self-contained batteries and vehicle power connections used for manipulating major vehicle elements and performing fine connections	4	2.4 t total
Fueling section	Plumbing, flange and "pumping" facility for transferring top-off propellant from an HLLV to the vehicle	1	0.5 t
Platform structure	Assembly platform basic structure, of trusswork, assembled on the ground and launched fully configured (hard lined) with the first launch element	1	6 t
Berthing port	Keyed passive berthing port to allow the docking of a CTV, CRV or HLLV payload at the platform	1	0.1 t
Vehicle com. bus	Data, communications and power transfer connection between the vehicle and the platform	2	0.2 t total
Rail system	Extending rail segments that allow the assembly platform to translate up and down the vehicle	2 rails	4 t
Solar arrays	Small 6 x 20 meter arrays used to give power to the saddle platform and charge the robotic arm batteries.	4	5t total
MIEA	Modified Integrated Equipment Assembly which will act as a power distribution, switching and integration system	2	600 kg total
Auxiliary batteries	Additional power storage and emergency supply source	1 set	600 kg total
Thruster pods	Attitude control propulsion system, consists of 5 thrusters in a manifold for each pod assembly	2	32 kg total
Propellant lines	Fixed lines from the GO ₂ and GH ₂ tanks to the thruster pods	2 sets	10 kg total
GO ₂ tanks and gas	Gaseous oxygen propellant oxidizer	2	0.349 t total
GH ₂ tanks and gas	Gaseous hydrogen propellant fuel	2	0.510 t total
Crossfeed propellant manifold	Crossfeed manifold for the propellant lines to permit both propellant tank sets to supply both thruster pods	1	0.1 t
CMGs	Control moment gyros for station keeping and position sensing	4	25 kg total
Total Mass			20.546 t

Total mass estimate with a 30% growth ~ 2671 t

Figure 2-17. Saddle assembly platform parts list

2.3 METEOROID/ORBITAL DEBRIS PROGRAM (MOD)

Debris shield mass trades for probability of no penetration (PNP) in LEO orbit have been made using the Meteoroid/Orbital Debris Simulation Program (MOD). Several simulations were done for debris shields over the habitat, central tanks and aft tank-engine assembly in PNP versus shield mass. These data were based on the worst possible case of a 6 year on-orbit stay time (from 2010 through 2016) with a target .99 PNP, and were used in the calculation of lofted mass in section 2.1 on packaging and sizing. They were the heaviest expected configurations.

Reducing the on-orbit stay time did lighten the expected mass. Data for the aft tank-engine assembly, a central tank and habitat with the input conditions for one years LEO residence are given in figures 2-18a through 2-18c. The knee of the PNP versus Shield Mass cure is shown in these figures, but the minimum acceptable mass has not been pinpointed. Reevaluating the data for the currently recommended PNP of .95 will lighten the expected shield mass even further.

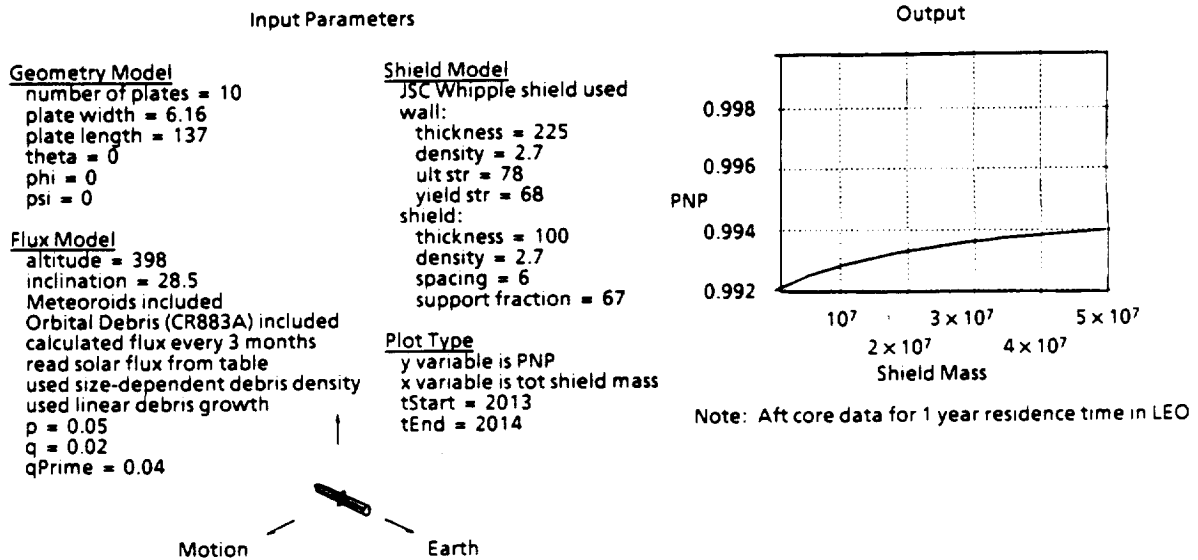


Figure 2-18a. LEO Debris Shielding Model-1

TD036

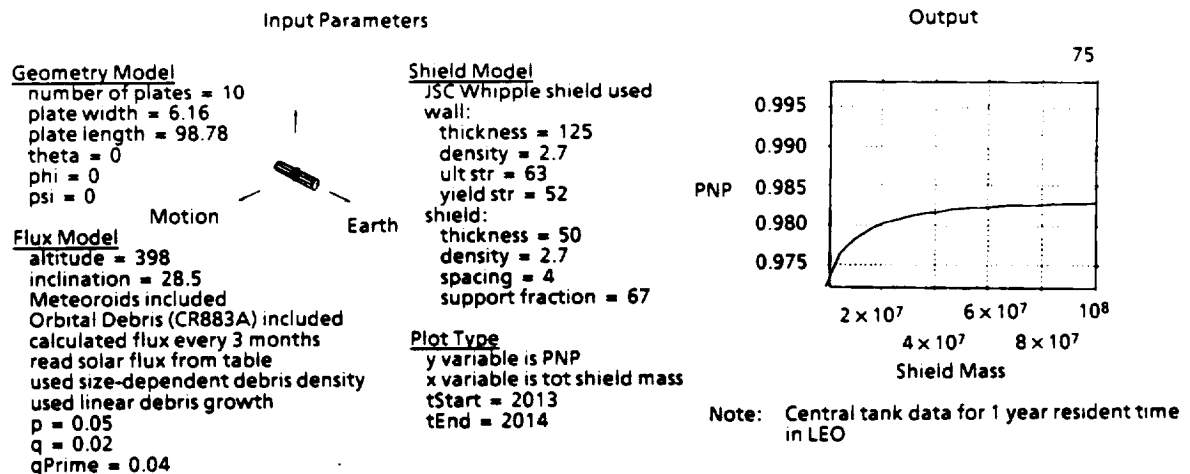


Figure 2-18b. LEO Debris Shielding Model-2

TD037

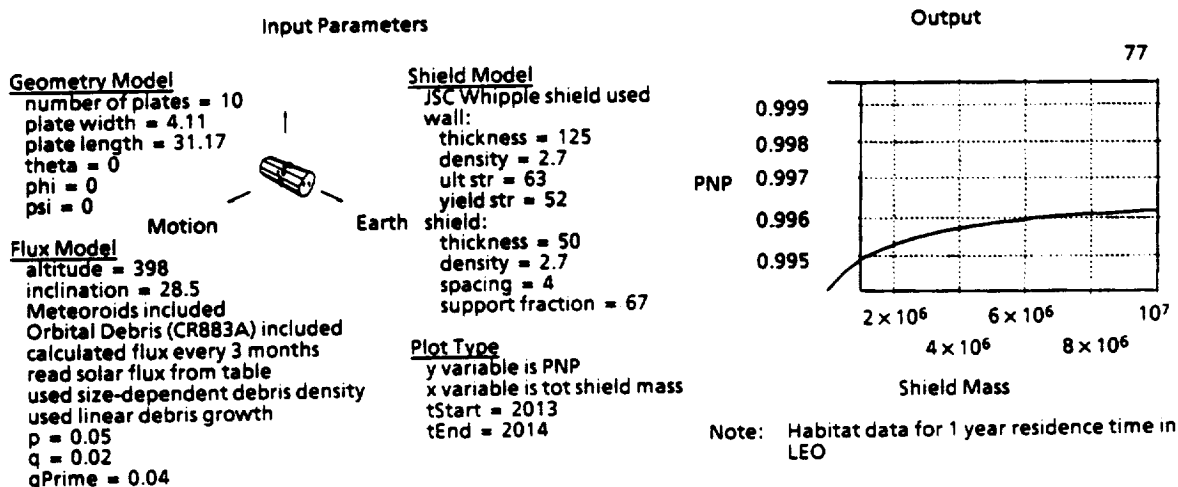


Figure 2-18c. LEO Debris Shielding Model-3

TD038

2.4 DELTA-V AND DESCENT ANALYSIS

2.4.1 Introduction

Analyses and results shown in this section were in direct support to nuclear thermal propulsion-Mars transportation system sizing efforts. The topics include:

- a. Delta-V Sets
- b. Mars parking orbit descriptions
- c. 2016 TEI delta-V reduction
- d. Low-L/D landing site access
- e. High-L/D landing site access
- f. Nuclear reactor disposal.

2.4.2 Delta-V Sets

Mission delta-V profiles are required as data input to vehicle sizing algorithms. The delta-V data provided in sections 2.4.2.1 and 2.4.2.2 represent distributed minimum energy trajectory data derived from patched conic algorithms. Section 2.4.2.1 describes Boeing optimized trajectories where the parking orbits are minimum delta-V, elliptical and the transfers times are of intermediate durations. Section 2.4.2.2 describes delta-V data for NASA Level II mission dates with Boeing optimized elliptical parking orbits and of significantly faster transfer times as compared to the Boeing transfers. The net results of faster transfer times is essentially higher energy missions. Section 2.4.2.3 provides data indicating reserves, losses, midcourse contingencies, and reactor cool-down budgets. These off-nominal fuel requirements increase the end-to-end mission delta-V.

2.4.2.1 2012-2020 Mission Delta-V Data, Boeing

Boeing generic mission data and delta-V components for the opportunity years 2012 through 2020 are provided in figure 2-19. Mission data provided includes gravity, plane change, and apsidal rotation losses. An in-plane capture with a periapsis-to-periapsis transfer is assumed for MOI with the exception of the 2016 mission. The 2016 mission includes an off-periapsis MOI maneuver to reduce the TEI delta-V (see section 4).

Mission type	Launch date	TMI* ΔV	Outbound (days)	MOI* ΔV	Mars Stay - time (days)	TEI* ΔV	Return (days)	Return V _{inf} *	Mission Duration (days)	Total ΔV	Abort Type
Cargo 1	11/9/11	3960	300	982	---	---	---	---	300	4942	---
Cargo 2	12/4/13	3988	294	1184	---	---	---	---	294	5172	---
Piloted 1	1/17/14	4318	175	3457	100	3840	290	5482	565	11595	---
Abort Option 1	1/17/14	4318	175	---	flyby	1224	376.6	5166	552	5714	flyby
Abort Option 2	Piloted 1 has sufficient delta-V budget for abort from surface of more than 50 days before nominal departure										surface
Piloted 2**	3/14/16	4152	170	2200	610	1720	150	8072	930	8072	---
Abort Option 1	3/14/16	4152	170	---	flyby	1776	275	5484	445	5922	flyby
Piloted 2***	2/25/16	4022	157	3790	575	3680	160	8997	907	11492	---
Abort Option 2	2/25/16	4022	157	4060	31	3740	246	7200	434	11822	surface
Piloted 3	5/26/18	4034	170	1340	610	2000	150	3585	930	7374	---
Abort Option	5/26/18	4034	170	---	flyby	2551, 1549†	312	7066	482	8134	flyby
Piloted 4	7/13/20	4205	170	1620	600	2434	150	6539	920	8259	---
Abort Option	7/13/20	4205	170	---	flyby	1599	346	7033	516	5624	flyby
Average for piloted missions	4150	168	2510	600	2370	245	6500	670	8400		

NOTE: TMI g-loss = 300 m/s, MOI g-loss = 50 m/s, TEI g-loss = 30 m/s, TMI worst plane change = 400 m/s for 2014 and 100 m/s for 2016 - 2020.

- * Delta-V and V_{inf} are in the units of m/s.
- ** Optimized for a Mars flyby abort.
- *** Optimized for an abort from surface within 31 days of arrival.
- † Deep space maneuver of 1549 on 5/5/19.

Figure 2-19. 2012 - 2020 Mission Delta-V Data

The mission data divided into the categories of cargo missions 1 and 2 and piloted missions 1 through 4, along with their related abort mission options are shown in figure 2-19. In addition to the above mentioned data categories, an average is provided for delta-V, transfer times, stay times, Earth return V-infinity, and mission duration. The average Mars stay time was not computed with the short stay 2014 missions and abort option 2 stay time for the 2016 mission. General ground rules that were followed in analyzing the mission opportunities described in figure 2-19 are given below:

- a. If a swingby can be found, aborts utilize a Venus swingby (VSB) on Earth return to reduce mission delta-V requirements.
- b. If no VSB can be found on Earth return leg of abort, then a deep-space maneuver on return is utilized to reduce mission delta-V.
- c. In the effort to analyze only intermediate fast transfers times, no missions with transfer times of less than 150 days were analyzed. Intermediate transfer times have a moderate impact on the total delta-V budget.

Cargo Missions. Cargo mission 1 supports the 2014 piloted mission 1, and cargo mission 2 supports the 2016 piloted mission 2. Cargo mission 2 arrives at Mars while the 2014 mission astronauts are on the surface of Mars. Thus, the cargo supporting the 2016 mission could be used to support the 2014 crew in the event of an emergency. The cargo missions are minimum energy conjunction style missions with transfer times of approximately 300 days and delta-V of about 5000 m/s. These cargo missions are close to the lowest energy missions possible for their concomitant opportunity years.

2014 Piloted Mission. Piloted mission 1 is an opposition style mission with a relatively short stay time of 100 days nominal and a total delta-V requirement of 11595 m/s. This 2014 mission is, within Synthesis architecture 1, the first piloted mission and is slated as an opposition style mission. The Earth return trajectory utilized a Venus swingby in route, lowering the Earth return Vhp and lowering the Mars TEI delta-V. This mission has the necessary delta-V budget required for an early return of greater than 50 days before the nominal Earth return date. The 2014 opportunity scenario and corresponding delta-V set was used to size the Boeing Mars transportation vehicle and is considered the reference opportunity.

2016 Piloted Mission. Piloted mission 2 is launched during the 2016 opportunity date and has two options, viz. 2** and 2***. The first option is a conjunction type mission with the relatively long Mars stay time of 610 days and a total delta-V of 8072 m/s. This mission option was optimized for a Mars flyby abort and therefore does not have the delta-V capability for an abort from orbit or surface. The aborted mission profile for piloted 2** is designated as abort option 1 and indicates a lowered total delta-V of 5922 m/s, which is in part attributed to no occurrence of a capture maneuver in a flyby abort scenario.

In the case of the 2016 piloted 2***, the mission was optimized for an abort from surface requirement, reflected in the much higher total delta-V as compared to the 2** mission. The delta-V requirement for this mission is 11492 m/s for a successful mission (no abort is required). If an abort from surface is necessary, the total delta-V required is

11922 m/s for an abort within 31 days of Mars arrival. This mission can also be considered as the first piloted mission of Synthesis architecture 4, (Reference 3) following an opposition type profile with a short stay time of 31 days and having an indigenous early departure capability corresponding to the 2014 opposition mission abort capability. An early return of the Synthesis architecture 4 opposition mission could occur any time within the 31 days of nominal Mars stay time.

2018 Piloted Mission. Piloted 3 corresponds to a 2018 conjunction style mission with a Mars stay time of 610 days and a total delta-V of 7374 m/s. This total delta-V is the lowest mission delta-V of the four mission opportunities analyzed, reflecting the over all "easy" opportunity year of 2018. No Venus swingby opportunity could be found for the 2018 return trajectory to aid in lowering the delta-V requirements for an aborted mission. This mission was thus optimized for a flyby abort capability with a deep-space maneuver of 1549 m/s on 5/5/19 during the Earth return trajectory. The deep-space maneuver can be thought of as replacing the gravity assist that could be provided by Venus if the planetary geometry was right for a Venus swingby on the 2018 return leg.

2020 Piloted Mission. Piloted 4 corresponds to a 2020 conjunction style mission with a Mars stay time of 600 days and a total delta-V of 8259 m/s. There was no counterpart mission provided by Level II (see the following section of Level II missions). This mission was analyzed and optimized only for a flyby abort scenario, but a Venus swingby opportunity does exist on the Earth return trajectory and could be analyzed.

2.4.2.2 Reference Delta-V Set, Level II

Level II mission data and delta-V components for the opportunity years 2012 through 2018 are shown in figure 2-20. Mission data provided includes gravity, plane change, and apsidal rotation losses. An in-plane capture with a periapsis-to-periapsis transfer is assumed for MOI. In the next to the last column, a comparison is made to indicate savings that may be realized with elliptical vs circular parking orbits: elliptical orbit can save over 1 km/s in delta-V over circular orbits for the same Level II mission opportunity dates.

Architecture ref.	Opportunity year/type	Maneuver/ dates	Level 2 ideal delta-V	Finite burn loss	Plane change loss	Elliptic orbit savings	Elliptic orbits delta-V
1	2012 cargo conjunction	TMI 11/28/11	3653	300	100	N/A	4053
		MOC 8/6/12	2538	50	N/A	1198	1340
1	2014 crew opposition	TMI 2/1/14	4127	300	100	N/A	4627
		MOC 7/1/14	5299	50	N/A	1259	4090
		TEI 9/29/14-12/4/14	4370	30	72	1042	3430
1	2014 cargo (for 2016)	TMI 1/17/17	3808	300	100	N/A	4208
		MOC 8/29/14	2802	50	N/A	1192	1660
1	2016 crew conjunction	TMI 4/11/16	4958	300	100	N/A	5358
		MOC 8/08/16	4700	50	N/A	1120	3630
		TEI 5/19/18-8/17/18	4212	30	37	989	3290
4	2016 crew opposition	TMI 3/12/16	3789	300	100	N/A	4189
		MOC 8/04/16	4685	50	N/A	1175	3560
		TEI 9/23/18-5/11/17	5454	30	54	-32	5570
1 & 4	2018 crew conjunction	TMI 6/18/18	4615	300	100	N/A	5015
		MOC 10/01/18	3916	50	N/A	976	2990
		TEI 8/8/20-11/1/20	5309	30	46	703	4606

Figure 2-20. Reference Delta - Set, Synthesis Report

2.4.2.3 2014 Reserves, Losses, Mid-course

A delineation of the 2014 reference mission excess fuel requirements is shown in figure 2-21 and provides additional information concerning the end to end delta-V budget that was used in sizing the Mars transportation vehicle. Those requirements are indicated as reserves, losses, midcourse, and reactor cool down. For reserves and reactor cool down, the excess fuel requirements are provided as a percentage of the total applicable maneuvers.

	Explanation	ΔV (m/s)	Comments
Reserves	Provided for contingencies	---	2% of maneuver TMI, TEI descent, and ascent
Reactor cooldown	NTP operational requirement	---	3% of maneuver TMI, MOI, and TEI
Midcourse	Correction for TMI, MOI, TEI, and Venus swingby	10	Provided by RCS; recharges each 15 to 20 days. Use main engine if greater ΔV needed
Losses	g-loss estimates	50 30	~ on MOI ~ on TEI These values will be updated by numerical integration
	Parking orbit plane and apsidal	263	Losses on arrival and departure from parking orbit

Figure 2-21. 2014 Reserves, Losses, Midcourse

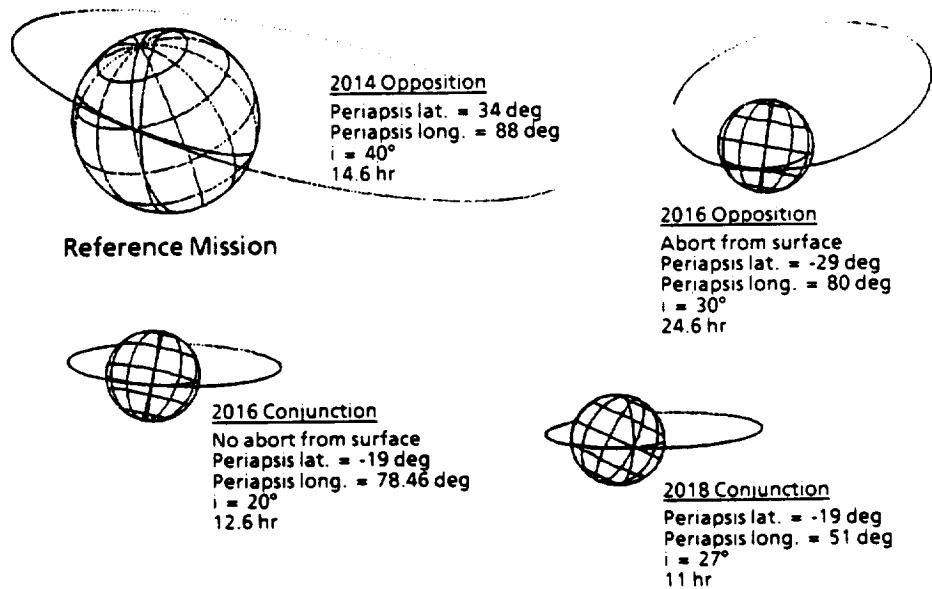
2.4.3 Mars Parking Orbit Descriptions

An end-to-end minimum energy mission requires the optimization of the Mars parking orbit, in addition to optimizing the interplanetary trajectories (minimum energy means lowest energy missions relative to particular transfer dates and times that have been chosen as "fast", i.e., Mars direct transfers from 90 to 170 days). Minimum energy elliptical parking orbits will generally vary widely in period, inclination, periapsis latitude, and periapsis lighting from opportunity year to opportunity year. This variation

in parking orbit as a function of opportunity year is described in section 2.4.3.1. A comparison of elliptical and circular parking orbits for Boeing and NASA Level II missions, emphasizing that circular parking orbits are significantly higher in mission energy requirements is described in 2.4.3.2.

2.4.3.1 Parking Orbits Depictions

Depicted in figure 2-22 are Mars parking orbits for the piloted missions 2014 through 2018. The 2016 opposition mission is included to satisfy architecture 4 of the Synthesis report. For each parking orbit, the inclination, period, periapsis latitude, and periapsis longitude has been chosen to minimize the Mars departure delta-V and provide daylight landing over a range of latitudes. That range of latitudes chosen is between 20 degree north or south of the Martian equator, due to the potential of scientifically interesting areas.



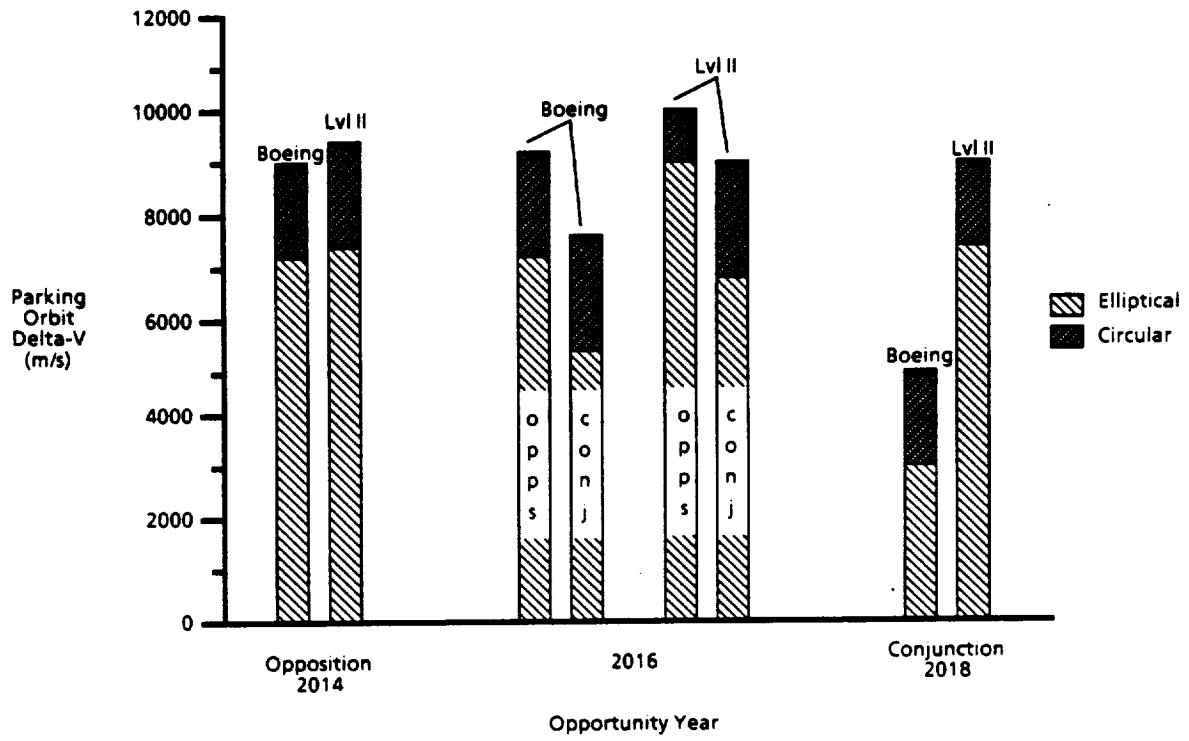
TD039

Figure 2-22. Mars Parking Orbits

2.4.3.2 Parking Orbit Delta-V

Provided in figure 2-23 is a comparison of circular with elliptical parking orbits for Boeing generic missions and the NASA Level II missions. Comparisons are made for the 2014 and 2016 opposition (short Mars stay time) missions as well as the 2016 and 2018 conjunction (long Mars stay time) missions. The delta-Vs are found from the sum of MOI and TEI for the mission opportunity dates indicated in figures 2-19 and 2-20. As shown in

figure 2-23, optimized elliptical Mars parking orbits can require 1 to 2 km/s less delta-V than corresponding circular Mars parking orbits.



Elliptical parking orbits require 1000 to 2000 m/s less delta-V than circular parking orbits.

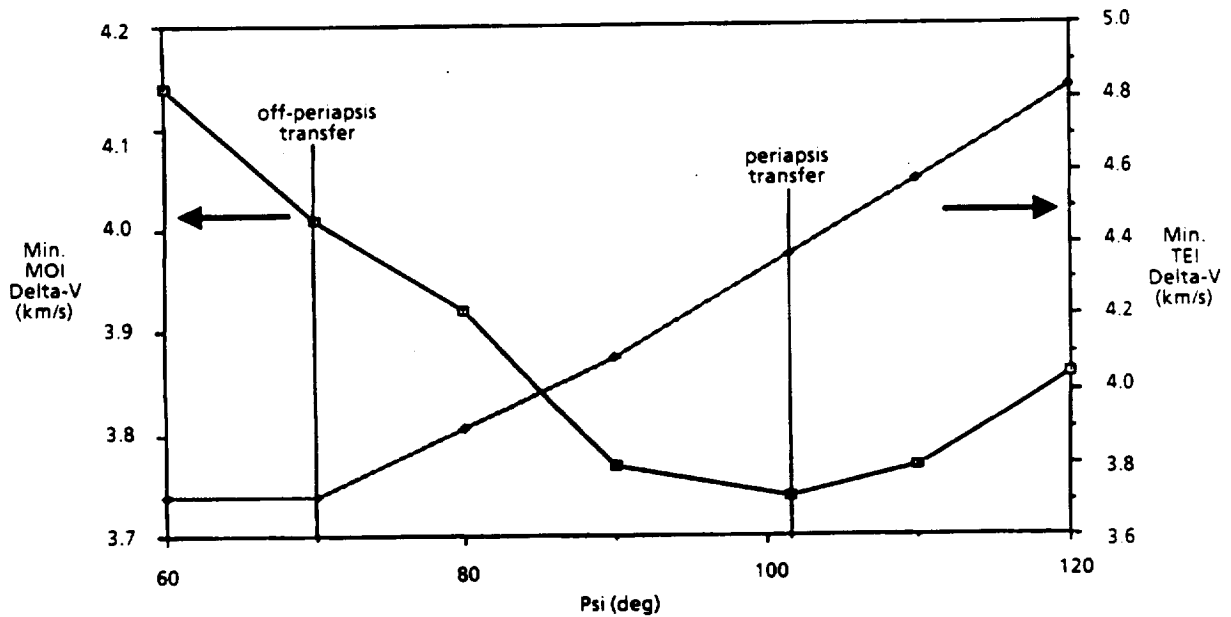
Figure 2-23. Parking Orbit Delta-V

2.4.4 2016 TEI Reduction

The 2016 opportunity for Synthesis Architecture 1 is a long stay conjunction mission (Boeing's 575 day stay) designed with relatively fast transfers, reducing the astronaut exposure to harmful space radiation. This mission also has the requirement to provide vehicle performance allowing for an early return (abort) within approximately 30 days from Mars arrival. It should be noted, however, that the NTP Mars transportation system has been baselined on the 2014 opposition (short stay time) class mission. With the intent of assuring the 2016 TEI performance requirement matches or is less than the requirements of the 2014 TEI stage, analysis was performed showing that the 2016 TEI delta-V could be reduced to the level of the 2014 mission TEI delta-V. The results of this TEI delta-V reduction analysis are shown in sections 2.4.4.1 and 2.4.4.2.

2.4.4.1 Analysis Parameters and Procedure

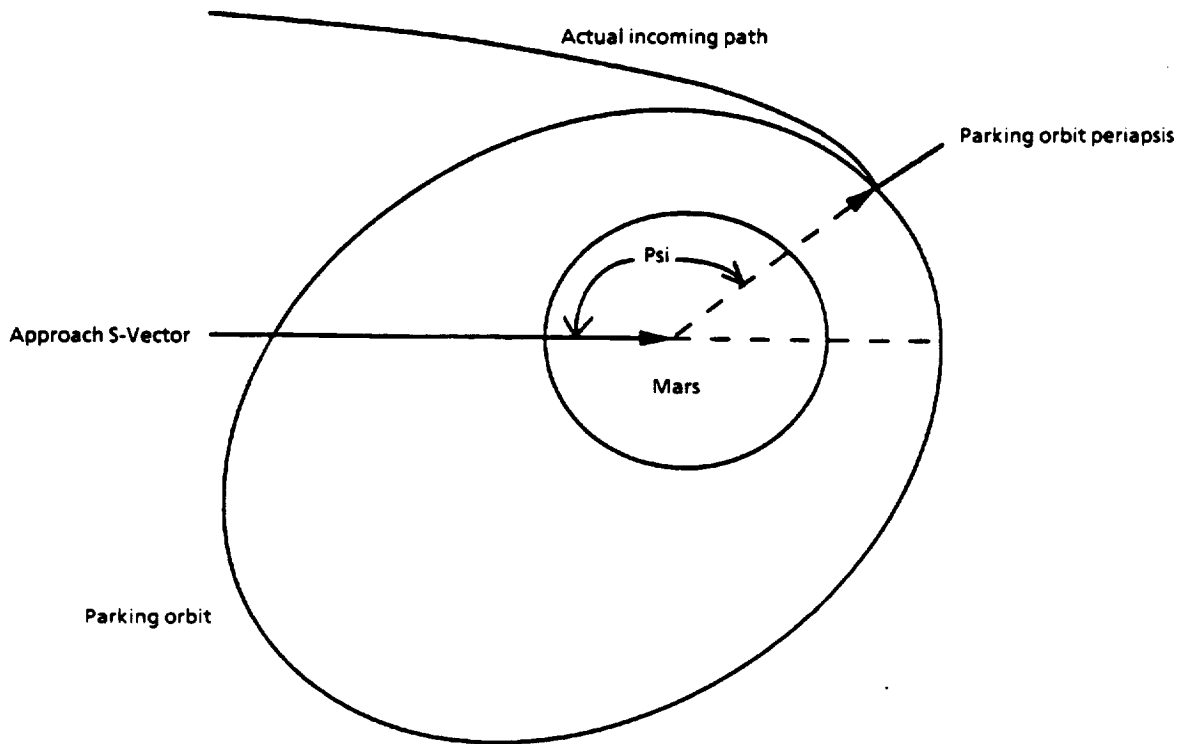
This section attempts to clarify the relationship between the MOI delta-V and the position that the MOI maneuver is performed on the approach hyperbolic trajectory. Likewise, the required delta-V to capture in the optimal elliptical parking orbit is related to the position that the concomitant MOI impulse is made on the approach trajectory. Shown in figure 2-24 is the relationship of minimum MOI and minimum TEI with a parameter termed Psi. Psi is the angle between the tail of the arrival V-infinity vector and the point on the arrival hyperbola that MOI impulse occurs, as shown in figure 2-25. A comparison of MOI and TEI for the 2014 reference mission with the 2016 mission is found in figure 2-24. The periapsis-to-periapsis transfer impulse is indicated by "periapsis transfer" and an off periapsis transfer impulse is indicated by "off-periapsis transfer". It is clear that the TEI for the 2016 mission can be lowered by a related increase in the MOI. The net effect is a decrease in 2016 total mission delta-V that results from a decrease in Mars departure plane-change/apsidal-misalignment losses.



Parking orbit delta-V is dependent upon the angle Psi at MOI

TD040

Figure 2-24. 2016 Opposition, Split Delta-V



TD041

Figure 2-25. Definition of Angle Psi

2.4.4.2 MOI/TEI Split Delta-V Budget

Continuing the discussion of the 2016 delta-V split, the data of figure 2-26 is provided as a delta-V budget for the 2016 opposition mission. The off-periapsis maneuver on the 2016 Mars approach reduced the plane and apsidal losses by over 600 m/s, with a reduction in the total delta-V of 390 m/s. The 2016 TEI delta-V was reduced to below the 2014 TEI delta-V, thus, showing that the 2016 TEI stage can be identical to the 2014 TEI stage. Also, the 2016 early departure requirements can still be met.

Delta-V Budget (m/s)						
Mission	MOC maneuver	TMI	MOC	TEI	Plane & apsidal losses	Total delta-V
2014 Ref	Periapsis	4318	3457	3840	263	11,595
2016	Periapsis	4022	3740 + 50*	4370 + 30	1060	12,212
2016	Off periapsis	4022	4010 + 50	3710 + 30	400	11,822

- Vehicle sized by 2014 reference mission delta-V
- Vehicle must meet 2016 abort from surface delta-V requirement
- Reduction in 2016 TEI to below 2014 reference mission TEI by apsidal rotation of arrival parking orbit
- * The values preceded by a "+" sign are estimated g-losses.

Figure 2-26. 2016 Split Delta-V

2.4.5 Low-L/D MEV Landing Site Access

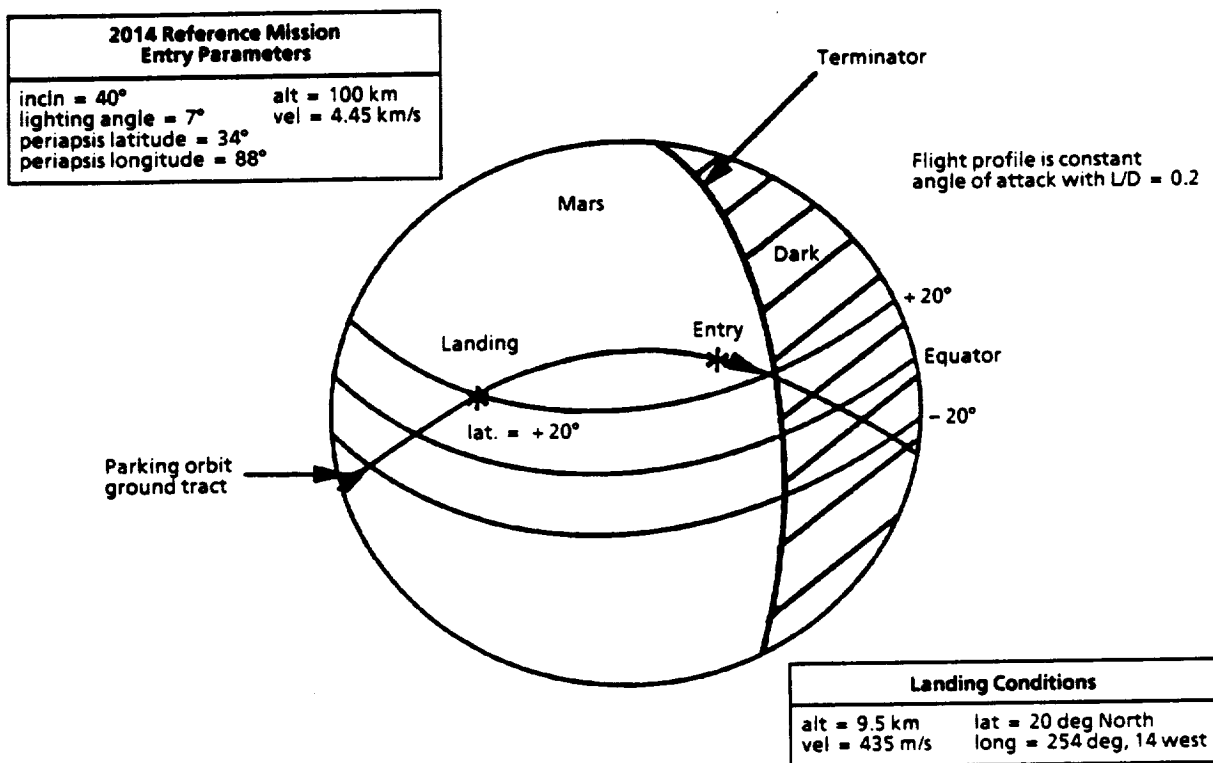
The MEV performance requirements play a significant role in sizing the NTP Mars transportation system. An ongoing issue in MEV configuration concerns the L/D requirements for meeting the sometimes conflicting landing requirements such as daylight landing in conjunction with landing anywhere in a Mars latitude range of 20 degrees north or south. The current section indicates the results of an investigation performed to ascertain the viability of using an MEV with L/D of 0.2 to meet the previously mentioned landing requirements, and meet those requirements for the widely varying elliptical parking orbits of opportunities 2014 through 2018. It should be noted that the 2014 reference mission and the 2018 mission represent the extremes of landing geometries that were encountered for the missions analyzed.

2.4.5.1 2014 Landing Site Access

The analysis results of this section were derived from an assumed 2014 elliptical parking orbit initial descent conditions as indicated below:

- entry altitude = 100 km
- entry latitude = 40 degree
- entry longitude = 0 degree (assumed)
- apoapsis altitude = 21,800 km
- periapsis altitude = 40 km
- inclination = 41.5 degree
- argument of periapsis = 129.8 degree
- periapsis latitude = 36 degree
- periapsis lighting angle = 7 degree.

The 2014 parking orbit, shown in figure 2-27, will allow a daylight landing within latitudes of 40 degree north/south of the Martian equator. This landing range can be achieved with a controlled atmospheric skip-out of a vehicle with max L/D of 0.2.



TD042

Figure 2-27. 2014 Landing Site Access

2.4.5.2 2018 Landing Site Access

The 2018 parking orbit, shown in figure 2-28, has a periapsis longitude of 51 degree east of the noon meridian and 19 degree south, with a node position close to the evening terminator. This southerly location of periapsis in conjunction with the position of the node relative to the terminator restricts accessible daylight landing sites of the low L/D vehicle to approximately 0 to 20 degree south.

2.4.6 High-L/D MEV Landing Site Access

An analysis was performed to provide some indication of the extent to which an high L/D vehicle could traverse the surface of Mars. The results of simulated MEV trajectory optimizations to maximize the southerly latitude and thereby attempt an approach to the Martian south pole are provided in the following sections. Trajectories were simulated for an MEV with max L/D = 1.6 (section 2.4.6.1) and with max L/D = 1.3 (section 2.4.6.2). All analysis results of this section were derived from an assumed 2014 elliptical parking orbit initial descent conditions as indicated in section 2.5.5.1. Final descent conditions are MEV relative velocity = 0 and, as previously mentioned, final latitude was maximized in the southerly direction.

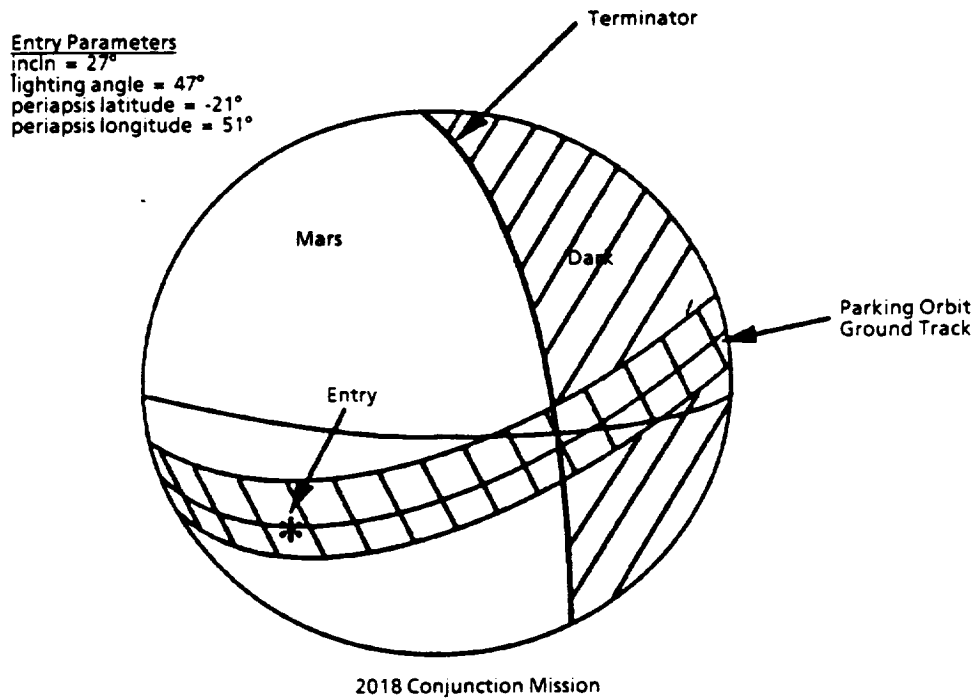


Figure 2-28. 2018 Landing Site Access

TD043

2.4.6.1 Polar Access with HMEV

To gauge the landing site access capability of the high-L/D Mev with max L/D = 1.6, a simulated descent was made in an effort to approach the Martian south polar region. In this simulation, the only control variable was roll and, therefore, the angle of attack was constant, implying a constant L/D descent. The initial and final conditions of this descent are given in figure 2-29 (the initial conditions are essentially identical to the 2014 reference mission initial conditions, section 2.4.5.1). The end Martian latitude calculated is approximately 85 degree south; the Martian permanent south-polar-icecap begins at 85 degree south. Also, the Martian permanent north-polar-icecap begins at approximately 75 degree north. Thus, the HMEV may be able to reach either the Martian north or south polar icecap region.

2.4.6.2 Polar Access with Biconic

In a similar fashion, an analysis was performed to gauge the landing site access capability of the high-L/D biconic based Mev with max L/D = 1.3. A simulated descent was made with this vehicle in an effort to approach the Martian south polar region. In this simulation, the only control variable was roll and, therefore, the angle of attack was constant, implying a constant L/D descent. The initial and final conditions of this

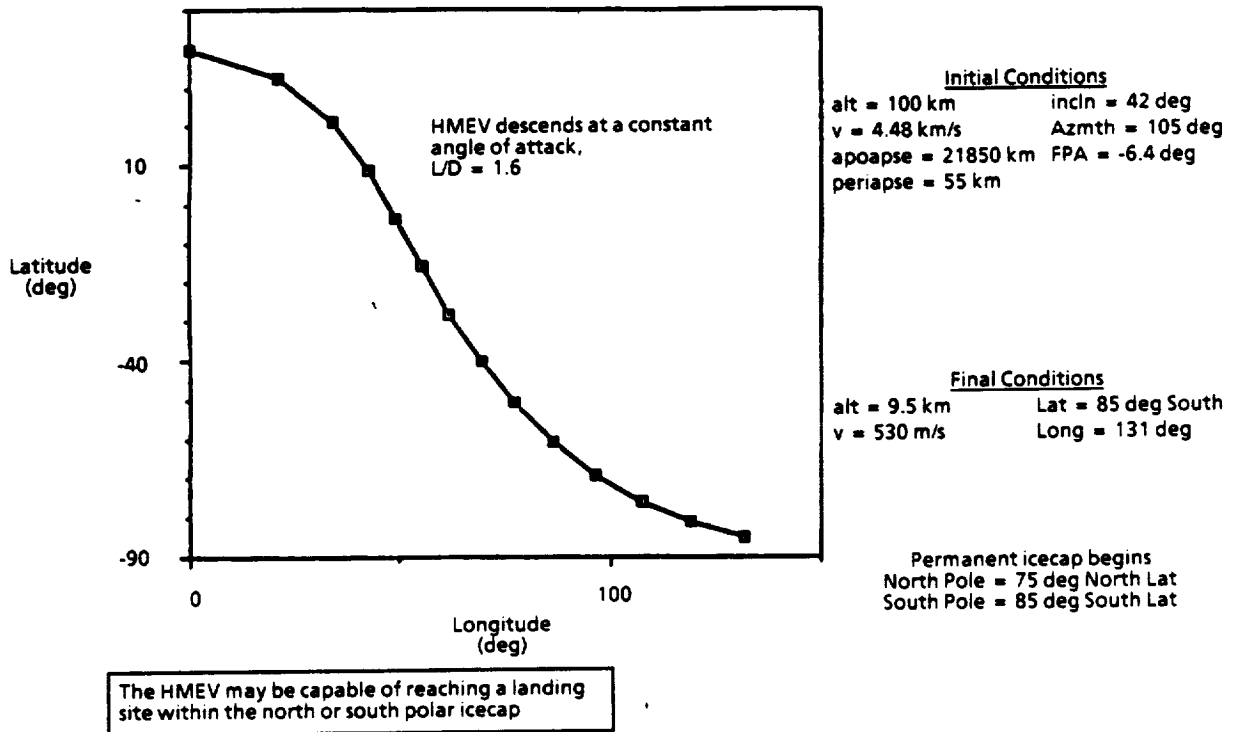


Figure 2-29. Polar Access with HMEV Lander

TD044

descent are given in figure 2-30. The initial conditions are essentially identical to the 2014 reference mission initial conditions, section 2.4.5.1. The end Martian latitude is approximately 72 degree south, with the Martian permanent south-polar-icecap beginning at 85 degree south. Also, the Martian permanent north-polar-icecap begins at approximately 75 degree north. Thus, the biconic MEV probably cannot reach the permanent south-polar-icecap, but may be able to reach the Martian north-polar-icecap region.

2.4.7 Nuclear Reactor Disposal

Options related to the disposal of spent nuclear reactor propulsion modules in a way that precludes or reduces the chances of Earth biosphere contamination with nuclear waste from the reactor are provided. A spent reactor is defined by a nuclear thermal propulsion system reactor that has been operated over one or more Mars missions and has come to the end-of-life usefulness for mission purposes. The reactor may or may not have some propulsive abilities remaining. If the reactor does not have self propulsive abilities and if it is in safe Earth parking orbit, then it will be assumed that measures will be taken to affix a dedicated disposal vehicle to the spent reactor to facilitate appropriate delivery to safe disposal orbit.

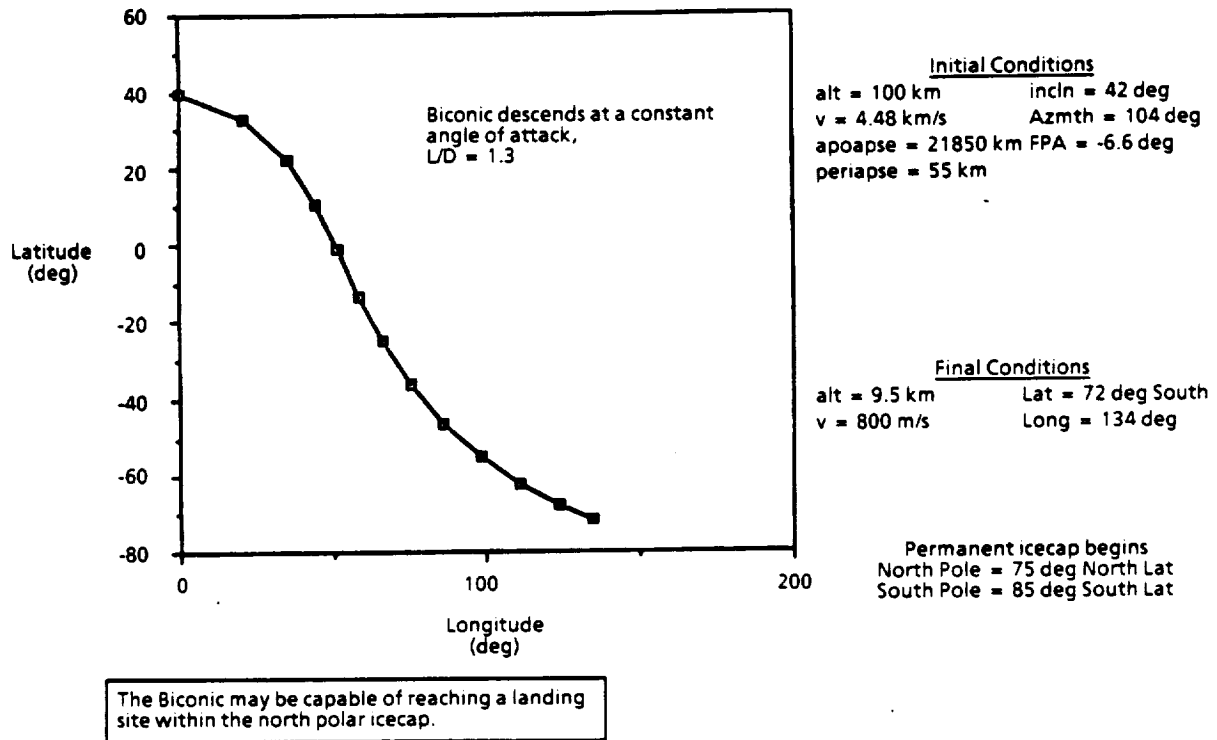


Figure 2-30. Polar Access With Biconic Lander

TD045

2.4.7.1 Safe Disposal Orbits

There have been several nuclear safe disposal orbits proposed: circular orbit between Earth and Venus, circular orbit between Earth and Mars, and circular orbits about Earth. The most promising from a low probability of Earth impact standpoint appears to be a circular orbit of 0.85 AU between Earth and Venus.

2.4.7.2 Nuclear Reactor Disposal Options

Listed below are some option scenarios for delivery of the spent nuclear reactor to a safe disposal orbit of 0.85 AU.

- a. Dedicated disposal vehicle delivers reactor from safe Earth parking orbit to safe disposal orbit between Earth and Venus; crew cab may be removed for reuse prior to disposal.
- b. Nuclear Thermal Propulsion system delivers itself from safe Earth parking orbit to safe disposal orbit between Earth and Venus; crew cab may be removed for reuse prior to disposal.
- c. NTP vehicle performs Earth gravity assist at Earth return. Subsequent maneuvers

will be required to circularize orbit to safe disposal orbit. For reuse purposes, crew habitat could be separated and aerocaptured (unmanned) at Earth.

2.4.7.3 NTP Reactor Disposal by Powered Earth Gravity Assist

Each of the above three option should be studied in greater depth to ascertain their impact on mission delta-V budgets. In this analysis, however, only the Earth gravity assist option has been analyzed.

A nuclear reactor disposal delta-V summary and comments chart is found in figure 2-31. For the 2014 and 2016 opposition missions, maneuver delta-Vs were found that are on the order of 4.5 km/s. These maneuvers place the vehicle in a nuclear safe circular orbit of 0.85 AU. The 2016 and 2018 conjunction missions, however, have excess Earth return Vhp which do not provide a sufficient turning angle to perform the Earth gravity assist disposal maneuver.

Disposal Maneuver: Earth gravity assist with propulsive maneuvers at Earth and at periapse (0.85 AU) of target orbit.*

Opportunity	Delta-V km/s	Comments
2014 opposition	4.43	Earth Vhp = 5.48 km/s; Earth closest approach radius - 113,000 km; Earth delta-V = 3.14 km/s
2016 opposition	4.68	Earth Vhp = 7.2 km/s; Earth closest approach radius - 27,000 km; Earth delta-V = 3.39 km/s
2016 conjunction	---	Insufficient turning angle to perform disposal maneuver; Earth Vhp = 9 km/s**
2018 conjunction	--	Insufficient turning angle to perform disposal maneuver; Earth Vhp = 3.59 km/s**

* Recommended approach is an unpowered Earth-Venus gravity assist, requiring no delta-V. (Need further work to identify/assess disposal profiles.)

** The Earth return Vhp could be reduced to increase the turning angle; this would significantly increase total delta-V for disposal maneuver.

Figure 2-31. Reactor Disposal Delta-V

An alternative approach to targeting a circular nuclear safe orbit would be to utilize an unpowered Earth-Venus gravity assist to place the spent reactor in an elliptical orbit with periapse at Venus' orbit and the apoapse of 1 AU. Also, in the case of the 2016 high Earth return Vhp of 9 km/s, an unpowered Earth-Jupiter gravity assist may be feasible, placing the vehicle in a high inclination orbit about the sun.

2.4.8 Summary

Indicated below is a summary of eight significant conclusions that may be reached based on the previous analysis results and data delineations.

- a. Mars optimal parking orbits differ widely from mission to mission, and landing site access will differ.
- b. Reserves, reactor cool-down, midcourse, and losses have been accounted for in vehicle sizing.
- c. Elliptical parking orbits require 1 to 2 km/s less delta-V than circular parking orbits.
- d. Vehicle sized for 2014 opposition mission can be made compatible with the 2016 abort from surface delta-V requirements.
- e. For the 2014 opposition mission, a low L/D MEV can land at daylight sites within lat = 20 degree north or south through partial skip-out.
- f. For the 2018 conjunction mission, low L/D MEV daylight landing sites are within the southern hemisphere.
- g. The Biconic lander may reach the northern polar icecap. The HMEV lander may reach the northern or southern polar icecap.
- h. Disposal of spent nuclear reactor into a "nuclear safe" orbit requires delta-V \approx 4.5 km/s; recommended approach is a low delta-V Earth-Venus gravity assist into an orbit with low probability of Earth impact.

3.0 MEV OPTIONS

The MEV options task examines aerobrake concepts which could result in reduced heating with extended crossrange capability, and allowing for an integral launch. The analysis covers a broad range of L/D from 0.2 to 2.0 with a close coupling between the materials, structural analysis and aerothermodynamic analysis for concept design.

3.1 SYMMETRIC BICONIC CONCEPTS

During the course of the STCAEM contract, several aerobrake shapes have been examined as options for the Mars excursion vehicle (MEV) in descent only mode (i.e., nuclear thermal propulsion mission profiles). Shown in figure 3-1 is a summary of these concepts, all of which have been discussed in either the STCAEM Phase 1 or the Phase 2 (references 1 and 2) except for the symmetric biconic shapes. Biconic concepts were analyzed during the current study in order to provide an alternative means of placing the MEV into orbit without on-orbit assembly while still providing adequate crossrange capability and reduced heating. Integral launch of a biconic Mars excursion vehicle (BMEV) will pose an even simpler problem than that of the side launched high L/D MEV of the earlier studies as the entire vehicle will be in line without a center of gravity (c.g.) offset. The biconic concepts have a base diameter of 10 to 12 meters to fit atop a heavy lift launch vehicle (HLLV).

3.1.1 Parametric Study

A parametric study of biconic cone angles and radii was performed to arrive at a biconic concept which provided a high L/D (>1.0) at large angles of attack, with aerodynamic performance comparable to the HMEV, and also allowing adequate packaging volume for the Mars surface habitat. Constraints and initial limits were used to aid in ruling out nonfeasible concepts. The independent variables used for this analysis included the base θ_b and nose cone θ_n half angles, the intermediate radius to base radius ratio R_i/R_b , and the nose cone radius to base radius ratio, R_n/R_b . A graphical definition of these parameters is displayed in figure 3-2.

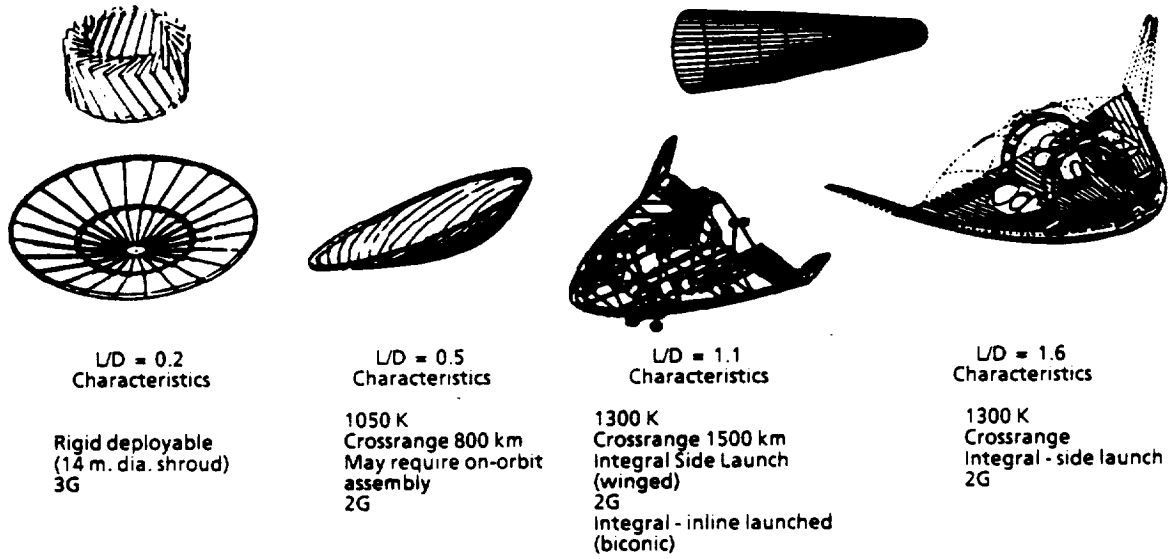
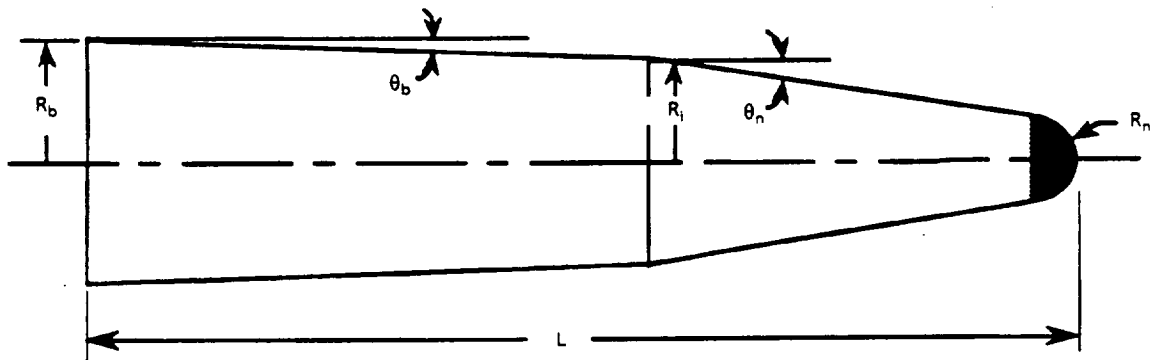


Figure 3-1. Types of Aerobrake Shapes Examined

TD001



θ_b = base cone half angle	R_b = base radius
θ_n = nose cone half angle	R_i = intermediate radius
L = Length	R_n = nose radius

Figure 3-2. Biconic Geometry Parameters

TD002

For the initial study, the following ranges were examined:

$$\begin{aligned}\theta_n &= 8^\circ \text{ to } 16^\circ \\ \theta_b &= 4^\circ \text{ to } 7^\circ \\ R_i/R_b &= 0.7, 0.8, 0.9\end{aligned}$$

The nose-to-base radius ratio was fixed at 0.33. This fixes the actual nose radius at 2 m for an HLLV with a 12 m shroud and 1.65 m for a 10 m shroud. The 2 m value corresponds to a nose radius which would result in minimal heating for an aerocapture maneuver at Mars (ref. 1). For the MEV descent only vehicle, aerocapture is not applicable and thus the nose radius should be as large as possible to reduce convective stagnation point heating. However, in order to decrease the drag, the nose radius needs to be small. The 2 m value was used as a compromise between heating and drag.

Aerodynamics of the biconic concepts were evaluated using the AERO program. This analysis used Modified Newtonian Impact Theory to compute the pressures at large angles of attack. Although this theory is in error at low angles of attack, it is adequate for initial concept screening.

The concepts' aerodynamic characteristics were evaluated at a trim angle of attack of 20° . All aerodynamic coefficients were computed using the plan area as the aerodynamic reference area (A_{ref}). This reference area is nondimensional as the base radius was set equal to unity, for this study. The lift-to-drag ratio as a function of drag coefficient times the nondimensional reference area ($C_D^*A_{ref}$) is displayed in figure 3-3. This figure shows the results for many biconic shapes, and is actually a function of all of the aforementioned independent variables. In this figure, concepts which fall in the upper right corner of the graph are the most desirable. The large $C_D^*A_{ref}$ values give small ballistic coefficient values which would result in lower heating and higher pull up altitudes. Values of $C_D^*A_{ref}$ for the biconics range from 1.3 to 1.5. If a 30-m length is assumed for both the HMEV ($L/D = 1.6$) and the biconics, the resulting scaled C_D^*A (where A is the dimensional area) would be 92 m^2 and 32 m^2 respectively. With identical masses assumed, this difference in $C_D^*A_{ref}$ would result in a 65% increase in ballistic coefficient over that of HMEV. Thus, these biconics will result in lower pull-up altitudes and the resulting heating will potentially be higher than the HMEV entry.

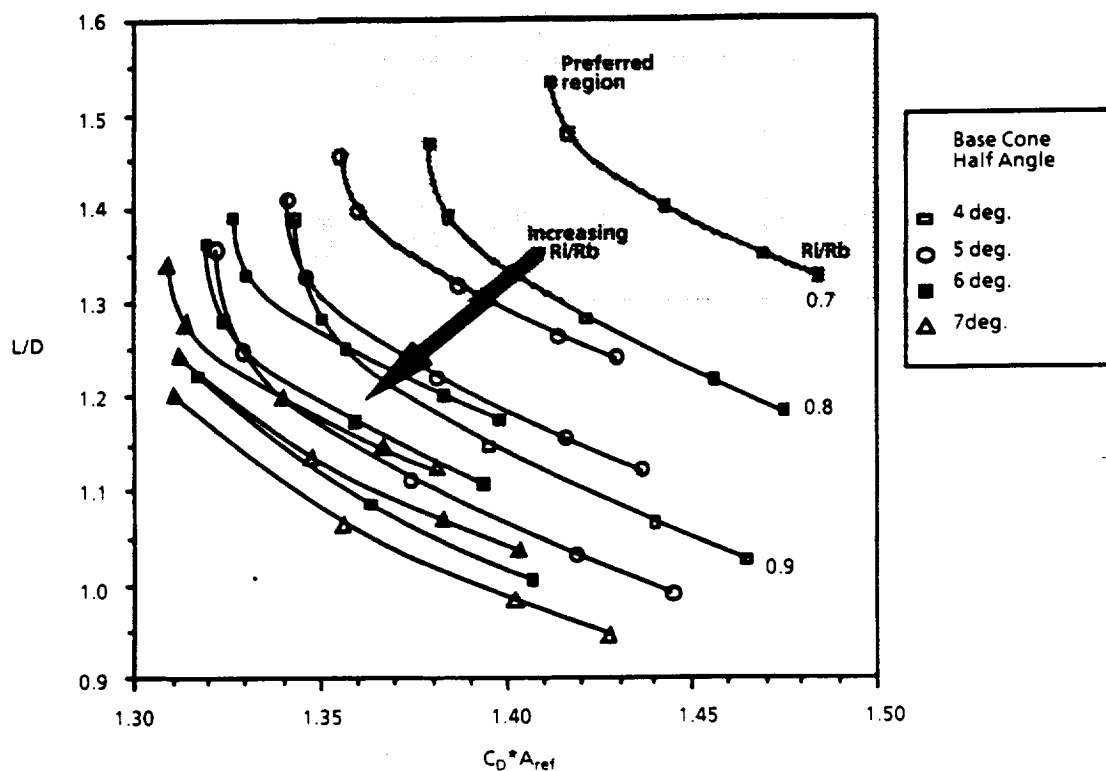


Figure 3-3. Biconic Lift And Drag Values

TD003

A large L/D value for the biconics is needed to provide aerodynamics similar to the HMEV. For this analysis, the L/D values were weighed with greater importance (best when L/D is 1.5 or greater). From figure 3-3, the better configuration is the one with a 4° base cone half angle, 8° nose cone half angle, and $R_i/R_b = 0.7$. The concepts will be numbered as "a bc de fg", where a is the base cone half angle, bc is the nose cone half angle, de is the intermediate radius percentage, and fg is the nose radius percentage. Therefore, the selected concept will be numbered 408.7033.

The effects of varying the nose cone half angle on L/D are more easily readable in figure 3-4. Smaller nose cone angles result in higher L/D values. The intermediate radius ratio was fixed at 0.7 for this calculation.

The location of the center of pressure (CP) plays a large role in the ability to package a biconic concept. Due to the generally narrow volumes of biconics, it is most favorable for packaging to have the CP located farther aft where the radius is the largest. However, this does not mean right against the base. In figure 3-5, the normalized x_{CP} location (distance from the base along the x-axis) is shown with a fixed base cone half angle of 4° . It can be observed that the best L/D and x_{CP}/L combination occurs for the 408.7033 biconic configuration.

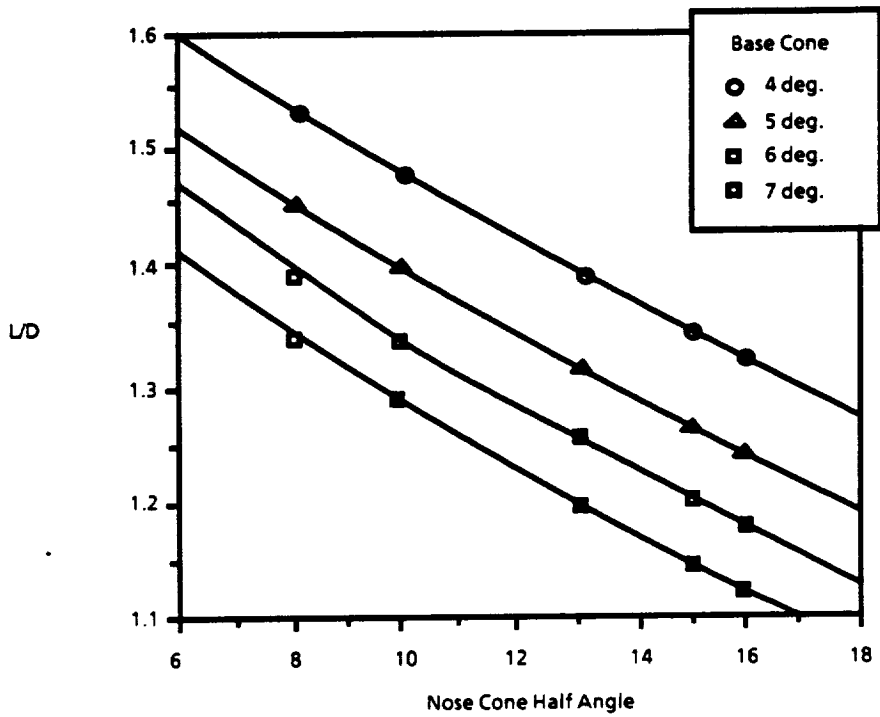


Figure 3-4. Nose Cone Angle Effects

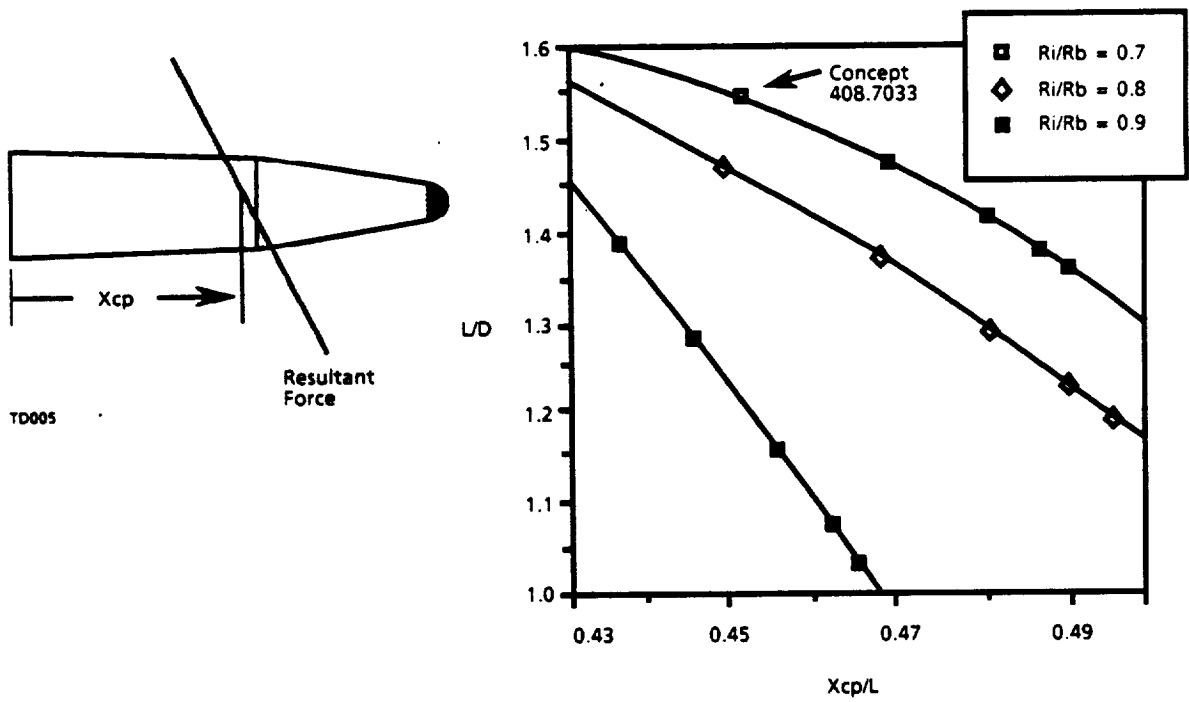


Figure 3-5. Center of Pressure Locations

From this analysis, the 408.7033 biconic concept was selected as the initial symmetric biconic shape. This concept provides an L/D of approximately 1.5 at a 20° trim angle of attack. The overall length of this concept, with a 6-m base radius, is 43 m. The aerodynamic coefficients, for Concept 408.7033, as a function of angle of attack are displayed in figure 3-6.

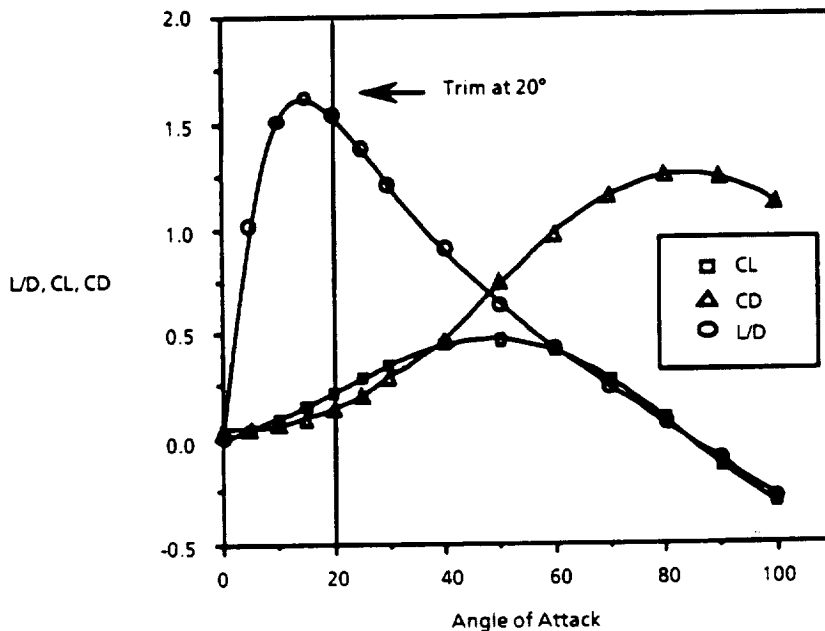


Figure 3-6. Concept 408.7033 Aerodynamic Parameters

TD006

3.1.2 Additional Studies

Further analysis was required to arrive at additional biconic concepts in order to reduce the overall length of the biconic MEV configurations. The Concept 408.7033 resulted in a 43-m length when scaled up to the 12-m launch shroud diameter. This aspect ratio (length/base radius) provided large longitudinal volumes, which are excessive for MEV surface habitat requirements. In order to decrease the aspect ratio and reduce the length of the MEV, additional concepts were evaluated.

A reduction in the length of these vehicles and thus a decrease in the aspect ratio was accomplished by increasing the intermediate radius of the shapes. However, as evident in figure 3-3, as R_i/R_b increases, the L/D decreases, which is not desirable. To avoid a reduction in L/D, smaller nose radius ratios were investigated in combination with the larger intermediate radius ratios. For this extended examination, the following parameter ranges were examined:

$$\theta_n = 4^\circ \text{ to } 7^\circ$$

$$\theta_b = 8^\circ \text{ to } 16^\circ$$

$$R_i/R_b = 0.7, 0.75, 0.8$$

$$R_n/R_b = 0.1667, 0.2, 0.33$$

A comparison of some of these biconic shapes with the Concept 408.7033 is shown in figure 3-7. The majority of these newer concepts have smaller aspect ratios and nose radii in comparison to Concept 408.7033. The L/D as function of $C_D \cdot A_{ref}$ for these updated shapes is shown in figure 3-8 along with the 408.7033 reference point. From this graph, it is noticeable that the product of $C_D \cdot A_{ref}$ is much smaller than that of the previous concept. Although these smaller values are less desirable, they will result in roughly a 10% increase in the ballistic coefficient, which is not significant. One other point to note is that as the nose radius ratio decreased, the L/D increased, which is a direct function of the drag decrease or $C_D \cdot A_{ref}$ decrease. Based on the values in figure 3-8, the best concepts are the 4° base cone half angle shapes, as they fall in the upper right portion of the graph.

Of the 4° base cone shapes, the 412.7516, 414.7516, 412.7520, 513.7520, and 414.7520 (where 412.7516 = 4° base, 12° nose, $R_i/R_b = 0.75$ and $R_n/R_b = .1667$) provide the best aerodynamic performance. For preliminary concept definition, the 414.7516 concept was examined in greater detail, as it results in values which are closest to the 408.7033 concept except in length. The aspect ratio (length/ R_b) of the 414.7516 concept is 6.04, which will result in a shorter more compact MEV configuration when compared to the 408.7033 values of 7.2.

As a result of the reduced nose radii for these shorter biconics, the heating rates that the MEV will encounter will increase. For the descent only MEV, convective heating is the only significant contribution to the stagnation point heating rates. The heating to the stagnation point varies inversely as the square root of the nose radius. The previous nose radius of 0.33 or a 2-m radius with a 6-m base diameter resulted in lower heating rates than the newer value of 0.1667 or 1 m for a 6-m base diameter (value for selected concept 414.7516). A graph of the peak stagnation point heating as a function of nose radii for an MEV descent is shown in figure 3-9. As can be seen, the heating rates increase significantly as the nose radius goes below one meter. The decrease in nose radius from two meters to one meter results in only a 40% increase in convective heating or temperatures of approximately 1450 K. This will result in the potential need for the use of a light weight ablator or reradiative TPS covering instead

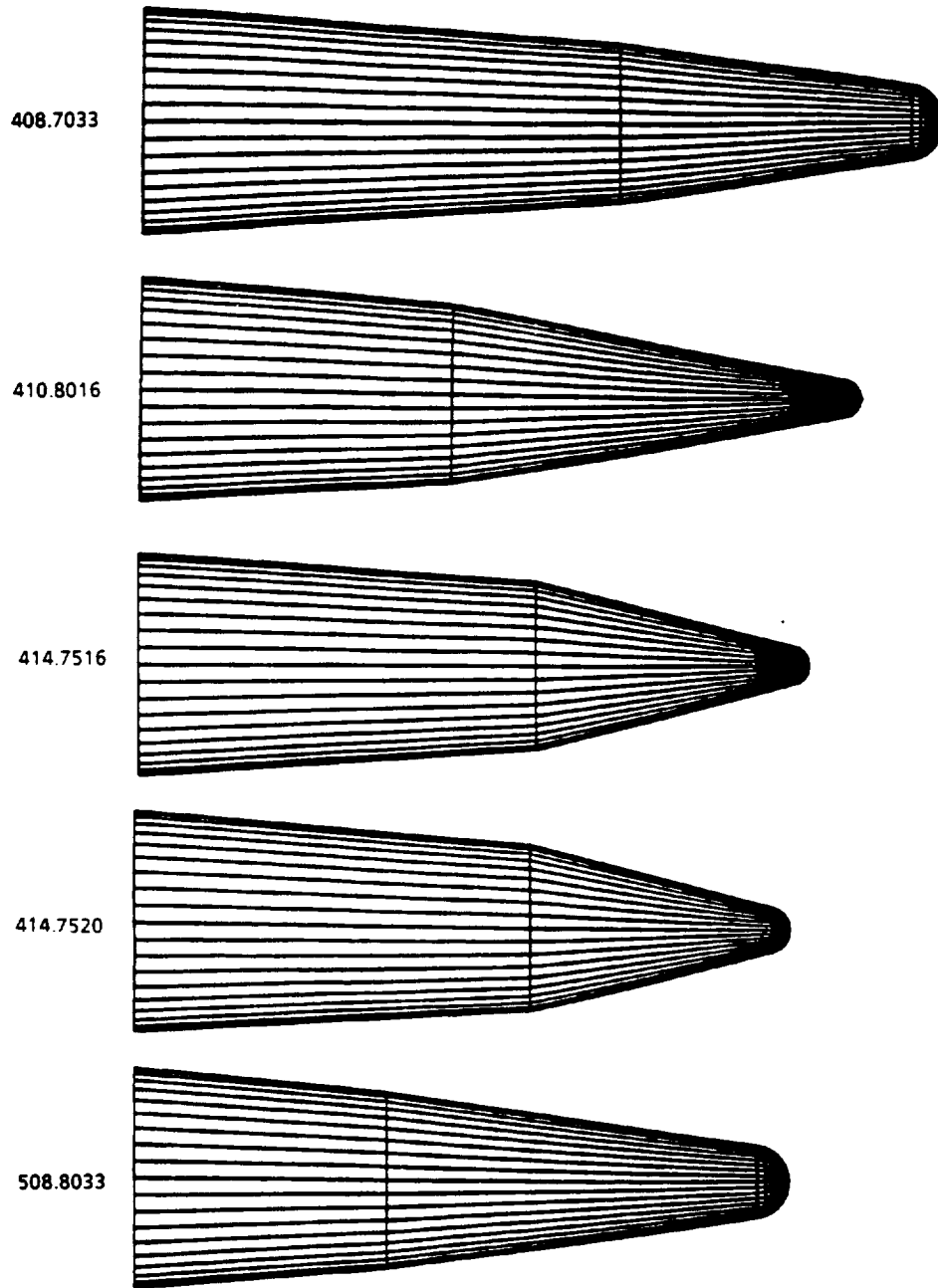


Figure 3-7. Comparison of Biconic Shapes

TD014

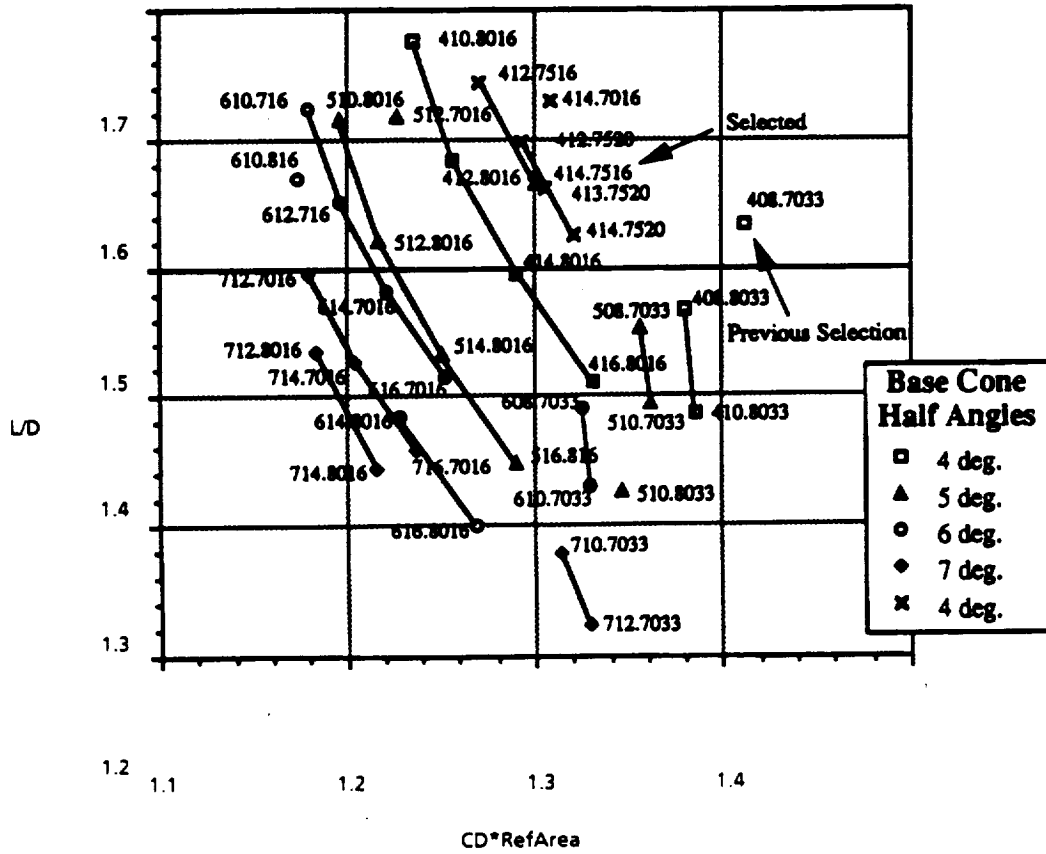


Figure 3-8. Biconic Lift and Drag Values

TD008

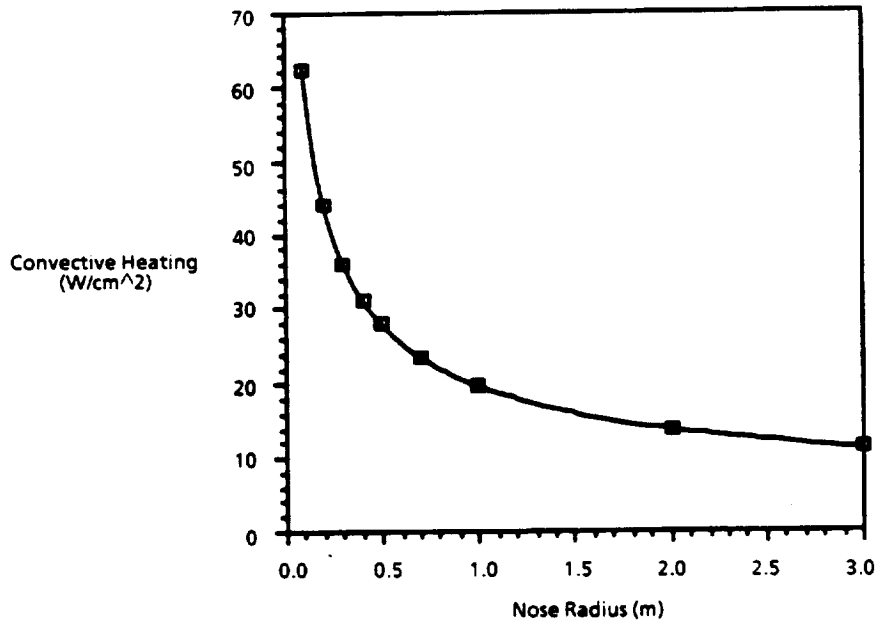


Figure 3-9. Scaled Peak Heating Rates for BMEV Descent

TD009

of hot structure only in the stagnation point region. However, as this is a small area, the additional TPS will not be a significant weight increase. Once again, a reduction in the nose radius was required to keep the L/D high while decreasing the overall length of the vehicle.

The lift and drag coefficients as a function of angle of attack for the 414.7516 concept and the HMEV are displayed in figure 3-10. The L/D ratios for these vehicles are displayed in figure 3-11. The aerodynamic parameters for the HMEV are shifted only slightly as compared to the biconic MEV 414.7516 concept. However, there is a significant difference in reference areas thus making the total lift-and-drag forces differ. For the pitching moment coefficients, the c.g. or reference point was chosen at the x_{CP} location for a 20° trim angle of attack. The 414.7516 biconic displays static stability in that the slope of the C_M vs. α curve, shown in figure 3-12, is negative for the higher angles of attack. At the lower angles of attack ($\alpha < 10^\circ$), the slope turns positive. The values at lower angles of attack are invalid as Newtonian Impact Theory was used, which does not give good results at low angles of attack, and additionally no viscous drag forces were included in the preliminary screenings. A more detailed analysis is required to determine the fully defined aerodynamic characteristics of the biconics.

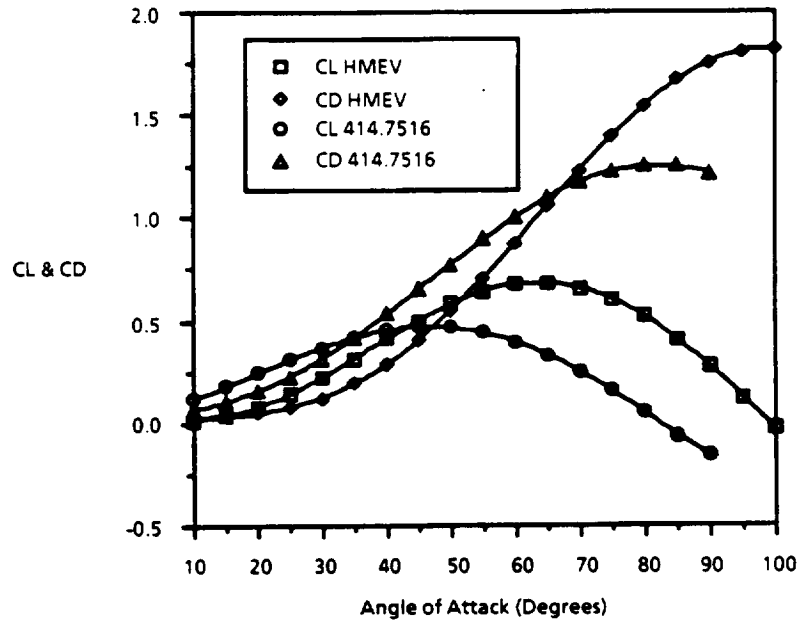


Figure 3-10. Aerodynamic Coefficients for BMEV and HMEV

TD010

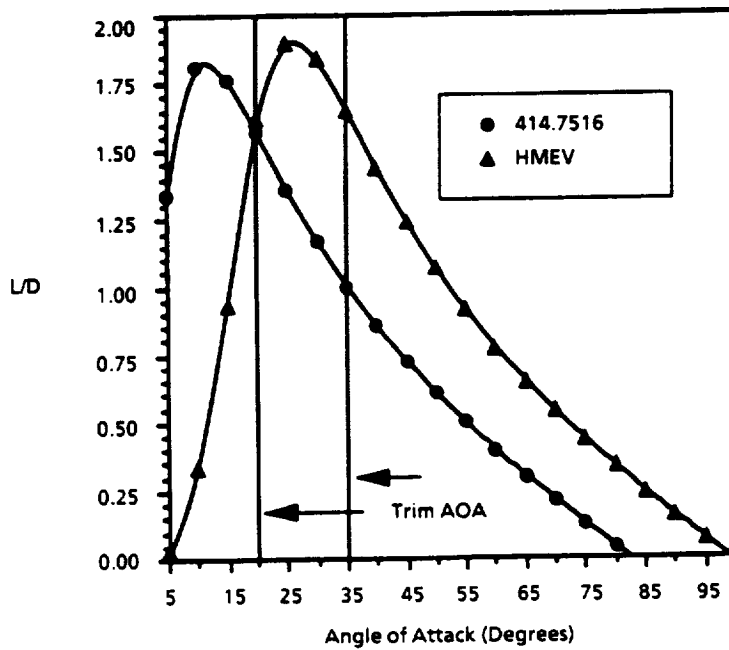


Figure 3-11. Lift-to-Drag Ratios for BMEV and HMEV

TD011

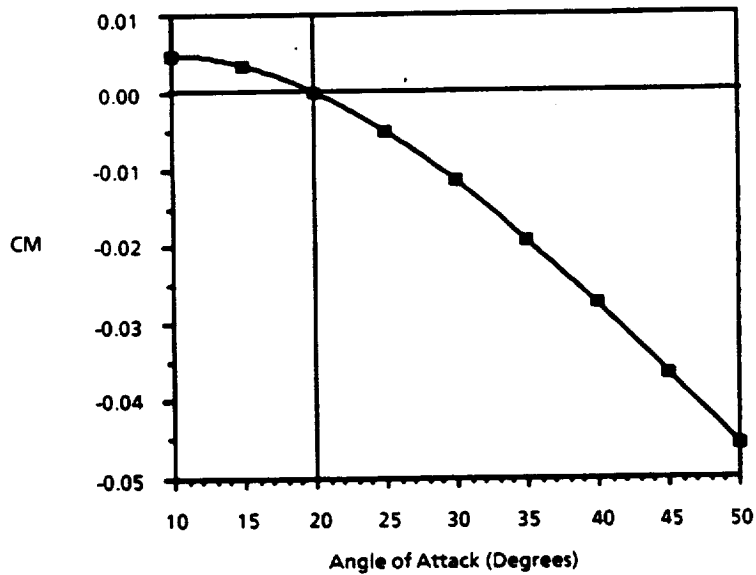


Figure 3-12. Moment Coefficient for Concept 414.7516

TD012

3.1.3 Biconic MEV Configuration Layout

Initial development of a biconic Mars lander concept has consisted of investigations into packaging of propulsion systems and payload into potential biconic shapes. Preliminary dimensions of approximately 35 meters in overall length, with a 12-meter diameter base were assumed for the BMEV. It is possible to incorporate both the Mars surface habitat and the crew delivery and ascent vehicles into the same size biconic structure. The surface habitat is sized at approximately 700 cubic meters for a crew of 6, and is integral with the vehicle structure. This assumption provides the biconic lander to serve a "campsite" function. The crew delivery biconic would land fairly close to the habitat lander, with surface transportation provided by a rover. Conceptual configurations for the crew and cargo BMEVs are shown in figure 3-13.

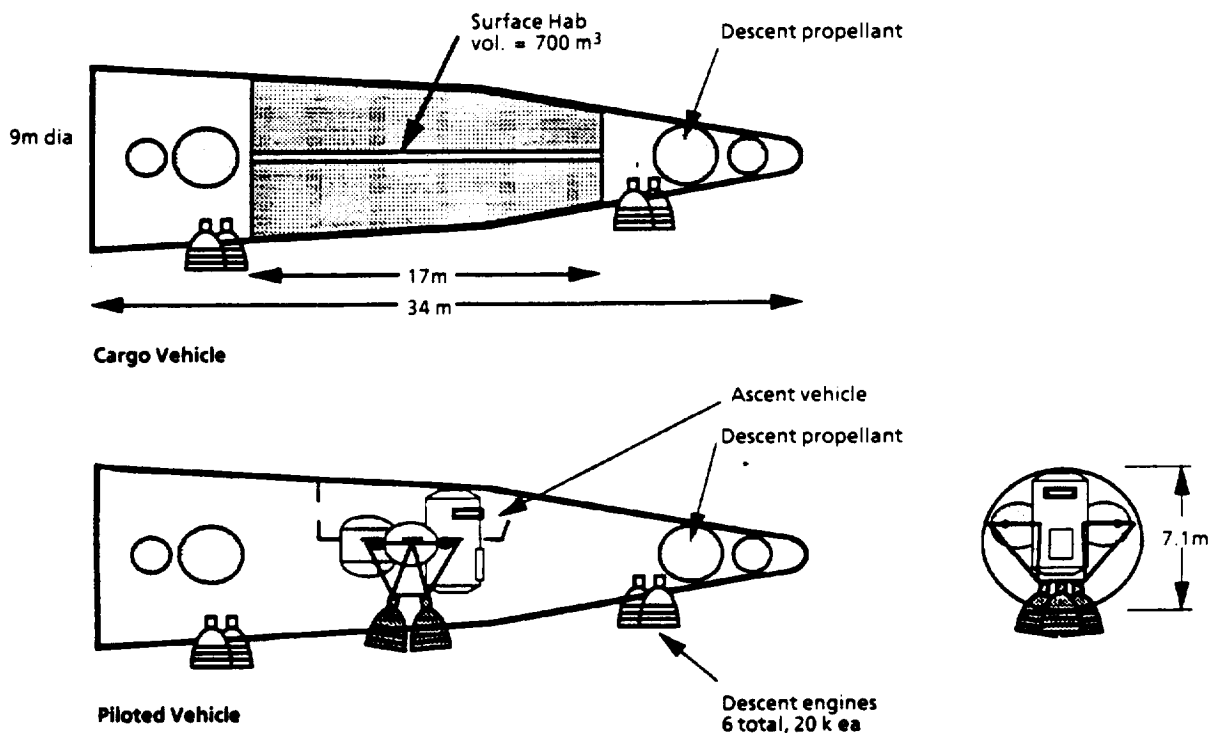


Figure 3-13. BMEV Conceptual Configurations

TD013

The crew delivery biconic will carry a Mars ascent vehicle that will use the lander stage as a launch platform. This is made possible by jettisoning a portion of the vehicle's upper surface during the terminal part of the descent maneuver, also allowing abort if necessary.

3.1.4 Biconic MEV Summary

The selection of a final biconic concept will involve an iterative process with the configuration layout and the aerodynamic characteristics of the shape. This will include determining in detail the system placements such as the surface habitat, ascent and descent engines, etc. The design process will hopefully lead to a BMEV with the minimum dimensions capable of packaging both the crew version and cargo versions in a common external structure.

3.2 STRUCTURAL ANALYSIS OF LOW L/D AEROBRAKE

A new Finite Element Model was generated for the Low L/D Aerobrake using PATRAN as a pre-processor resident on the SGI terminals. This model included the curved rim (or lip) which was omitted from the previous FEM. The curved rim provides stiffness to the free edge and helps cut down the deformations. The model was generated using mostly QUAD plate elements. The use of relatively stiffer triangular elements was kept to a minimum. A mesh was generated which would provide a minimum number of elements without compromising the true geometry and curvatures. This resulted in a model with approx. 6300 degrees of freedom and was dubbed as the Baseline model, figure 3-14.

3.2.1 Material properties

The aerobrake structure was fabricated using a metallic honeycomb sandwich structure. Each of the face sheets were 0.00173m thick titanium alloy (Ti-6Al-4V) with a 0.0381m thick 5056 aluminum honeycomb core separating them as shown in figure 3-15.

The sandwich structure was modeled as monolithic plate elements having bending stiffness and mechanical properties of the sandwich structure, figure 3-16.

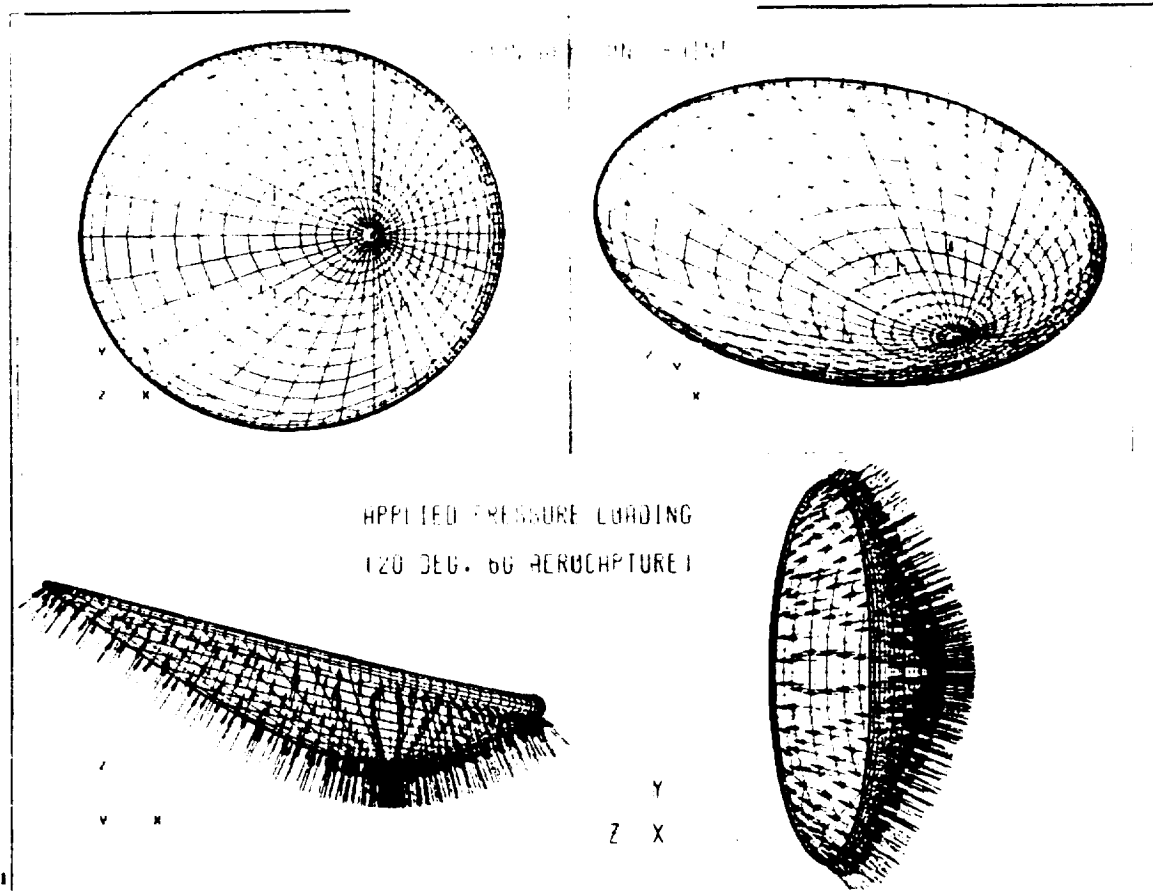


Figure 3-14. Loads and Boundary Conditions

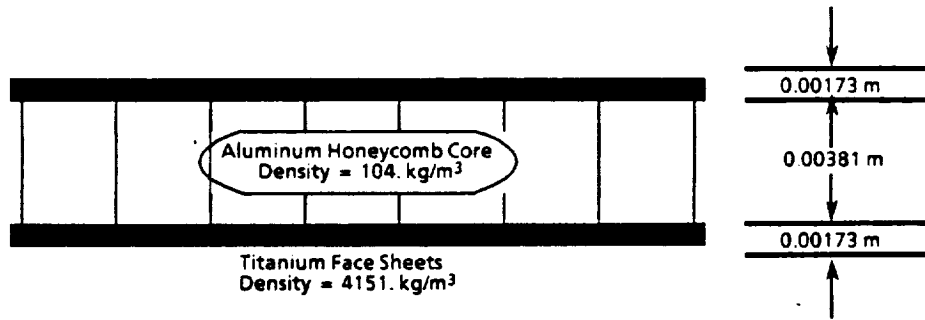


Figure 3-15. Aerobrake Honeycomb Sandwich Structure

	E (Pa)	G (Pa)	μ	ρ (kg/m ³)	σ_{xy} (Pa)	σ_{cy} (Pa)	σ_{su} (Pa)
Face Sheets	1.103e11	0.427e11	0.310	4.429e3	11.030e8	10.617e8	6.894e8
Honeycomb	0.690e11	0.270e9	0.330	2.656e3	2.4133e8	0.965e8	1.448e8

Figure 3-16. Sandwich Structure Physical Characteristics

3.2.2 Loading

Pressure distribution (C_p) over the aerobrake surface for a 20° entry angle was obtained from the AERO program. Using this C_p distribution, a three dimensional pressure surface was created using PATRAN. The 3-D surface was normal to the aerobrake surface and constituted the unit loading case, figure 3-14. Pressure loading for the 6-g aerocapture maneuver was generated by calculating the dynamic pressure (q_∞) for an 84mt mass at 6g's ($q_\infty = 7318$ Pa) and multiplying it by the unit loading (C_p). The MTV Payload is attached to the aerobrake at four locations. These locations were used as reaction points for the applied pressure loading.

3.2.3 Baseline Analysis Results

Structural analysis was performed using NASTRAN/ver 66, Linear Static Sol 101 on the Silicon Graphics workstation. PATRAN was utilized for post-processing. The results of the analysis showed that the structure is stiffness critical. Maximum displacement at the trailing edge was approximately 0.55 m. The total mass for the aerobrake was approximately 16 mt.

3.2.4 Aerobrake Configuration Update

In order to improve stiffness and reduce large deformations, the finite element (FE) model was revised. The most promising change included stiffening the rim since this is where the largest deformations occurred. Stiffness increase was accomplished by increasing the face sheet thickness from 0.00173m to 0.0020m and the core thickness from 0.0381m to 0.050m for the rim structure. New cross-section is shown in figure 3-17. Dish structure below the rim was left unchanged. The revised FE model was named AB2 (Aerobrake 2).

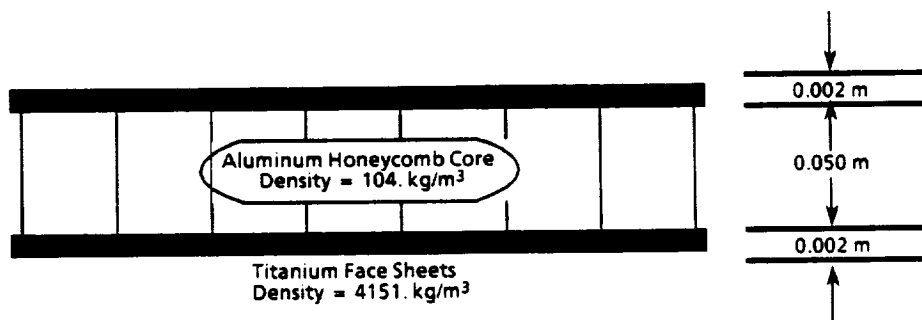


Figure 3-17. Revised Rim Configuration

3.2.5 Revised Rim

This modification resulted in a weight increase of 1.4mT (8.75%), but it reduced the maximum deformations by almost 50%. Results from this analysis are shown below. Deformed shapes and the displacement and stress fringe plots are shown in figures 3-18 to 3-20. There is a potential for further reduction in weight with design optimization and selection of advanced composite materials. A summary of the structural finding is provided in figure 3-21.

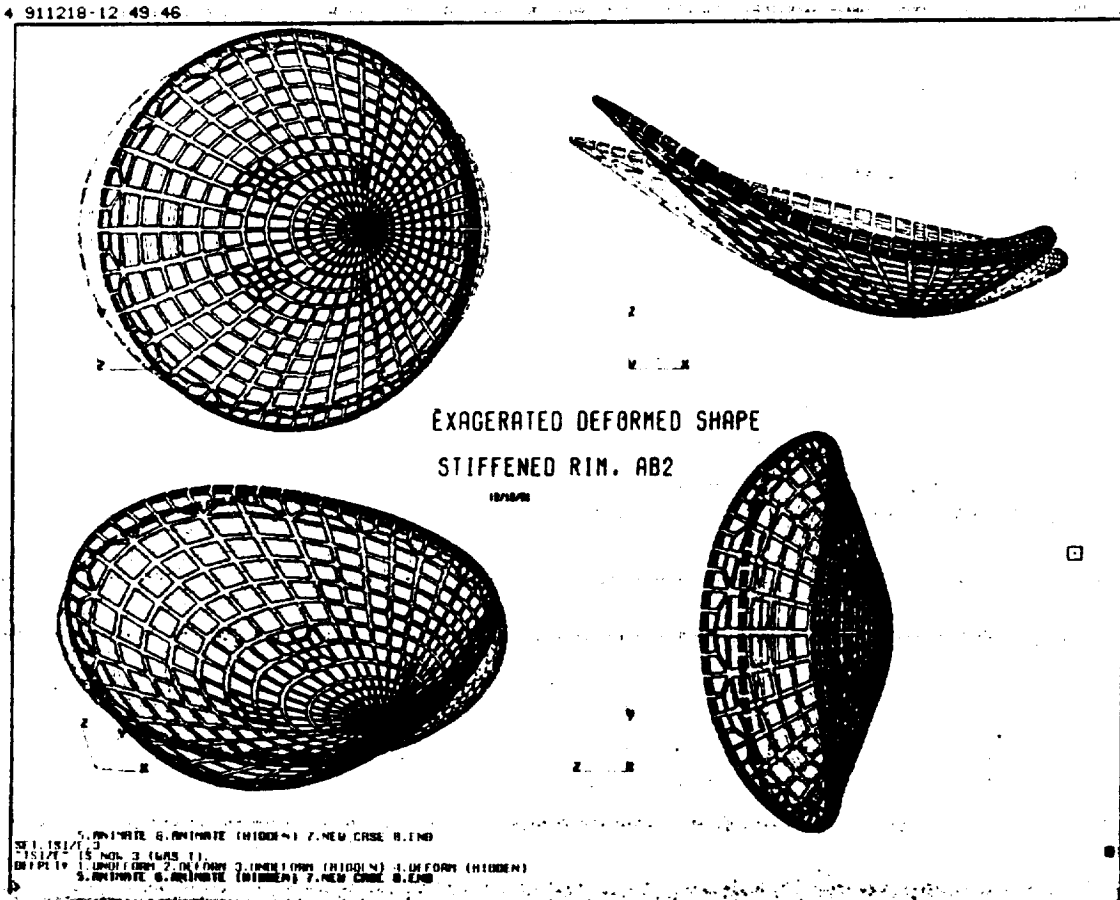


Figure 3-18. Exaggerated Deformed Shape, Blue - Undeformed, Black - Deformed

This page intentionally left blank

4 911218-12 58 27

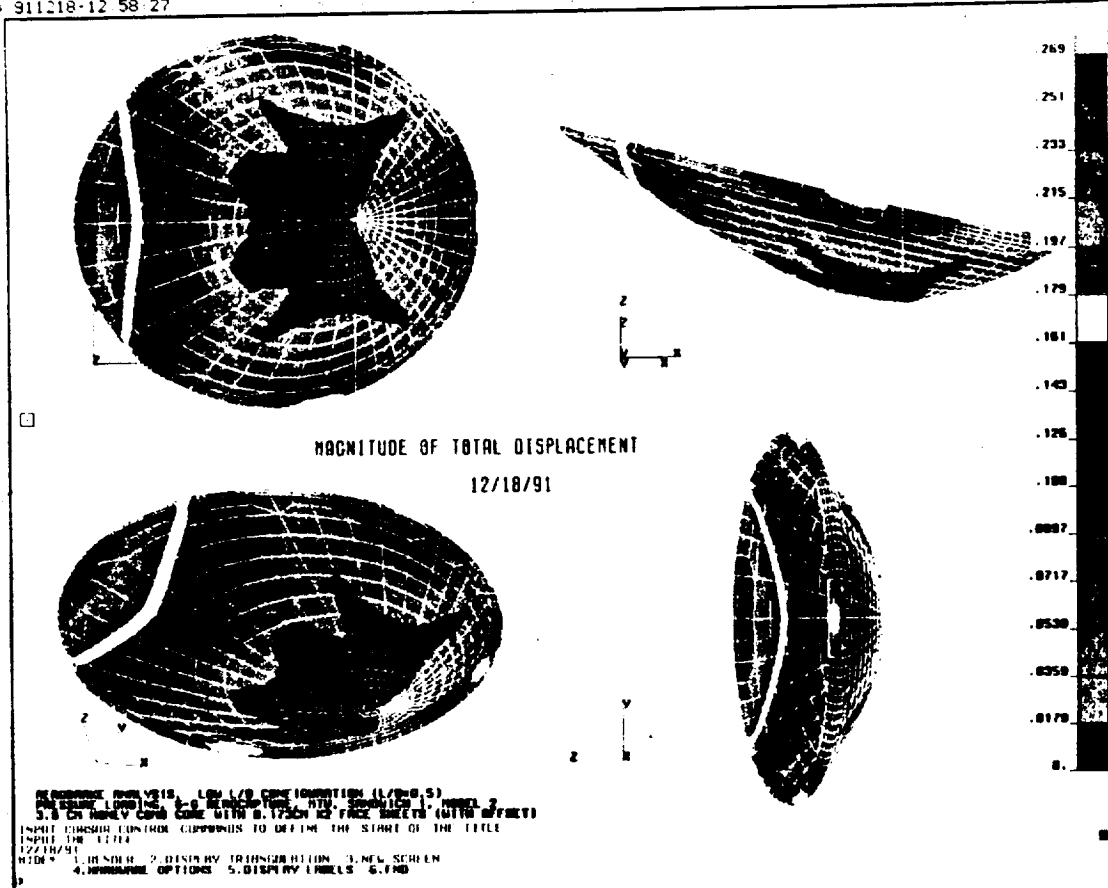


Figure 3-19. Magnitude of Total Displacements (meters)

This page intentionally left blank

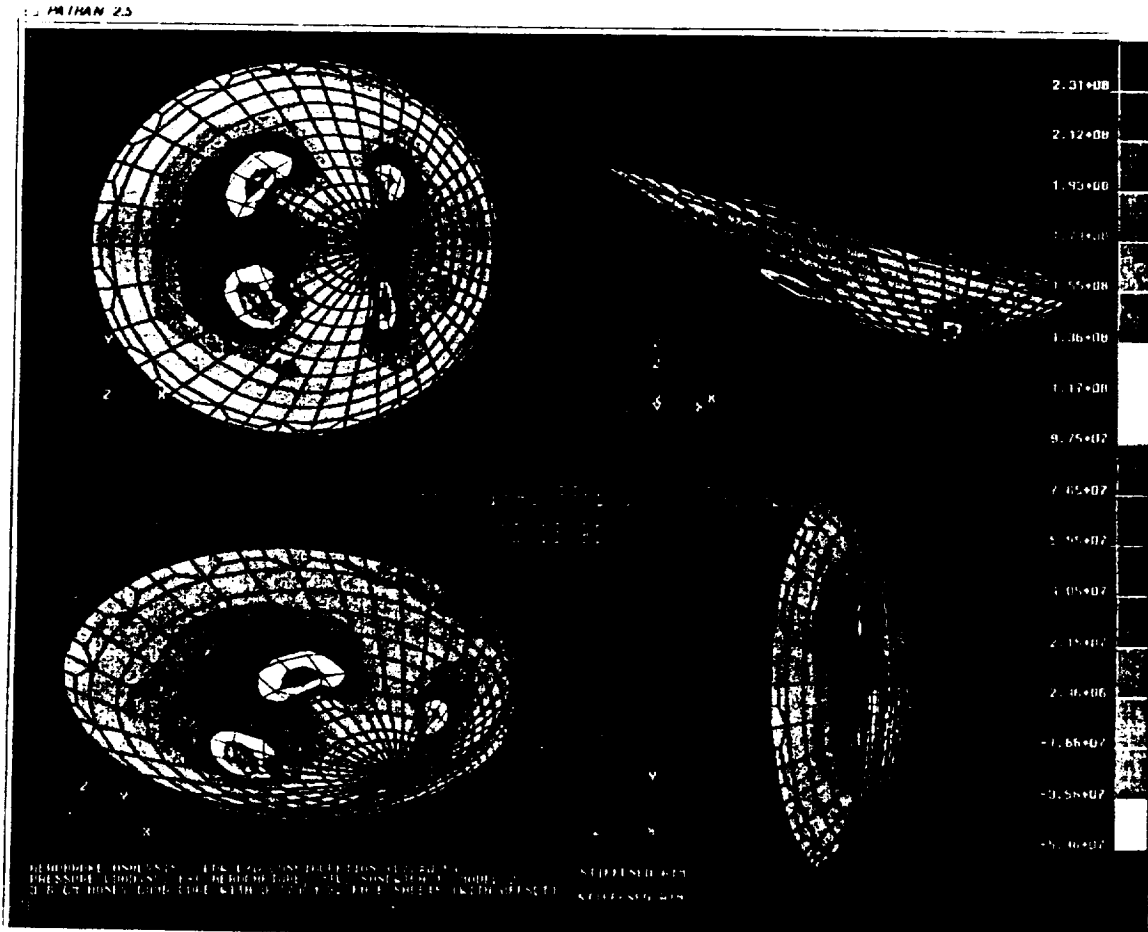


Figure 3-20. Major Principal Stresses on the Outer Surface (Pa)

Maximum displacement at the trailing edge rim	~ 0.26 m
Maximum displacement at the leading edge rim	~ 0.18 m
Margin of safety for maximum principal stress	~ 3.0
Mass of the face sheets (From NASTRAN)	~ 12.95 mT
Mass of the core (Hand calculated)	~ 4.40 mT
Total mass of the aerobrake	~ 17.35 mT

Figure 3-21. Summary of Structural Results

3.2.6 Thermal Loading

The finite element model for the Low L/D Aerobrake was updated in order to apply thermal loads and to investigate the effects of temperature gradients on aerobrake deformations. Since the temperature and pressure loads are out of phase, they do not peak simultaneously. Temperature peak is a function of the TPS. Thermal loading will be applied with reduced g pressure loading (possibly a 2g or 3g pressure).

Test cases were successfully run on a simple plate element. Complete analysis will be performed as thermal loads become available. This includes the study of optimizing the structure using spars and trusses.

3.3 HIGH L/D BICONIC MEV

A simplified structural analysis was performed in order to estimate an approximate weight of the biconic MEV, Concept 408.7033.

3.3.1 Loading

A total (vehicle plus payload) mass of 57.2 mT was assumed for this evaluation. Dynamic pressure q was calculated for a 4g, 20° entry loading as follows:

$$q_{\infty} = 0.1054 * g * Mass = 24116 Pa$$

The biconic vehicle was divided into three sections, section 1 (4 deg), section 2 (8 deg), and the nose cone as shown in figure 3-22. Pressure coefficients, C_p , vary along the diameter but are constant along the length of each respective section. For a simplified analysis, C_p along the largest diameter of sections 1 and 2 were averaged. Each C_p was applied along the length of the respective section to provide a constant pressure distribution. Since the nose section has double curvatures (semi-spherical), maximum C_p was applied there. Distributed loading per unit length of each section was calculated as follows:

$$w_i = F / L_i = q_{\infty} * C_{pi} * Diameter_i \quad \left(N/m \right)$$

where,

$$F = Total\ load\ (N)$$

$$C_{pi} = Coefficient\ of\ pressure\ for\ section\ (i)$$

$$L_i = Length\ of\ section\ (i)$$

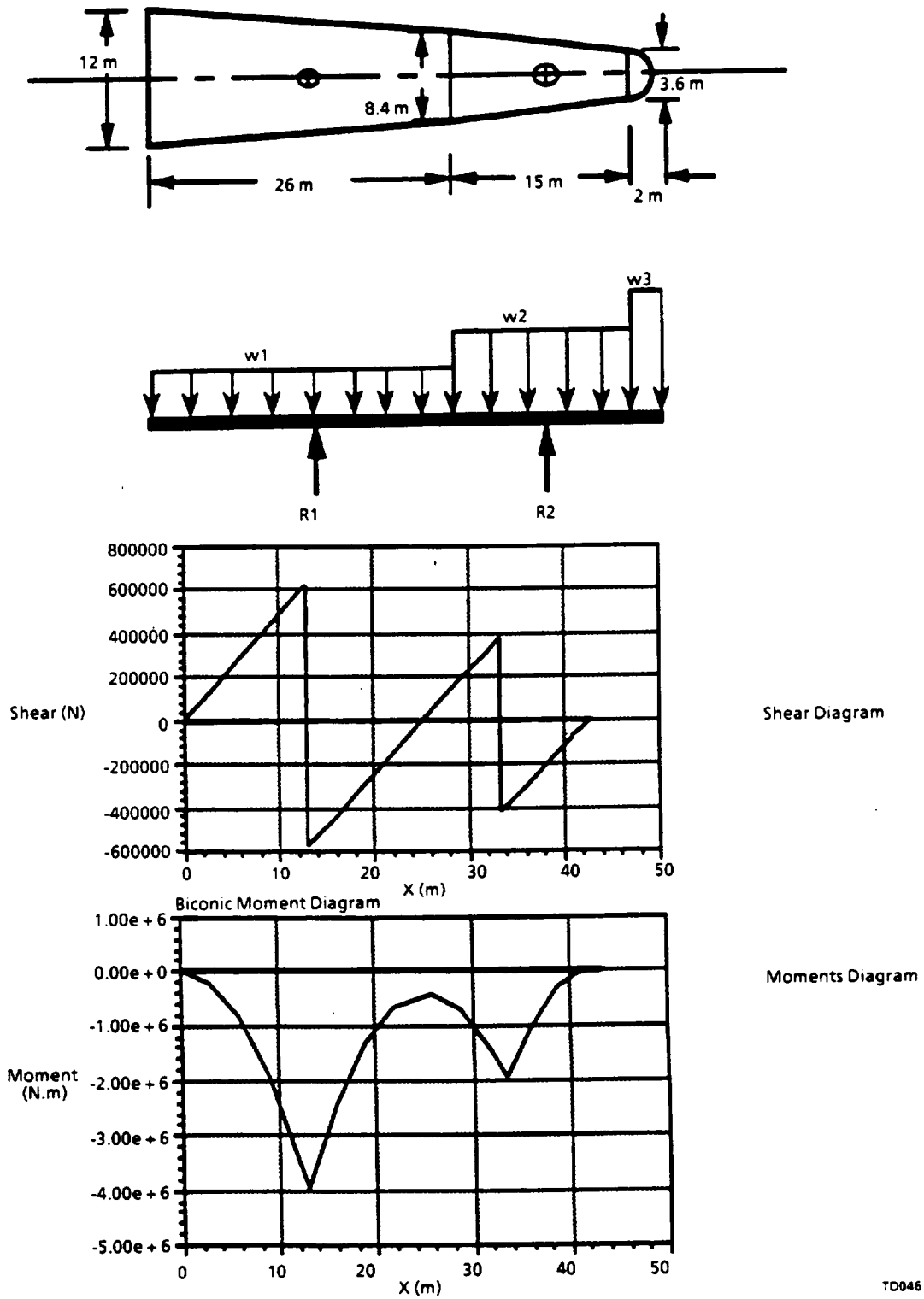


Figure 3-22. Concept 408.7033, Loading, Shear, and Moment Diagrams

3.3.2 Analysis

The biconic was analyzed as a beam with the assumption that the mass of each section was acting through its centroid. A free body diagram was constructed for this beam with lengthwise distributed pressure loading reacted at the centroids. Shear and moment diagrams were developed to find the maximum moment as shown in figure 3-22.

Using the maximum bending moment and radius for each section and a factor of safety of two (2), a minimum required thickness, t_i , was calculated. (For simplicity longerons and frames were not considered). The material for the biconic was assumed to be titanium, Ti-4Al-6V. The calculated skin thicknesses for each section were as follows:

$$t_i = \text{Moment} / \left(\pi * \sigma_{\text{yield}} * R^2 \right)$$

$$t_1 = 2.9894 * E-3 \text{ meter}$$

$$t_2 = 2.7290 * E-3 \text{ meter}$$

$$t_3 = 2.7290 * E-3 \text{ meter}$$

Material volumes for each of the sections and the nose radius were calculated using the geometry and the skin thicknesses and the total mass was calculated using the volumes and the Titanium density:

$$\text{Total Mass} = \text{Volume} * \rho = 14,750 \text{ kg}$$

The calculated mass is only a conservative approximation and will be updated as the biconic configuration becomes better defined.

4.0 LUNAR DRESS REHEARSAL ANALYSIS

4.1 INTRODUCTION

The Lunar Dress Rehearsal (LDR) task encompasses both the definition and the characterization of a piloted lunar mission in which a prototype Mars transfer vehicle is utilized for a checkout mission prior to committal to a multimission Mars program. The majority of the task study effort was focused on defining how this rehearsal mission is to contribute to insuring a successful Mars program. The program time table utilized in this study calls for a lunar checkout mission in 2010, to precede a first piloted Mars flight of 2014. This corresponds to the timetable originally set forth in the 1991 Synthesis Group Report Mars transportation implementations (ref. 3).

The primary objective of this study was to examine and characterize several options for a lunar dress rehearsal for the first piloted Mars mission. The lunar mission serves to validate key Mars vehicle subsystems and mission operations necessary to the initial Mars flight. The rehearsal mission crew will evaluate the spacecraft in its operational environment, as well as provide mission planners an opportunity to evaluate their response to their habitat for a duration approximating that of a Mars mission. By remaining within Earth-Moon space (a distance of relatively close proximity as compared to Earth-Mars distances), an emergency Earth return trip time of several days rather than months is always available. In this way, some of the risks associated with the initial use of the nuclear thermal propulsion system, and the closed-cycle ECLS crew habitation systems will be reduced over that of a first-time use of these elements at the more remote Mars distances encountered on the initial 2014 Mars flight.

In the STCAEM study, the broad initial base was selectively narrowed as the study progressed. Some detailed analyses was concentrated on specific, clearly defined SEI missions outlined in the Synthesis Report. With the selection of NTP as the preferred propulsive technology, and recommendation for a first piloted Mars flight in 2014, came a co-lateral requirement for a lunar mission to flight qualify the propulsion system and other essential technologies.

The scope of the dress rehearsal analysis included identifying and prioritizing secondary mission objectives, developing and refining a prototype vehicle concept and its subsystems, and identifying a baseline mission plan with viable options as pertaining to the objective of validating Mars mission hardware and operations. The major emphasis has been narrowed to the identification and assessment of a prototype Mars vehicle system, and a mission plan circumscribing the validation of those hardware systems and mission operations unique to the Mars missions.

4.1.1 Specific Areas of Investigation

Simulating the zero-g and radiation environment effects of the Earth-Mars outbound trajectory will be accomplished by operating, maintaining and monitoring the spacecraft for 175 days in lunar orbit or Earth-Moon space. This will supplement SSF man-tended phase findings relative to crew response to long duration habitability factors and provide the essential in-space operational experience with the prototype vehicle necessary for its flight qualification and modifications/refinements phase for subsequent Mars flights. During the study, analysis was divided into several specialized areas of evaluation. Priority items included assessments of the influence of ETO launch vehicle packaging (shroud size limitations) and on-orbit vehicle assembly operations in LEO on the reference vehicle design. Of primary importance to the qualification of a prototype vehicle is the mission data acquisition requirement, and postflight inspection of the two major hardware systems developed and utilized solely for Mars missions; the NTP and transfer habitat systems. Other investigations included identifying Mars surface mission elements to be delivered to the Moon, planning a lunar flight test of the Mars excursion vehicle ascent system and evaluating options to the reference mission plan.

4.2 MISSION PROFILE

4.2.1 Earth-Moon-Earth Transfer

A dual-engine NTP system is utilized for all major mission phases, including a three burn periapsis Earth departure to demonstrate the startup/shutdown cycling capability and post-burn cooldown operation that would be necessary for the later Trans Mars Injection (TMI) burn sequence. This system is to be as nearly identical to that of the piloted Mars mission vehicles as the development cycle will permit. After a 3-to-4-day outbound cruise period and capture into lunar orbit, a chemical LEV delivers the prototype Mars surface habitat module to the surface, where a 12-to-60-day surface mission is conducted as a means of partially 'simulating' a Mars surface mission. The low g-level Mars surface habitat module and its associated support systems hardware will be validated, as well as surface crew exploration activities anticipated for the initial Mars stay. The delivered surface hardware systems may be supplemented by existing lunar outpost power and rover systems. Subsequent to the surface mission, the NTP transfer vehicle departs lunar orbit for its 3-to-4-day return trip before being propulsively recaptured into LEO for inspection.

4.2.2 Reuse

Because of the relatively short NTP engine burn time associated with this (or any) lunar mission (approximately 1-1/2 hours total for the four burns), at least 75 percent of the expected engine operational life (in hours) is still available for use on follow up lunar missions, or for either the initial Mars cargo flight in 2012 or piloted flight in 2014. By returning the spacecraft to LEO, the crew transfer habitat module and NTP system are accessible for a detailed post-flight on-orbit inspection and are therefore available to be reused on subsequent missions. A significant front end cost reduction might result for the follow on Mars program, by completely eliminating the necessity for manufacture, launch and assembly of one "core" vehicle element (i.e. propulsion, habitat, and structural/interconnect systems). The additional resupply and reassembly required for reuse would be limited to providing a MEV, propellant tanks, and consumables.

4.2.3 Abort Modes

The transfer vehicle carries a Crew Return Vehicle (CRV) with a chemical propulsion Earth return stage, similar to the Apollo service module, to provide mission abort capability in case of main propulsion system failure.

4.3 VALIDATION OF MARS MISSION UNIQUE HARDWARE

The LDR task activity mandates a total mission transfer time of 175 days and a lunar surface stay time of 12 to 60 days. The 175-day mission duration approximates the outbound trip time of the initial 2014 Mars mission. The following key subsystems are to be validated over the course of the 175-day mission:

Space Transfer Vehicle Systems

1. Nuclear Thermal Propulsion systems
2. Transfer vehicle crew habitat module system
3. Mars vehicle truss strongback/interconnect system
4. Long term LH₂ cryogenic propellant storage
5. NTP Unique H₂ gas (boiloff/tank pressurant) RCS.

Surface Habitat Systems

6. Mars surface crew habitat systems

Surface Access Vehicle Systems

7. MEV ascent stage
8. Crew Return Vehicle (CRV)

Aerobrake Technology**9. MEV descent aeroshell**

Optional Earth entry test separate from transfer vehicle mission.

4.4 SPACE TRANSFER VEHICLE DESCRIPTION

Application was made of the preassembled tank/truss/propellant line NTP vehicle configuration, a refinement of the deployable truss NTR vehicle design developed earlier in the STCAEM study, to satisfy the requirements of the Synthesis Report Mars missions. This configuration was originally presented in the STCAEM Phase 2, Final Report (ref. 2), following a favorable assessment of its suitability to minimizing on-orbit assembly operations, launch vehicle packaging difficulties, and required ETO flights. The working configuration illustrated in figure 4-1, though optimized with respect to the aforementioned criteria relating to packaging and assembly, is not definitive of the latest Boeing Mars vehicle configuration. The current baseline Mars NTP configuration is also given in reference 2, though no finalized vehicle configuration will exist until all questions pertaining to a comprehensive Mars program, i.e., goals, requirements, payloads, support infrastructure, timetable, precursor missions, etc. are resolved.

4.4.1 Transfer Vehicle Systems

The lunar dress rehearsal vehicle utilizes NTP for all its major propulsive maneuvers. The 'core' configuration includes two NTP engines at 75,000 lbf (333.6 kN) thrust each, a tungsten/boron carbide/lithium hydride radiation shadow shield, an aft tank/RCS assembly, an interstage 'spine' truss structure that includes expendable tank attachment and connect provisions, a Mars transfer crew habitat, power, thermal control, attitude control and communications utility services, a LEV, and a small Apollo type, chemical propellant Earth return stage for a contingency abort return. This core configuration is launched in two 30-meter length by 12-meter diameter payload shrouds, with a 150-metric ton payload capability launch vehicle. Trans lunar injection H₂ propellant is provided in a single hydrogen tank launched separately. These three vehicle sections are berthed together at the two truss interface connect points in LEO. Separate propellant line installation is not required.

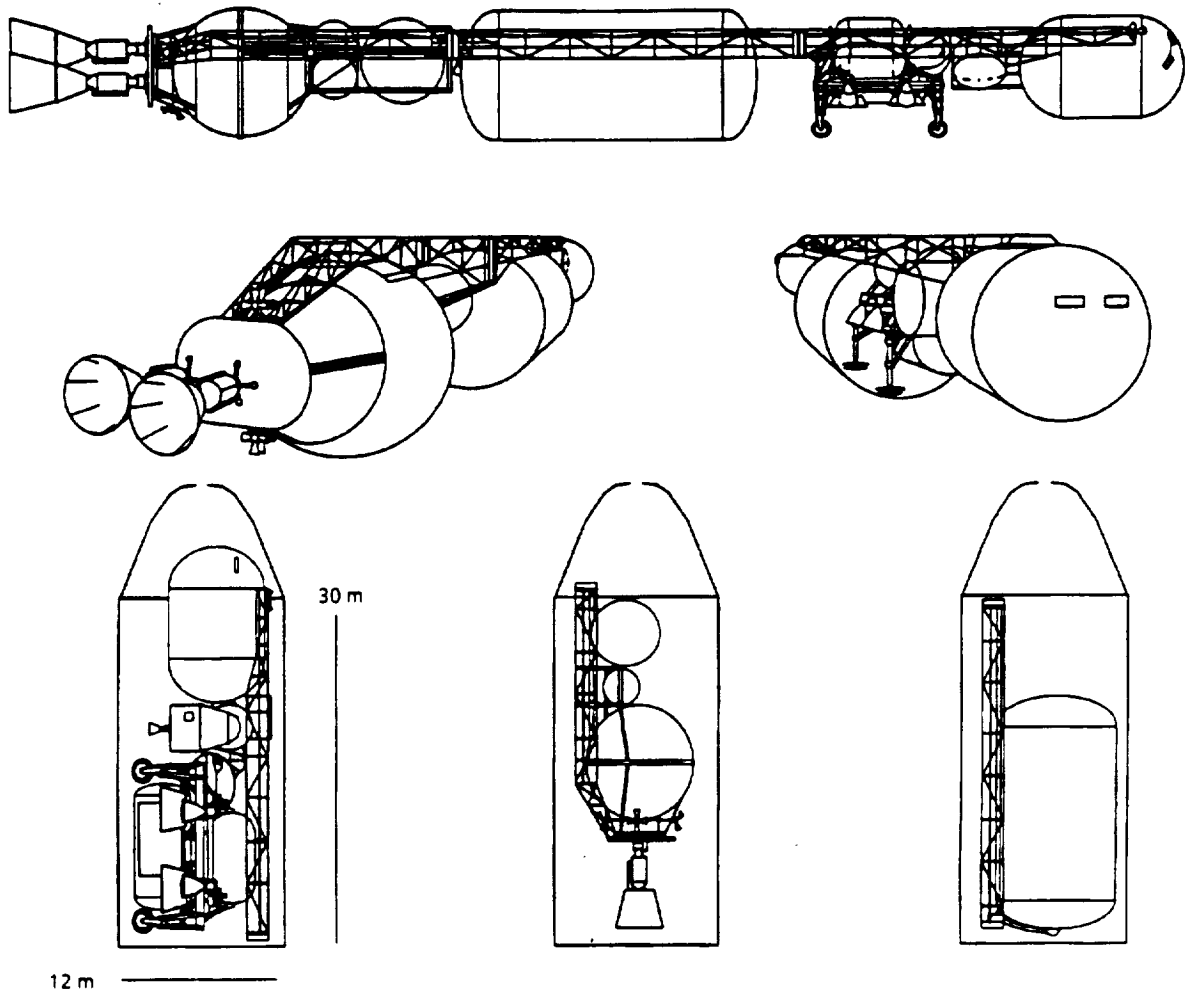


Figure 4-1. Lunar Dress Rehearsal Vehicle Sketch and Launch Manifest

TD015

4.4.2 Transfer Vehicle Performance and Mass

The vehicle IMLEO is shown as a function of lander mass and lander cargo mass in figure 4-2. For a nominal LEV delivered surface payload requirement of 30 mt, with vehicle return to LEO, the transfer vehicle IMLEO is about 400 mt. For return to a high energy elliptical orbit, IMLEO is about 315 mt.

4.4.3 Transfer Vehicle Propulsion System

The nuclear engines are advanced prismatic fuel or particle-bed engines with a thrust-to-weight ratio of 10 or greater. Isp is baselined at 925 seconds. This Isp corresponds to a 2700 K reactor fuel element temperature, a 1000 psia chamber pressure and a nozzle expansion ratio of 400. Liquid hydrogen is pressure fed, with warm hydrogen gas utilized for tank pressurization during burns. Vehicle tanks are passively

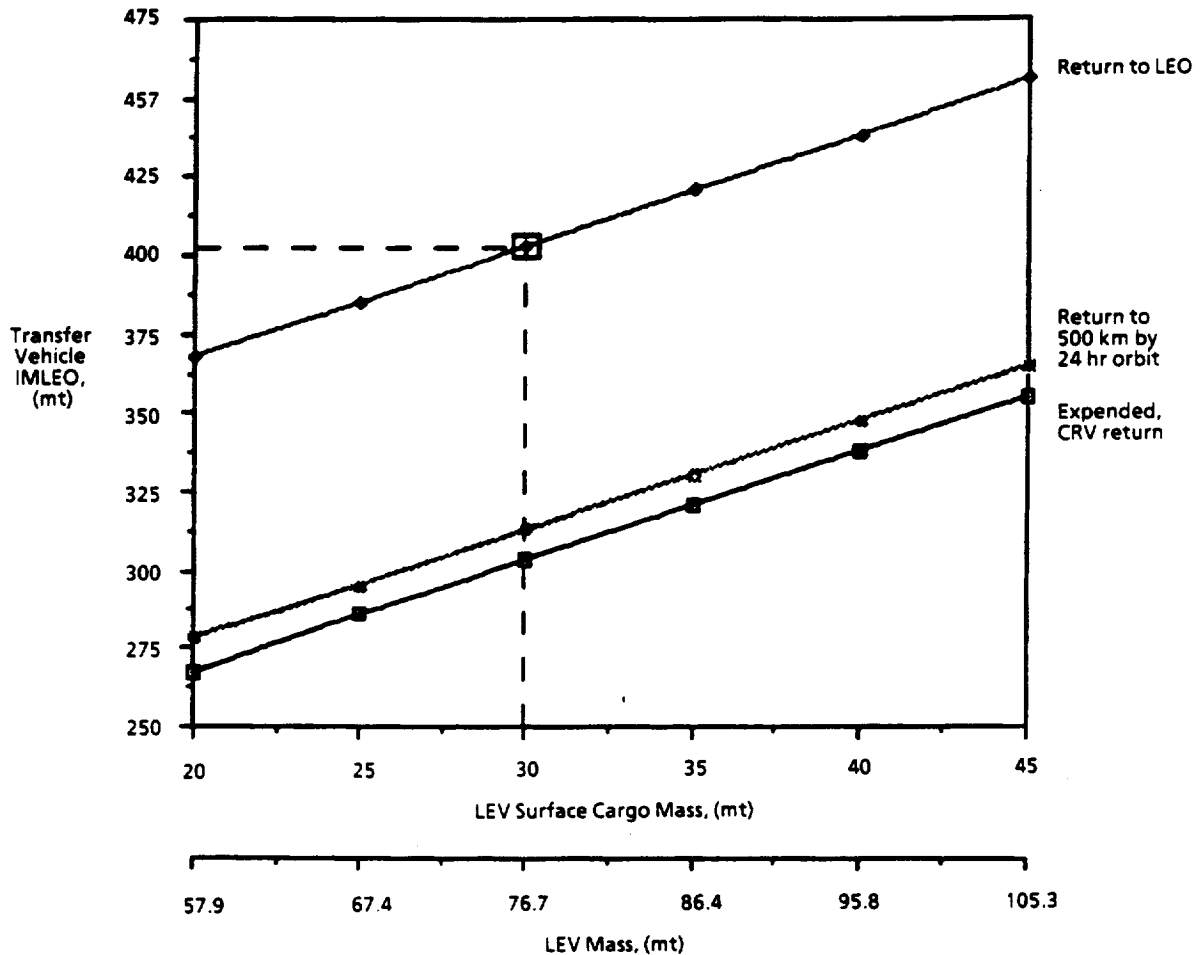


Figure 4-2. Vehicle Mass Variation with Surface Payload

TD016

insulated with multilayer insulation and vapor-cooled shields; active refrigeration is not used. Both engines are operated for all maneuvers unless one is inoperable. Mission rules provide for return-to-Earth abort in the event an engine failure. Reactor and engine-vehicle integration data (beyond that gathered during ground tests) needed to resolve NTP specific issues, or for engine qualification, include, but are not limited to, the following:

- a. Start cycle influence on fuel element cracking and reactor life. The Mars missions will require a total of 5 major burn maneuvers, including a three burn Earth departure maneuver. The impact of these thermal cycles on fuel element matrix/coating delamination and subsequent atomic H₂ fuel element erosion is a prime indicator of reactor life expectancy.

- b. **Maximum reactor temperature and reactor life.** The impact of the 1.5 hour lunar mission reactor operation time at peak temperature on fuel element integrity will provide additional data beyond that provided by ground testing.
- c. **Dual reactor neutronic interaction influence on reactor control.** The close proximity between two reactors may influence reactor neutronic control systems. Any undesirable 'control linkage' existing between the reactors is to be assessed. As an option for validating the 'engine out' failure margin requirement, a deliberate midburn single reactor shutdown might be undertaken as a means of determining what residual neutronic influence the shutdown reactor might have on the second operational reactor.
- d. **Aft tank heating effects.** Close placement of the aft H₂ propellant tank to the reactors may result in exaggerated H₂ boiloff if adequate radiation heating insulation is not provided. This may be hard to evaluate during a static ground test.
- e. **Real time measurement of transfer habitat radiation levels.** Determining transfer habitat module NTP generated radiation dose as a function of engine burn time and H₂ propellant shielding influence would be desirable, and would serve as a data point for verification of analytical radiation code predictions used during the vehicle design phase. The lower delta-V lunar mission results in a lower level of reactor total fission product buildup than that of the later higher delta-V Mars missions. Predicted NTP Mars crew habitat generated radiation dosages can be extrapolated from lower levels generated on the lunar mission.

4.4.4 Transfer Vehicle Crew Systems

The transfer habitat is an aluminum composite-reinforced metal matrix pressure vessel with unreinforced interior secondary structures. It provides full-service crew systems with private quarters, galley/wardroom, command and control, health maintenance, exercise and recreational equipment, and science and observation posts. Crew suggestions pertaining to placement and operation of habitat systems will allow for needed internal geometry reconfiguration and refinements prior to initial Mars missions.

4.4.5 Radiation Sources

Mars mission radiation exposure to the crew is a primary concern to mission planners due to the variety of radiation sources and uncertainties involved with estimating their magnitude and frequency. The exact levels and frequencies of exposure accumulated over the course of a Mars mission, and the biological sensitivity of

astronauts to these radiation sources are difficult to quantify. The uncertainties in this area are threefold:

- a. The quantitative characteristics of the radiation in space are poorly known (i.e., number of particles, energy spectrum etc.)
- b. The interactions of high-energy particles with various shield material are in doubt
- c. The effects of the particles of different energy on human tissue (i.e., the relative biological effectiveness) are largely unknown.

A real-time measurement of actual radiation dosages impacting the vehicle habitat module in an environment outside the Earth magnetosphere will serve to validate internal geometric attenuation methods. The primary radiation sources to be shielded against are:

- a. Van Allen. A belt of trapped radiation surrounds the Earth except in the polar regions. Two zones of intense radiation exist within the belt. The interzone contains many electrons, but more importantly, a large number of protons, of energies of over 30 mev confined to altitudes between about 400 and 5,000 nautical miles. The outer zone extends over a much wider range of altitudes but is mostly composed of electrons, which are easily stopped by a thin sheet of metal.

To minimize large Earth departure gravity losses for the high delta-V Mars missions (brought on by small vehicle thrust-to-weight ratio at Earth departure), a three burn periapsis maneuver is employed. This would mean that three passes would be made through the Van Allen belt.

- b. Cosmic Ray. Cosmic radiation consists of very energetic atomic nuclei, over 90 percent of which are protons. However, heavier particles, such as alpha particles, comprise more than 30 percent of the total by weight and also have far more deleterious effects on man. Cosmic-ray fluxes exhibit a significant variation with time which is related to solar activity.
- c. Solar Flares. At irregular intervals, the Sun emits bursts of radiation which are classified according to the area of the visible disturbance on the Sun's surface. Class 1 and 2 flares occur almost continuously, but their accompanying radiation is believed to be sufficiently low in energy that it is stopped by even thin walls. Class 3 flares, which occur on the average of about once a month, emit mostly protons (of energies up to 500 mev) with possibly 10 percent alpha particles.

At rare intervals there occur giant major flares. These are large flares of the Class 3 category which may emit up to 10,000 times the usual intensity radiation

with particle energies as high as 20 bev. The greatest portion of shielding attenuation is aimed at this Class of event.

- d. NTP. NTP reactor radiation is composed of gamma rays and neutrons, which are of fairly low energy in comparison with the naturally occurring particles.

The above information on radiation sources and uncertainties was taken from reference 4.

Dedicated radiation shielding is not provided in the baseline Mars transfer vehicle habitat module; radiation dose calculations indicate that the shielding provided by the transfer habitat structure, systems and consumables is adequate to protect the crew, assuming the crew uses the galley as a storm shelter during severe solar proton events.

4.4.6 Transfer Vehicle Attitude Control Propulsion System

The control propulsion system is provided by mechanically compressed hydrogen gas obtained from the main H₂ tank boiloff or tank pressurant GH₂. Hydrogen gas accumulators provide sufficient storage for any one auxiliary propulsion maneuver and are recharged during coast periods; the accumulator capacity is sized by Earth-Mars leg midcourse correction requirements. Nuclear engines have low-rate gimbal capability for center of gravity tracking; the attitude control propulsion system provides attitude damping during thrust periods.

4.4.7 Transfer Vehicle Truss Strongback/Interconnect System (Structures)

Propellant tanks are constructed of aluminum-lithium alloy, or metal matrix composites pressurized to 25-35 psia. Intertank and other main structures employ advanced composites for reduced mass. The truss strongback or 'spine' uses a simple rigid (load carrying) truss arrangement that allows for preassembly and integration of tanks, propellant lines, pressurant lines, and other umbilicals directly to the truss at the ground station assembly building. These elements are preassembled and flown in the ETO vehicles as complete preintegrated units to minimize the on-orbit assembly task. The transfer vehicle is divided into three elements as shown in figure 4-1. This configuration was developed as a means to minimizing the complexity and number of assembly tasks required on orbit, as well as for facilitating launch vehicle packaging. All tank gas pressurant lines, power lines and communication lines, (i.e. cable trays) are connected at these two interfaces. Only a single H₂ propellant connection is required at the aft-mid truss interconnect. Filled tanks are flown up to orbit. The only assembly required on-orbit is the joining of the three vehicle segments at the two truss

interconnect planes. This represents the absolute minimum in assembly operations that is possible for a three ETO vehicle delivery. It may be possible to eliminate the need for an assembly platform altogether by attaching RMS/RCS packages to two of the three vehicle elements to provide for autonomous self assembly. A description of the ETO flight manifests is given below. No less than two operations is possible. Further reductions in assembly operations can only be had by utilizing larger ETO vehicles that can deliver the complete spacecraft in only one or two flights.

4.4.8 Earth-to-Orbit Vehicle Flight Manifests

Three flights are planned to perform this portion of the mission.

- a. Flight one delivers the transfer habitat system, forward truss section, CRV/chemical abort stage, solar panel system and the LEV.
- b. Flight two delivers the engine/aft tank/RCS/Lunar Orbit Capture (LOC) propellant assembly.
- c. Flight three delivers the large TLI tank/midtruss assembly.

4.5 VALIDATION OF MARS MISSION UNIQUE OPERATIONS

In-orbit and in-flight operations unique to the Mars mission will be conducted to insure that the capability to accomplish these operations is in place before the first Mars mission elements are delivered to orbit. These operations are listed according to their chronological order in the mission timeline, figure 4-3.

4.5.1 On-Orbit Assembly/Assembly Platform

On orbit delivery and construction of the vehicle assembly platform precedes all other space activities. This platform, co-orbiting with SSF in LEO will serve the rehearsal and all Mars missions. Its design may be transfer vehicle configuration dependent and specific. It is delivered as a one piece unit and assembles spacecraft sections utilizing SSF or ground control. The optimal extent of automation vs. man-in-the-loop control/monitoring vs. EVA assistance was not addressed in this study. After assembly, preflight checkout tests are conducted before the crew board the craft. Additional checkouts and crew training follow, with the vehicle under assembly platform control until the spacecraft is given authority to separate and fly in formation in LEO with SSF and the assembly platform. The delivery, assembly and checkout sequence for the rehearsal mission may represent the first truly autonomous vehicle construction task in space. Validation of these operations is key to meeting the Mars program assembly timetables planned for the 2012 - 2018 time period.

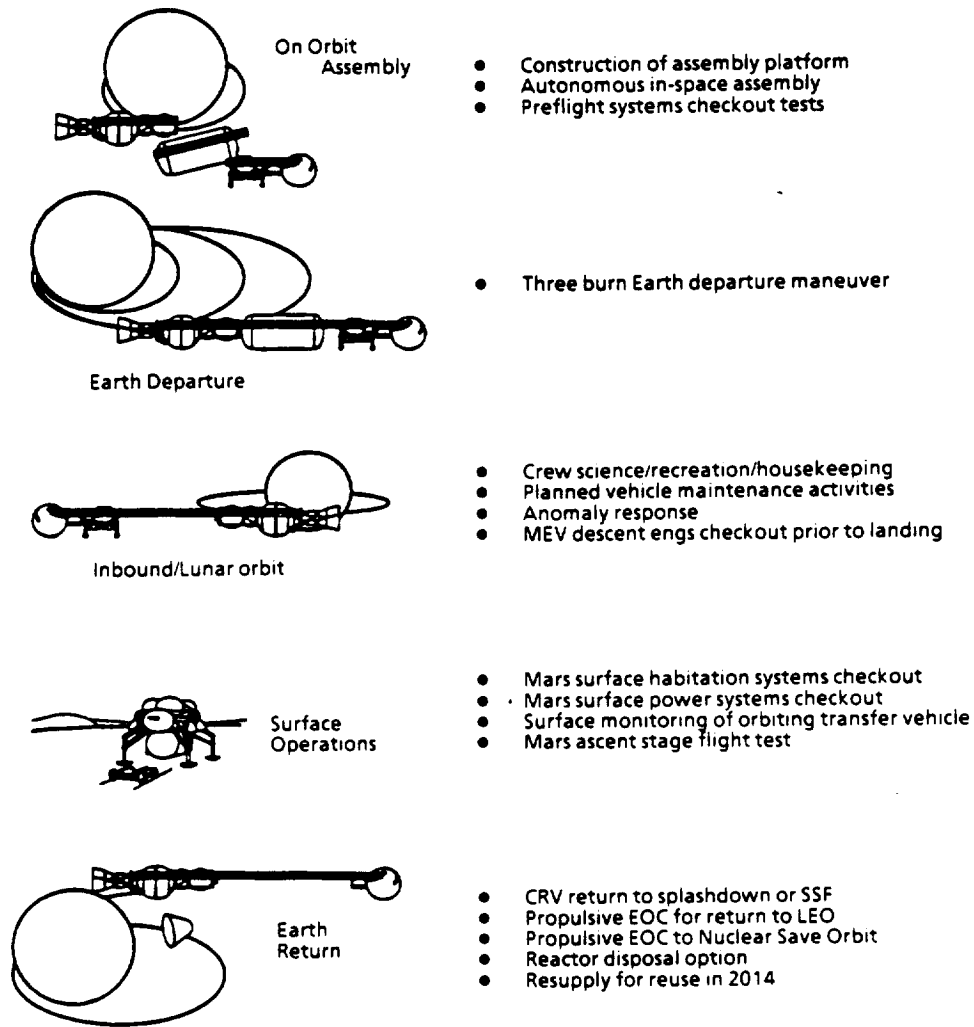


Figure 4-3. Validation of Mars Mission Unique Operations at the Moon

T0017

4.5.2 Outbound Flight/Lunar Arrival/Lunar Orbit

During this phase, crew science/recreation/vehicle housekeeping and maintenance activities are carried out. Anomaly response, as required, is carried out and documented for hardware modification/upgrades for the Mars flight vehicles. Propellant tank jettison occurs at the end of Earth departure and lunar capture burns. LEV descent engine checkout tests may be conducted as a review for the Mars missions.

4.5.3 Surface Operations

The following operations fall into this category: (1) Mars surface habitation systems checkout (see section 4.6); (2) Mars surface power systems checkout; (3) verification of

surface system control and monitoring of orbiting transfer vehicle capability; and (4) Mars ascent flight test (see section 4.8).

4.5.4 Inbound Flight

Continuation of crew science/recreation/housekeeping/maintenance and anomaly response activities. Crew response to zero-g isolated environment data documented. Real-time radiation assessments continued.

4.5.5 Earth Return

In this category are the following: (1) propulsive vehicle EOC burn for return to LEO for inspection, (2) EOC burn for return to nuclear safe orbit for inspection, (3) reactor disposal option (see section following), or (4) CRV return to SSF or splashdown.

4.6 SURFACE MANIFEST

A surface stay duration of 90 days is planned for the 2014 first piloted Mars mission as outlined in the Synthesis Group Report (ref. 3). A JSC supplied surface habitation/exploration manifest for this mission is given in figure 4-4. The total cargo allotment according to this manifest, to be delivered and deployed at Mars, is 115 metric tons. This equates to more than 1.2 metric tons of mass per day of stay time and 15 metric tons per individual crew member. This total includes two surface habitat modules, two airlocks, surface power generation equipment, spares, exploration equipment and other items. It was assumed in this study that a lunar lander capable of delivering up to about 30 metric tons would be available. This vehicle is described in some detail in section 4-7. It was determined that the rehearsal mission would deliver one LEV cargo load to the surface, which means that only about one quarter of the planned 90 day Mars surface mass could be delivered and operated on the Moon for checkout purposes. Those elements selected for the rehearsal flight are indicated in figure 4-4 as the boxed items. These include a 23.9 metric ton outfitted habitat module, a 5.5 metric ton 2 person airlock and 1 metric ton of communication equipment. It was also assumed that surface power is available to these systems from a lunar outpost or base power supply. The rehearsal mission surface stay time must be commensurate with the surface habitation systems actually delivered. A question arises as to what extent a crew of 6 outfitted with a 30-ton portion of the planned 115-ton manifest can validate the surface systems necessary to the follow-on Mars missions, especially the conjunction class missions that are characterized by stay times of as much as 600 days.

		<u>Flight 1</u>	<u>Flight Mass</u>	<u>Total</u>
		Equipment: offloading/construction	5.75	34.81
		Power: Martian module (100 kW)	5.98	
		Power management and distribution	2.50	
		Rover: Pressurized Mars	6.50	
		25 kW power cart	6.00	
		Experiment/sample trailer	3.45	
		Flare warning system	0.23	
		Mars geology/exobiology equipment	0.56	
		---	---	
		---	---	
~30 mt		<u>Flight 2</u>	<u>Flight Mass</u>	<u>Total</u>
				34.84
Habitat, Airlock & Equipment →	Habitat Module 1 (Martian)	23.85		
	Airlock: 2 person, Martian	5.50		
	Communication equipment, Martian	0.94		
chosen for Lunar validation	Habitat analytical lab instruments	0.15		
	Biomedical lab	0.50		
	Discretionary	0.30		
	---	---		

		<u>Flight 3</u>	<u>Flight Mass</u>	<u>Total</u>
		Habitat Module 2 (Martian)	25.50	34.75
		Airlock: 2 person, Martian	5.50	
		Power: Mars PVA/RFC system (25 kW)	2.65	
		---	---	
		---	---	

Figure 4-4. Mars Surface Exploration Manifest - 2014, 90-day stay

4.7 SURFACE HABITAT SYSTEM DELIVERY

It was assumed in the analysis that a "heavy delivery" lunar cargo lander would be available for a 2010 mission. Initial lander work was concerned primarily with refinement of an earlier STCAEM study Lunar Excursion Vehicle (LEV) single-stage lander design for application as the delivery vehicle for the prototype Mars surface crew habitat module and airlock. This lander design, outfitted in its piloted/cargo configuration as shown in figure 4-5, was chosen because of its effectiveness in delivering the combination of a single large surface habitat module of up to 30 metric tons and a six man excursion crew cab.

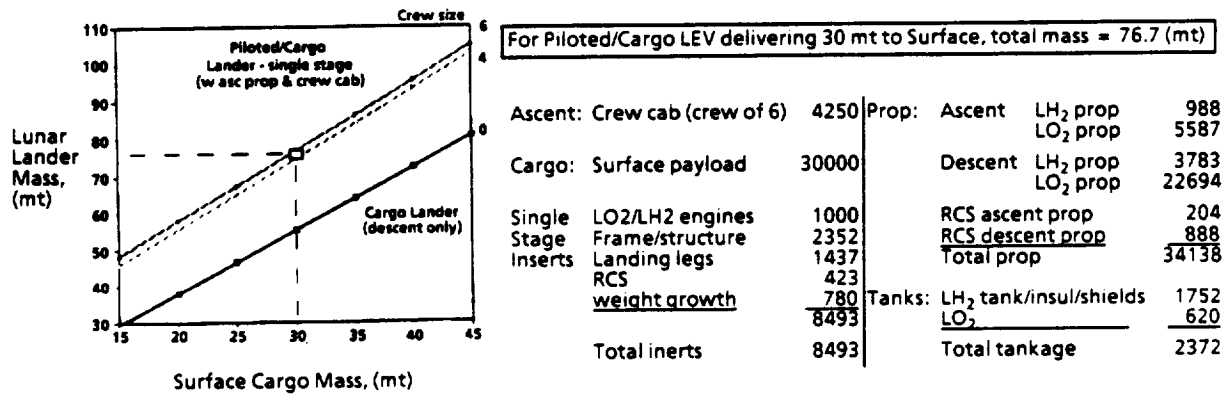
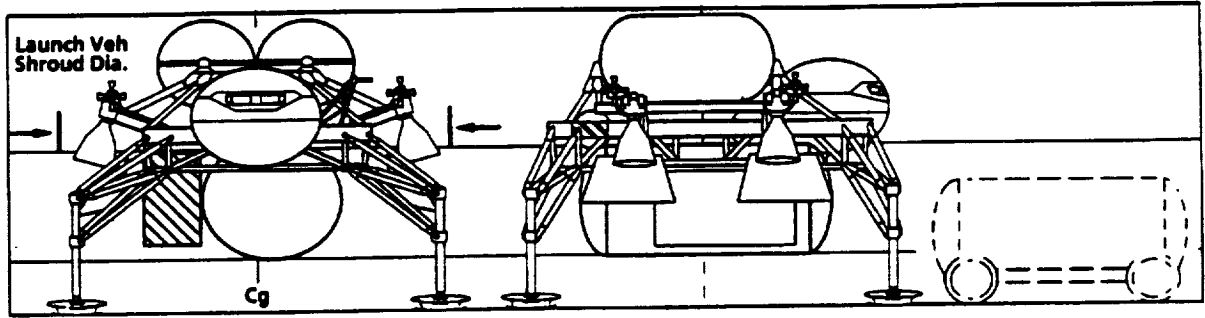


Figure 4-5. Lander Mass Variation with Surface Payload

TD019

4.7.1 Lunar Lander Design and Application

This vehicle provides for unassisted cargo downloading directly to the surface by mounting the cargo underneath its propellant tankage/propulsion system instead of above it or to each side. Positioning the cargo in this fashion is the key to providing for safe and efficient unloading operations. The cargo module or pallet is attached from above to the cargo bay, which lies below the base of the engine extension frame structure and propellant tanks. The vehicle illustrated utilizes four engines, arranged at four 'corners', with each engine extending out over the cargo bay as shown. In this 'over-top' position, the engines are positioned around the vehicle c.g. and above the surface a few meters, well out and away from the cargo. LO₂/LH₂ main engines at 475 Isp and N₂O₄/MMH storable propellant RCS thrusters at 280 Isp are used. Engine nozzles are canted slightly outward from the vehicle and have plume impingement shields to prevent exhaust gas impingement on the cargo (the Apollo lunar Excursion Module LEM utilized similar shields for its RCS thrusters). Opposed engine shut down, engine gimbaling and RCS compensation is used for engine out recovery. Two pairs of LO₂ and LH₂ tanks sit atop frame/cargo bay structure and are positioned such that vehicle c.g. does not shift during the descent burn.

4.7.2 Lander Cargo Downloading

This 'undercarriage' design specifically eliminates the difficulties inherent to the 'top-loaded' and 'side-loaded' cargo lander designs since no assistance is required from a separate overhead crane or gantry type off-loader (top-loader lander design requirement), and the cargo does not have to be divided for side placement (side-loader lander design requirement). Increased access to the cargo by surface transporters, ease of cargo ejection for an emergency descent abort maneuver, immediate cargo drop for emergency ascent to orbit, and contiguous placement of the surface habitat module and excursion crew modules are the advantages provided by this configuration. The design incorporates lessons learned from terrestrial cargo delivery helicopter operations (ref. 5).

4.7.3 Lander Mass and Performance

Required lander mass is plotted vs. surface cargo mass (Mars habitat module in this case) for two versions of this vehicle type: the piloted/cargo version, and an unmanned cargo only design. The cargo only version differs in the lack of the crew cab and ascent propellant. With 30 metric tons of cargo, the piloted version weighs approximately 76 metric tons including descent and ascent propellant. Vehicle thrust-to-weight ratio is approximately 1.6 with two (of the nominal four) engines operating. The following delta-Vs were used: descent: 2000 m/s, ascent: 1900 m/s, descent RCS: 35 m/s, ascent RCS: 35 m/s. Vehicle maximum width and depth is less than the allowed 12-meter ETO shroud diameter. A flatbed surface transporter can be carried underneath the cargo for immediate transport after touchdown.

4.8 MARS ASCENT STAGE CHECKOUT TEST AT THE MOON

Demonstrating MEV ascent stage performance prior to committal to piloted flight is the objective of this addition to the baseline mission plan. Propulsion systems, flight control systems, and propellant thermal insulation systems are three key technologies to be validated in a lunar test of a Mars ascent system. Testing of a Mars only lander on the lunar surface as an option in a development and test program was considered as early as 1967 in one major MEV study (ref. 6).

4.8.1 Flight Plan for Propulsion and Flight Control Systems

The propulsion and flight systems can be demonstrated by an unmanned ascent to lunar orbit flight. Selection of a descent stage for delivery of the prototype Mars ascent stage are presented for three options.

- a. **Option One.** Assuming that some form of lunar transportation system is already operational by 2010, an option entails the utilization of a pre-existing lunar vehicle descent stage for delivery of the ascent stage test article and seems the most obvious choice. Since current analyses tend to favor cislunar optimal single-stage vehicles, however, a significant modification to the lunar lander design would be necessary to configure a two-stage vehicle consisting of a lunar system descent stage with the MEV ascent stage as its second stage.
- b. **Option Two.** This option consists of utilizing a prototype MEV descent stage as the descent delivery stage. The MEV must accommodate entry heating and will employ aerodynamic braking to reduce descent propellant mass; the lunar vehicle descent is unaffected by descent heating and cannot make use of aerobraking. Since this stage is primarily an aero-deceleration driven design, a modification would be necessary for its use as a delivery stage for a lunar test. Following this approach, a complete two stage Mars excursion vehicle would have to be delivered 2 or 3 years earlier than would otherwise be necessary, compressing an already busy hardware delivery schedule.
- c. **Option Three.** Due to the extent of the modifications necessary to either a LEV single stage or MEV aerobraked stage, the development of a 'one use only' descent stage from either of these two options might be undesirable. A lower cost alternative is available that can satisfy the test objective. The reference MEV ascent stage test article propellant tank capacity is sized to provide the 4500 to 5000 (m/s) of Martian ascent delta-V needed to reach the transfer vehicle orbit for rendezvous. In contrast to this, the sum of both the lunar descent and ascent-to-orbit burns is approximately 3900 (m/s), well below the capability of a MEV ascent stage if flown with its tanks completely full. Consequently, it is proposed that this ascent stage fly both the lunar descent and ascent to orbit maneuver as a single stage, with the sole addition of a minimum weight landing leg set for touchdown. Option three was assessed as making minimal impact to the development schedule and cost. An ascent stage vehicle concept of option 3 is illustrated in figure 4-6.

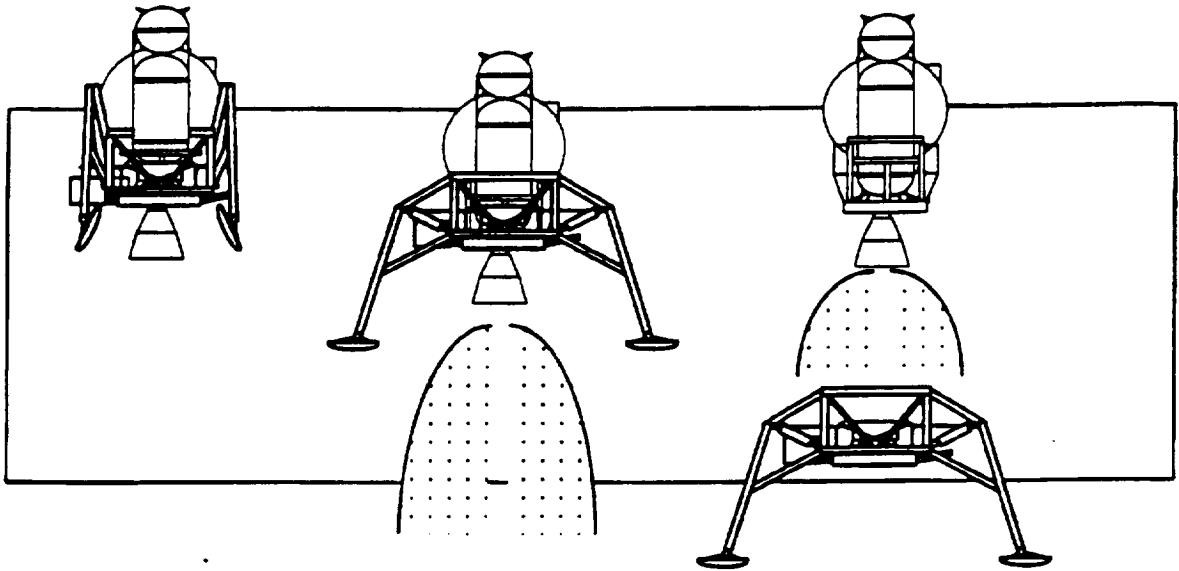


Figure 4-6. Mars Ascent Stage Lunar Checkout Flight

TD020

4.8.2 Cryogenic Propellant Thermal Insulation Validation

Advanced passive thermal insulation systems required of the high Isp cryogenic propellant propulsion systems need validation over long periods in the space environment. The performance of the insulation systems are of critical importance; uncertainty concerning their capability would force a program decision to drop that technology in favor of the significantly lower performing storable propellant systems, reducing the available cargo delivery capacity of the MEV for all but the long stay conjunction missions. Cryogenic thermal insulation systems are very sensitive to failures in the vacuum jacket system, reference 7. Small penetrations in the jacket could result in a significant loss in thermal insulation integrity, resulting in H₂ boiloff rates so excessive that surface mission activities would of necessity be abandoned to effect an immediate ascent to orbit while sufficient propellant was still in the tanks. Therefore, for MEV ascent stage designs utilizing the cryogenic propellants, the test plan should allow a reasonable period of thermal insulation system exposure to the environment of space to validate analytical predictions of boiloff rates and meteoroid damage assessments to vacuum shell integrity.

4.8.3 Mars Descent Aerobrake Qualification Flight

The approach to an MEV test plan is outlined in this section. An MEV checkout test plan involves boosting the Mars excursion vehicle to LEO and allowing it to descend to Earth in such a manner as to duplicate, as much as possible, the loadings and velocities that will be encountered on Mars mission descents. Because of the differences in gravity fields and atmospheres between the Earth and Mars, descent corridor entry conditions and trajectory profiles will necessarily be different. The entry to descent point will be higher to compensate for a more dense Earth atmosphere, however it is not possible to match the lapse rate with that of Mars. Offloading weight could compensate for the larger Earth gravity under steady state conditions but that would influence the dynamics and controllability of the vehicle, an important checkout point, and therefore offloading is not considered. It is assumed that actual flight hardware is to be used, i.e., a full scale version of the MEV. It is clear that the entire flight corridor of a Mars descent cannot be reproduced in its entirety, but we can match one or more points or segments of that trajectory. The hypersonic portion of the flight is deemed as most important for testing, as the more severe loads are placed on the vehicle in this regime. The potential Mars flight corridors can be uniquely defined by dynamic pressure vs. relative velocity profiles. A constant angle of attack is maintained during the hypersonic portion of the descent. Thus, the plan is to determine an Earth descent which will most nearly match a nominal dynamic pressure vs. relative velocity profile with emphasis on the hypersonic regime. It will be desirable to examine as much of the corridor as possible, therefore it might be possible to extend the flight test domain by investigating a skip out trajectory which would intersect the corridor multiple times. Finally, analysis must verify that a boost vehicle is capable of placing the descent vehicle in desired entry corridor. No further analysis has been done at this point.

4.9 LUNAR DRESS REHEARSAL MISSION SCHEDULES

Schedules were developed from data generated in Phase 1 of the STCAEM study, references 8 and 9. These, together with the program schedule generated from the Stafford Committee Report, dictate the timing and extent of the required development.

Program Full Scale Development (FSD) was based on the required commitment to project FSD for the reactor and engine development to produce a flight qualified, man rated system available for integration into and testing of mission flight article prior to the first launch date in mid- 2010.

Man rating involves qualifying several critical early-needed Mars systems that will be placed in trial checkout by the lunar dress rehearsal. These items, previously

identified, are shown on individual schedules under the man rating heading. These do not constitute the entire systems that must be developed. As an example, the ECLS is part, but not the whole, of the required habitat development. The habitat development, therefore, is shown as a separate schedule. Some items have an importance that is not apparent from the program schedule; an example of this is the Self-Check techniques, where the procedures must be incorporated into other systems prior to their qualification testing. This indicates that there is some cross schedule influence. Where possible, those items that directly affect each other are shown in the same schedule page. As many as possible of the schedules that have a major impact on the overall program were done in the time available in this study. These schedules are shown in figures 4-7 to 4-13.

4.10 FOLLOW ON LUNAR MISSIONS

Early exploration, extended exploration, and exploitation of lunar resources represent three categories of manned lunar operations. If SEI plans eventually call for extended exploration or resource exploitation, a period of heightened lunar operations would be entered into which would create the need for larger accumulations of equipment on the Moon. Extended operations in this phase would call for a further reduction in transportation costs. Reusable surface-to-orbit vehicles would be used at the Earth and at the Moon, and a reusable ferry would carry the larger payloads between their orbits. NTP vehicles such as the one described may provide economy over other propulsion vehicles such as the lunar chemical propulsion vehicle, paving the way for the accomplishment of two national space program goals.

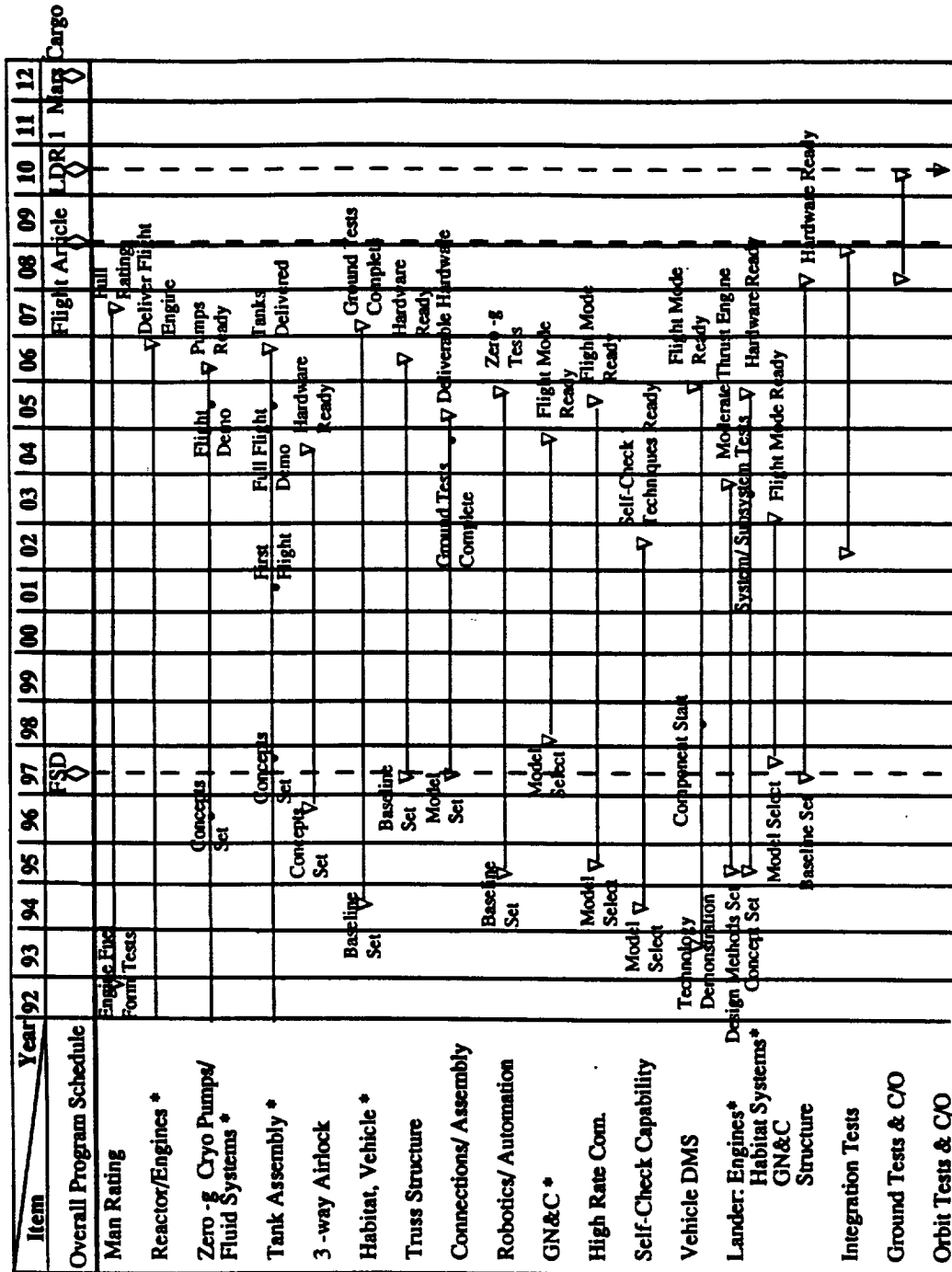


Figure 4-7. Lunar Dress Rehearsal - Top-Level Development Schedule

Item	Year	92	93	94	95	96	97	98	99	00	01	02	03	04	05	06	07	08	09	10	11	12
Overall Program Schedule																		Flight Article	LDR 1	Mars		
Nuclear Rocket : Begin Fuel Form Tests		▽																				
Test Facility Requirements & Design Approach			▽																			
Reactor Design & Technology Level Selected																						
Electric Furnace Fuel Tests Complete								▽														
Reactor/ Engine Tests										▽												
Engine Development Tests										▽												
Engine Qualification Tests Complete																	▽					
ECLSS: CELSS Baseline Select																						
SSF ECLSS Qualification																						
CELSS Brassboard Demo																						
Mars ECLSS Select																						
Mars ECLSS Full-Scale Development																						
SSF CELSS Experiments																						
Ground Qual. Tests Complete																						

Figure 4-8a. Lunar Dress Rehearsal - Man-Rating Approach

02

Item	Year	92	93	94	95	96	97	98	99	00	01	02	03	04	05	06	07	08	09	10	11	12	
Overall Program Schedule							FSD										Flight Article	LDR 1				Mars Cargo	
30 K Cryo Engine (lander): Ground Test for high Isp & throttling																							
LTV Transfer/ Landing Engine Qualification																							
LTV Flight Measurements																							
LTV Engine Lunar Mission																							
Transfer & Gaging Systems																							
LTV/LEV Transfer & Gaging First Use																							
Cryo Propellant System: Insulation System																							
Zero - Tests Cryo Simulations																							
Ground Test Demo Transfer & Gaging Tech.																							
Qual Tandem LTV Cryo System																							
LTV Cryo System First Flight																							
Lunar Mission																							
Transfer &Gaging Flight																							
LTV/LEV Transfer/ Gaging First Use																							

Figure 4-8b. Lunar Dress Rehearsal - Man-Rating Approach

Item	Year	92	93	94	95	96	97	98	99	00	01	02	03	04	05	06	07	08	09	10	11	12
Overall Program Schedule							FSD										Flight Article		LDR 1		Mars Cargo	
Avionics:																						
Component Technology Demonstration																						
Brassboard Demonstration																						
Software Development Environment Ready																						
SIL Ready																						
LDR Model Select																						
Lunar Avionics Qualified																						
First Lunar Mission																						
LDR Modifications																						
LDR Avionics Qualified																						

Figure 4-8c. Lunar Dress Rehearsal - Man-Rating Approach

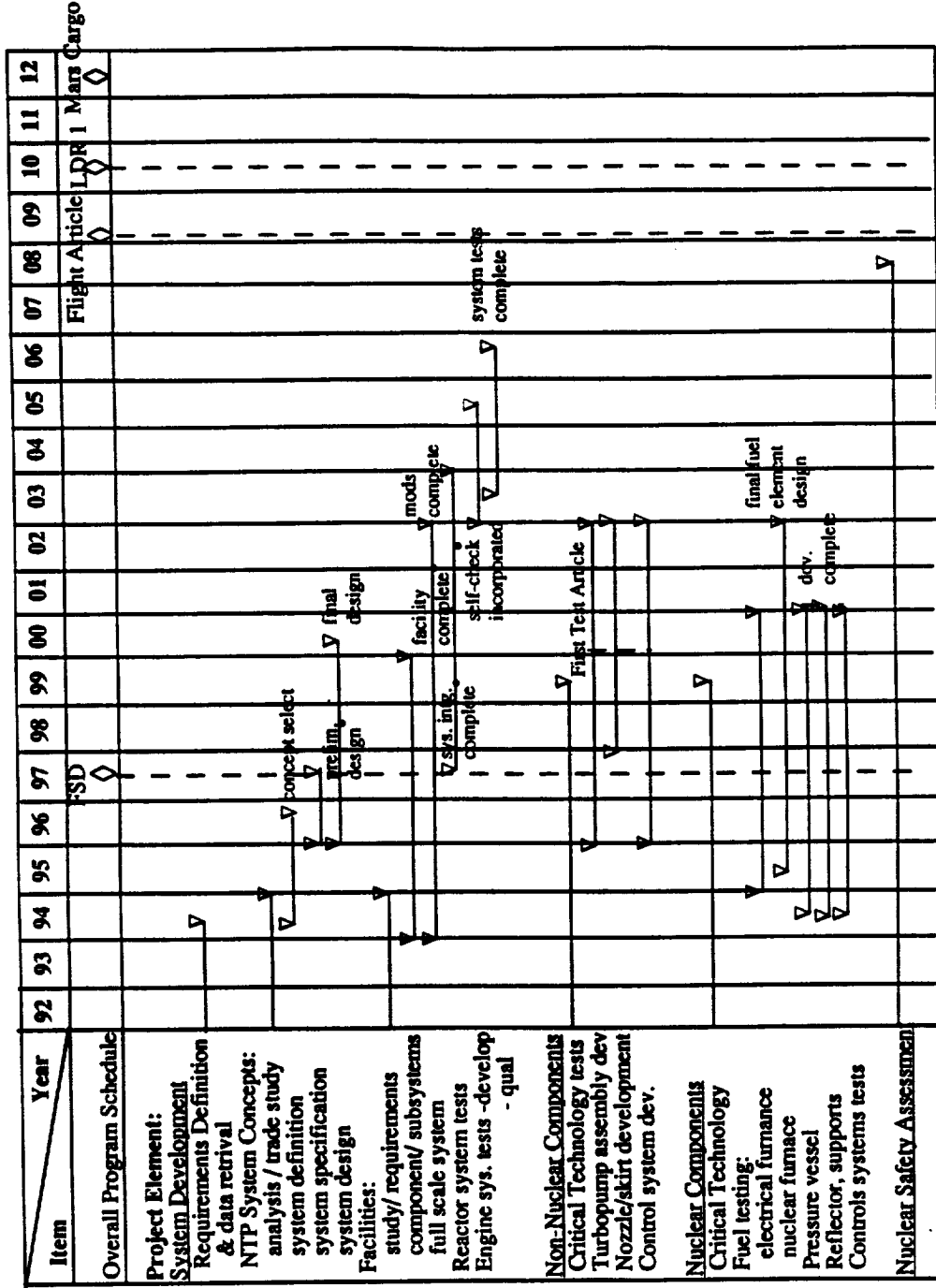


Figure 4-9. Lunar Dress Rehearsal - NTP Engine Development

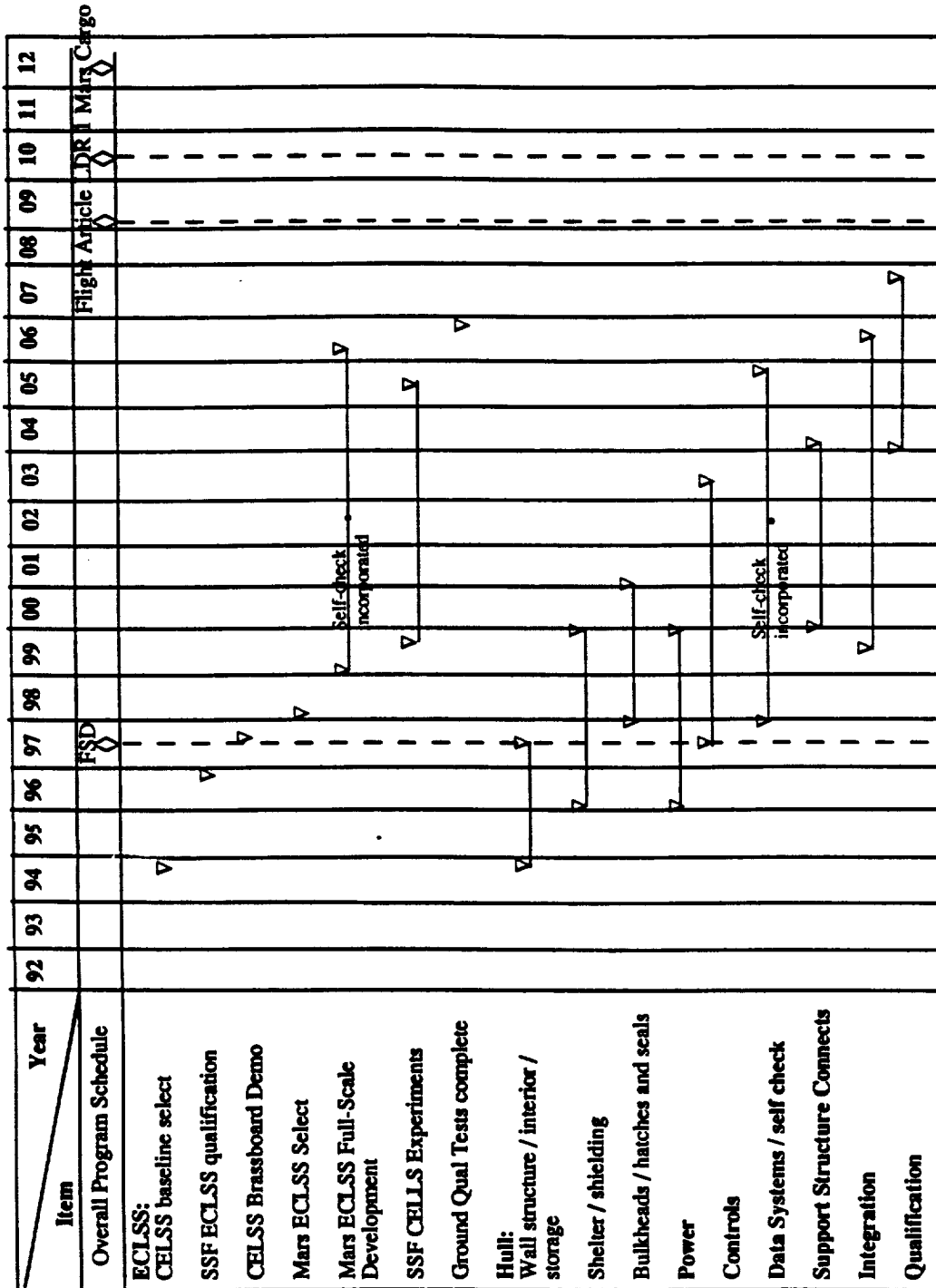


Figure 4-11. Lunar Dress Rehearsal - Vehicle Habitat

Item	Year	92	93	94	95	96	97	98	99	00	01	02	03	04	05	06	07	08	09	10	11	12
Overall Program Schedule							FSID										Flight Article		LDR 1			Mars Cargo
Truss Structure: Joint model							▽															
Material selection							▽															
Interface plane model (between sections)								▽														
Truss model dynamics									▽													
Section development																						
Section tests: assembly bending moment mass disengagement (dropping a mass) vibration radiation/ environment																						
Qualification																						
Connections/ Assembly: Quick connections models: electrical cryo fluid																						
Connection development																						
Connection tests																						
Environment tests																						
SSF Flight experiments																						
Qualification																						

Figure 4-13. Lunar Dress Rehearsal - Structures

5.0 RADIATION ANALYSIS - LUNAR CREW RETURN VEHICLE (LCRV)

5.1 INTRODUCTION

A radiation assessment of the LCRV has been performed to evaluate potential exposure to the crew resulting from large solar proton events. A similar study was previously performed on the Mars Crew Return Vehicle (reference 2). The two primary differences between the analysis performed on the LCRV and Mars CRV included the LCRV's shield distribution and the nature of the incident radiation field used to determine crew dose and dose equivalent rates.

The radiation evaluation of the Mars CRV has been completed. Current mission design operations call for astronauts to enter the Apollo style capsule, separate from the Mars transfer vehicle (MTV) for a direct Earth entry. This study investigated acute crew exposure resulting from the October 19, 1989 SPE. The spectra was obtained directly from the GOES-7 satellite. GOES-7 monitors the temporal development and energy characteristics of the emitted protons. The arrival of the the shock-front occurs at roughly 25 hours. The start of the event is declared as the ≥ 10 MeV protons reach a flux greater than 10 protons/cm² - sec. The initial and third twelve hours hours of the event were used in the investigation to simply characterize the potential impact to the crew from a large SPE. The period from 24 to 36 hours was included in the analysis because of the arrival of the shock front.

The LCRV follow-on study used the same reference flare as used on the Mars return but now included the full integrated spectra. In addition, added protection was provided by the incorporation of the LCRV's service module. The service module was "stacked" in the same fashion as the Apollo command and service module. The LCRV command module was the same as the Mars CRV with a crew of six.

5.2 MODELS AND METHODS

5.2.1 Background and Description of the Analysis

Evaluating the radiation environment within a spacecraft involves determining the incident radiation flux at the surface of the spacecraft and "transporting" the radiation through the vehicles structure to derive the attenuated internal radiation environment. To determine the exposure and resulting risk to the crew, the internal radiation environment is then transported through a simulated astronaut to determine the radiation field at specified critical organs. Accurate radiation assessment requires precise models or measurements of the natural space radiation environment and non-uniform distribution of shielding provided by the spacecraft's inherent mass and

anatomy of the astronaut. In addition, attenuation of the incident radiation field by the shielding, and biophysical models used to convert the radiation field at critical organs to a measure of medical risk consequences resulting from the exposure must also be determined.

5.2.2 Natural Radiation Environment Models

When astronauts leave the relative protection of the geomagnetic field, they are exposed to unpredictable solar proton events. The level of solar activity and modulation of radiation sources is tied directly to the strength of the sun's pervasive magnetic field. During the course of the roughly eleven year solar cycle, several tens of solar flares will produce sufficient energy to release elevated charged particle fluxes, primarily protons. Typical events are classified as "ordinary" and would have little effect on crew or spacecraft. Detailed radiation analysis should evaluate probable exposure from ordinary flares as part of the total mission exposure. Historically, an average of two to four flares release tremendous energy and particle fluxes and are classified as Anomalously Large Solar Proton Events (ALSPE). The cumulative fluence resulting from proton events during the solar cycle are dominated by the few occurrences of ALSPE. Large solar proton events can deliver debilitating or lethal doses to unprotected astronauts. Two such ALSPE were used in the investigation of the LCRV: the October 19, 1989 and August 8, 1972 events.

5.2.3 The Boeing Radiation Exposure Model

The Boeing Radiation Exposure Model, BREM, has been employed to perform the Radiation Analysis task. BREM combines computer aided design (CAD) capabilities with established NASA transport codes permitting fast, accurate and consistent radiation analysis. BREM uses an Intergraph workstation to create the solid models of the vehicles. VECTRACE (VECTor TRACE), a custom ray-tracing subroutine contained within BREM was used to establish the shield-distribution about the desired analysis points within LCRV. VECTRACE divides the 4π solid angle surrounding a "detector" into a number of equal solid angles as specified by the analyst. Vectors originating at the detector point and co-aligned with the centers of solid angles traverse the spacecraft shielding to determine the shield thickness and composition. Previous widespread techniques to determine the shielding provided by very complex and in homogeneous spacecraft structures either relied on oversimplifications, such as using an average shield thickness, or modeling the spacecraft structure through a process known as combinatorial geometry. The latter method is extremely slow, labor intensive, tedious

and sufficiently complex, significantly increasing the potential for errors. Design programs today rely heavily on the use of CAD based systems which allow unparalleled advantages in understanding the integration and compatibility of large complex systems. The logical development progression was to make use of these systems for radiation protection studies.

A modified version of Hardy's PDOSE (Proton DOSE Code) (reference 10), was used to determine crew exposure. PDOSE has adopted a continuous slowing down approximation to calculate the attenuation and propagation of particles in various shield materials. Secondary particles generated by nuclear interactions are not included in PDOSE. Results from PDOSE have been extensively compared against Shuttle measurements by NASA's Radiation Analysis Branch (Johnson Space Center) and has been found to be fairly accurate. Organ dose calculations, necessary for risk assessment, were performed using a detailed mathematical anthropomorphic phantom. The phantom model, known as the Computer Anatomical Man (CAM), represents the anatomical structure of a fifty percentile Air Force male. The shield distribution for critical organs are generated using a method similar to that employed by the routine VECTRACE previously described. The CAM model provides a more realistic shield distribution for the blood forming organs (BFO), ocular lens and skin than simple water sphere geometries. In the assessment, the BFO and skin represent the average distribution of 33 points distributed throughout the BFO and skin organs.

5.2.4 Solid Modeling

One of BREM's greatest attributes is its use of CAD technology to produce the spacecraft shield distribution at points or areas of interest. The strengths of this type of approach include its tremendous saving in time, accuracy, and functionality. Three-dimensional solid CAD models not only portray hardware geometry but serve as the database for structural, thermal, and human factors analysis.

The CAD system can keep assessment costs at a minimum. The system relies on the use of engineering databases that would be created in any spacecraft design program. By using CAD-based systems, the analyst can tap into the many man-hours of careful work that has been invested in their construction. Radiation analysis does not have to rely on the duplication of this effort. Additionally, CAD-based systems produce shield models with fewer errors (i.e., undesirable voids or overlapping regions) and greater accuracy compared to combinatorial geometry models. This reduces the high overhead in model error checking and verification and improves confidence in results which rely on the shield model distribution. Finally, CAD solid models allow for easy removal, addition, or

rearrangement of spacecraft components and the subsequent impacts produced at the analysis points. Changes in spacecraft configuration as the vehicle design matures, or changes in vehicle configuration as the mission progresses can be evaluated interactively for its impact on dose rates inside the structure. This flexibility also lends itself to parametric analyses to determine optimal vehicle designs in terms of radiation exposure.

Solid elements are assigned densities relating to either their mass properties (i.e., equipment racks) or the material composition (i.e., metal matrix composite used in construction of the pressure vessel). The densities serve three roles: (1) the product of the density and the measured slant path length of the projected vector give the areal density (g/cm²), a standard parameter used in transport analysis; (2) densities serve as flags to access nuclear and atomic cross-section data files; and (3) finally, densities allow access to data files used to convert the defined materials to an equivalent aluminum form based either on mass properties or the ratio of stopping powers

5.3 ANALYSIS RESULTS

Dosimeter locations were established at each of the six crew couch positions. It was assumed that crew members would stay positioned in their couches during the full transfer period. It was necessary to construct solid anatomical figures that would provide some degree of radiation protection. The anatomical figures are constructed of water which simulates the bodies self shielding capabilities. Five of these figures were "turned-on" while the shield distribution for the sixth was being established. The Computerized Anatomical Man model provided the shield distribution analytically for the sixth crew member. A typical dosimeter location was established, located roughly at a mid chest position. Results of the analysis are provided in figure 6-1 below.

SPE	Position		1	2	3	4	5	6
	Organ							
'72	BFO		10.3	10.3	12.0	12.0	16.4	16.4
	Skin		63.4	63.4	95.5	96.8	102.0	102.0
'89	BFO		11.5	11.6	11.7	11.7	15.8	15.8
	Skin		40.2	40.2	57.0	57.0	59.4	59.5

Figure 5-1. LCRV dose equivalent in rem/event

As expected, the dose equivalent values obtained for the LCRV are greater than the Mars CRV. Even though the shielding provided over a portion of the solid angle is greater for the LCRV as a result of the addition of the service module, it is not enough to greatly influence the full event integrated spectra. The dose equivalent results are below the current annual and monthly limits but would not be sufficient to meet the accepted principle of ALARA, (As Low As Reasonably Achievable) used by NASA. New concepts in shield materials or methods should be investigated for the LCRV. The amount of dedicated shielding needed can be reduced, however, by first shielding with the vehicles inherent mass. The Boeing Radiation Exposure Model allows vehicle designers to make such design changes and decisions early in the program where their impact is minimized.

CONCLUDING REMARKS

In the two phases of study conducted under the "Space Transfer Concepts and Analyses for Exploration Mission" contract a broad range of topics were discussed relating to human exploration missions to the Moon and Mars. The current short study addressed primarily three areas. In the trade study relative to the NTP vehicle an assessment was made of packaging the NTP in a launch vehicle, platform concepts for the NTP at LEO and delta-V budgets associated with the NTP Mars transportation system. The second area was a parametric study of biconic configurations to be used as a MEV. Parameters considered were the cone angles (front and rear), nose bluntness and intermediate body radius influence on lift, drag and stability. The third area examined several options for a lunar dress rehearsal for the first piloted mission to Mars. Schedules were developed to have a lunar check-out in 2010 for the piloted Mars mission of 2014.

REFERENCES

1. "Space Transfer Concepts and Analysis for Exploration Missions," Phase 1, Final Report, Boeing Defense and Space Group, Huntsville D615-10030-2, March, 1991
2. "Space Transfer Concepts and Analysis for Exploration Missions," Phase 2 Final Report, Boeing Defense and Space Group, Huntsville D615-10045-2, December, 1991
3. "America at the Threshold", The Synthesis Group on America's Space Exploration Initiative, May, 1991
4. Himmel, S. C., Dugan, J. F., Jr., Luidens, R. W., and Weber, R. J. "Nuclear-Rocket Missions to Mars," Aerospace Engineering, July, 1991
5. Donahue, B. D., "Logistics Impacts on Lunar on Mars Lander Design," AIAA 91-4131, November, 1991
6. Canetti, G. S., "Definition of Experimental Test for a Manned Mars Excursion Module," North American Rockwell Corporation Contract #NAS9-6464, 1966 - 68
7. "Evacuated Reflective Insulation in Cryogenic Service," American Society for Testing and Materials, Annual Book of ASTM Standards, C740-82
8. "Space Transfer Concepts and Analysis for Exploration Missions, IP and ED Volume I: Major Trades, Books 1 and 2," Boeing Aerospace and Electronic, Huntsville D615-10026-1, March, 1991
9. "Space Transfer Concepts and Analysis for Exploration Missions, IP and ED Volume 6: Lunar Systems," Boeing Aerospace and Electronics, Huntsville D615-10026-6, March 1991
10. Hardy, A. C., Personal Communication, October, 1991

